THESIS FOR THE DEGREE OF DOCTOR OF PHILOSOPHY

Decarbonization in Carbon-Intensive Industries

Frameworks for Enhanced Early-Stage Identification of Optimal Decarbonization Pathways

THARUN ROSHAN KUMAR

Department of Space, Earth and Environment

CHALMERS UNIVERSITY OF TECHNOLOGY

Gothenburg, Sweden 2025

Decarbonization in Carbon-Intensive Industries
Frameworks for Enhanced Early-Stage Identification of Optimal Decarbonization Pathways
THARUN ROSHAN KUMAR
ISBN 978-91-8103-294-9

Doktorsavhandlingar vid Chalmers tekniska högskola
Ny serie nr 5752
ISSN 0346-718X

Department of Space, Earth and Environment
Chalmers University of Technology
SE-412 96 Gothenburg
Sweden
Telephone + 46 (0)31-772 1000

Printed by Chalmers Digitaltryck
Gothenburg, Sweden 2025

Decarbonization in Carbon-Intensive Industries
Frameworks for Enhanced Early-Stage Identification of Optimal Decarbonization Pathways

THARUN ROSHAN KUMAR
Division of Energy Technology
Department of Space, Earth and Environment
Chalmers University of Technology

Abstract

Carbon-intensive industries account for a quarter of global annual CO_2 emissions. Achieving mandated climate targets requires rapid deployment of decarbonization technologies in these industries. Such deployment typically involves substantial upfront investments amidst technical, economic, and policy uncertainties. Consequently, careful selection of decarbonization technologies or a combination thereof, coupled with measures such as process electrification and energy efficiency, is crucial.

This thesis presents limitations in existing methodological approaches for comparing decarbonization pathways, spanning systems-, plant-, and site-level considerations. A generalized assessment framework was developed that addresses these limitations, with individual methodological frameworks developed in the appended papers. At the system level, extended boundaries and exergy as a metric were used to compare two CO_2 capture technologies with inherently different heat and electricity demands per unit of CO_2 captured, considering the perspectives of both plant owners and end-users. At the plant level, an iterative exergy-pinch analysis, combined with techno-economic analysis, was developed to identify promising process modifications in unabated process plants that maximize overall exergy utilization and CO_2 avoidance, leading to successive designs towards net-zero emissions. At the site level, a site-specific techno-economic analysis was developed by incorporating quantitative and qualitative site-specific factors expected to influence the choice of decarbonization technologies. Finally, to address deployment barriers for low-emissions hydrogen, an integrated system of complementary production technologies was evaluated using a generalized optimization framework, enabling cost-optimal supply strategies under site constraints and market uncertainties. The frameworks were demonstrated in case studies on bio-CHP in a district heating system, propane dehydrogenation, and a steam cracker plant.

The case study results show that integrating amine-based CO_2 capture with industrial heat pumps in bio-CHP plants could enable greater district heat delivery and provide product flexibility across heat, power, and CO_2 emissions. The iterative exergy-pinch analysis applied to the propane dehydrogenation plant identified an unconventional process modification, resulting in a substantial reduction in CO_2 avoidance cost (58–70%) compared to CO_2 capture from its highly diluted flue gas stream from the unmodified process. The site-specific techno-economic analysis revealed that incorporating site-specific cost factors yields higher avoidance cost estimates than standardized assessments, underscoring the risk of suboptimal technology selection. Finally, the integrated hydrogen production system demonstrated how combining multiple distinct production technologies can reduce costs, improve operational flexibility, and system redundancy. In summary, the generalized assessment framework, combining these individual framework methodologies, provides a comprehensive early-stage indication of the optimal decarbonization pathway for specific industrial sites.

Keywords: carbon-intensive industries; decarbonization; CCS; process integration, exergy and pinch analyses, techno-economic assessment

List of publications

The thesis is based on the work contained in the following appended papers, referred to by Roman numerals in the text:

I. Roshan Kumar, T.; Beiron, J.; Biermann, M.; Harvey, S.; & Thunman, H. "Plant and system-level performance of combined heat and power plants equipped with different carbon capture technologies," *Applied Energy*, **2023**, 338, 120927, https://doi.org/10.1016/j.apenergy.2023.120927

II. Roshan Kumar, T.; Beiron, J.; Marthala, V.R.R.; Pettersson, L.; Harvey, S.; & Thunman, H. "Combining exergy-pinch and techno-economic analyses for identifying feasible decarbonization opportunities in carbon-intensive process industry: Case study of a propylene production technology", *Energy Conservation & Management: X.*, **2024**, 25, 100853, https://doi.org/10.1016/j.ecmx.2024.100853

III. Roshan Kumar, T.; Beiron, J.; Marthala, V.R.R.; Pettersson, L.; Harvey, S.; & Thunman, H. "Enhancing early-stage techno-economic comparative assessment with site-specific factors for decarbonization pathways in carbon-intensive process industry," *Carbon Capture Science & Technology,* **2025**, 14, 100338, https://doi.org/10.1016/j.ccst.2024.100338

IV. Roshan Kumar, T.; Beiron, J.; Marthala, V.R.R.; Pettersson, L.; Harvey, S.; & Thunman, H. "Strategies for large-scale deployment of low-emissions hydrogen for CO_2 abatement in petrochemical clusters," *Submitted for publication.* **2025**

Author contributions

Tharun Roshan Kumar is the principal author of all papers included in this thesis. Dr. Maximilian Biermann contributed to method development, modeling (MEA model), discussions, and editing of **Paper I**. Dr. Johanna Beiron contributed to modeling (CHP plant model) in **Paper I**, method development in **Papers I**, **III**, and **IV**, and discussions and editing of **Papers I–IV**. Dr. V.R. Reddy Marthala and Lars Pettersson contributed to discussions and review of **Papers II–IV**. Professor Henrik Thunman supervised the work and contributed to discussions and editing of all papers. Professor Simon Harvey contributed to discussions and editing of all papers.

Other related publications not included in this thesis

V. Roshan Kumar, T.; Mattisson, T.; & Rydén, M.; & Stenberg, V.; "Process Analysis of Chemical Looping Gasification of Biomass for Fischer–Tropsch Crude Production with Net-Negative CO_2 Emissions: Part 1," *Energy & Fuels*, **2022**, 36 (17), 9687-9705. https://doi.org/10.1021/acs.energyfuels.2c00819

VI. Roshan Kumar, T.; Mattisson, T.; & Rydén, M. "Techno-Economic Assessment of Chemical Looping Gasification of Biomass for Fischer–Tropsch Crude Production with Net-Negative CO_2 Emissions: Part 2," *Energy & Fuels*, **2022**, 36 (17), 9706-9718. https://doi.org/10.1021/acs.energyfuels.2c01184

VII. Saeed, M. N.; Shahrivar, M.; Surywanshi, G. D.; Roshan Kumar, T.; Mattisson, T.; & Soleimanisalim, A. H. “Production of aviation fuel with negative emissions via chemical looping gasification of biogenic residues: Full chain process modelling and techno-economic analysis,” *Fuel Processing Technology*, **2022**, 241, 107585. https://doi.org/10.1016/j.fuproc.2022.107585

VIII. Stenström O.; Roshan Kumar, T.; Rydén M. “Using a Million Scenarios to Identify Conditions for Robust Bioenergy Carbon Capture in Sweden,” *International Journal of Greenhouse Gas Control*, **2025**, 104411. https://doi.org/10.1016/j.ijggc.2025.104411

IX. Hoseinpoori, S.; Roshan Kumar, T.; Beiron, J.; Svensson, E.; Pallarès, D.; & Johnsson, F.; “Integration of Sorbent-Based Direct Air Capture into Combined Heat and Power Plants with Carbon Capture and Storage,” *Energy*, **2025**, 36509. https://doi.org/10.1016/j.energy.2025.136509

Conference contributions

- Roshan Kumar, T.; Fortet Casabella, J; Beiron, J; Harvey, S.; & Thunman, H. “Optimal Design and Integration of Flexible Hydrogen Production Technologies for Carbon Neutrality in Carbon-Intensive Industries,” *Proceedings of the 17th Greenhouse Gas Control Technologies Conference (GHGT-17)*, **2024**. http://dx.doi.org/10.2139/ssrn.5065733

- Roshan Kumar, T.; Svensson, E., Beiron, J., Harvey, S.; & Thunman, H. “Towards Carbon-Neutral Petrochemical Industries: Optimizing Investment Trade-Offs in Decarbonization and Defossilization Under Uncertainty,” *Proceedings of the 13th Trondheim Conference on* CO_2 *Capture, Transport and Storage (TCCS-13),* **2025**.

- Fortet Casabella, J.; Beiron, J.; Roshan Kumar, T.; Harvey, S.; & Thunman, H. “Comparison of RED III Compliance for Synthetic Fuel Production Routes Using Exergoeconomic Analysis Tools,” *Proceedings of the 13th Trondheim Conference on* CO_2 *Capture, Transport and Storage (TCCS-13)*, **2025**.

Project reports

- Axelsson L., Edvall M., Harvey S., Roshan Kumar, T., Jannasch A. -K., Westin J., Starfelt F., Pettersson L., Edman A. P., Hellesöy F. “Future hydrogen supply in Stenungsund – Pre-study of a SOEC pilot plant and analysis of large-scale integration of SOEC and ammonia cracking plants,” *RISE Research Institutes of Sweden Report*, **2024**, 2024:78. https://urn.kb.se/resolve?urn=urn:nbn:se:ri:diva-76205

Acknowledgments

First and foremost, I would like to thank my supervisors, Henrik Thunman and Simon Harvey, for giving me the opportunity to work on this project and for guiding me in my research. To Henrik, thank you for your constant guidance and support. I am especially grateful for the trust and freedom you gave me throughout this journey. Your enthusiasm, vision, and endless stream of ideas have been a true source of inspiration. To Simon, thank you for your keen eye for detail, your critical feedback on my work, and your support that made everything run smoothly until the very end. I have truly enjoyed being part of your course, and I will always cherish the four years I spent within Industrial Energy Systems.

A big thanks to Maximilian Biermann and Johanna Beiron. Max, thank you for your help during the early days of my PhD. It is something I have learned from you and have tried to carry forward for others throughout my journey. Johanna, thank you for your valuable and timely input on my manuscripts, especially the first drafts. Your early obliteration of those drafts always made sure they ended up far better than they started.

My gratitude goes to all my co-authors and to everyone I had the pleasure of working with in the projects I was involved in. A special thanks to Lars Pettersson, Reddy Marthala, and Anna-Karin Jannasch for the many interesting discussions and valuable insights. I greatly appreciate your contributions to this work. As with any challenging journey, staying committed and consistently inspired would not have been possible without the right team, and I thank you all for that.

This PhD journey would not have started without the year-long opportunity that opened the doors of this wonderful division to me and gave me the confidence to pursue my doctoral studies. For this, I sincerely thank Tobias Mattisson and Magnus Rydén.

I would also like to thank everyone in the Gasification group—Adam, Chahat, Eliette, Iacopo, Isabel, Ivan, Judit, Martin, Nidia, Rene, and Teresa for all the interesting discussions and for keeping up the spirits, as well as to everyone in the Industrial Processes and Systems group.

Thank you to all my amazing colleagues at Energy Technology for creating this exceptional workplace we share. Special thanks to Anna, Katarina, and Marie for all the help and effort you have put in to make our lives easier at the division. To Alla, Anh, Aaron, Chahat, Farha, Henrik, Maria, Sebastian, and Sina, thank you for all the wonderful times outside of work. Thanks also to my office mate, Hyunkyo Yu, for sharing this journey with me and for making everyday life at the office much more enjoyable.

Finally, I would like to thank my family for their patience, support, and love. A special mention goes to my cats, Freja and Mimi, who have also been by my side throughout this journey.

Tharun Roshan Kumar,
Göteborg, 7th September 2025

Notes

This work was financially supported by the Swedish Energy Agency (project no. 49831-1), Borealis AG, and Preem AB within the framework of the project '*Transformative change towards net negative emissions in Swedish refinery and petrochemical industries*' (FUTNERC), a collaboration between Chalmers University of Technology, Borealis AG, and Preem AB. In addition, a part of this work was carried out within the framework of the project '*Förstudie om möjlig pilotanläggning för högtemperaturelektrolys (SOEC) i Stenungsund*', in collaboration with Borealis AB, Uniper, Vattenfall, Preem AB, RISE, and Chalmers University of Technology, and funded by Klimatledande Processindustri.

List of abbreviations

AC	Ammonia Cracker
ATR	Autothermal Reformer
BECCS	Bio-Energy with Carbon Capture and Storage
CAC	CO_2 Avoidance Cost
CAPEX	Capital Expenditure
CBAM	Carbon Border Adjustment Mechanism
CC	Carbon Capture
CCS	Carbon Capture and Storage
CEP	Combined Exergy-Pinch
CHP	Combined Heat and Power
COR	Cost of Retrofitability
DH	District Heating
ETS	Emissions Trading Scheme
GHG	Greenhouse Gas
GSHP	Ground Source Heat Pump
GT	Gas Turbine
HPC	Hot Potassium Carbonate
LCOH	Levelized Cost of Hydrogen
MEA	Monoethanolamine
NG	Natural Gas
OHSC	On-site Hydrogen Supply Costs
PC	Process Configuration
PDH	Propane Dehydrogenation
Post-CCS	Post-combustion Carbon Capture and Storage
PPA	Power purchasing agreements
Pre-CCS	Pre-combustion Carbon Capture and Storage
RCF	Recycled Carbon Fuels
SMR	Steam Methane Reformer
SOEC	Solid-Oxide Electrolyzer Cells
s-TEA	Standardized Techno-Economic Assessment
TRL	Technology Readiness Levels
VF	Value-Function
MVR	Mechanical Vapor Recompression
NZE	Net-Zero Emissions
MILP	Mixed-Integer Linear Programming

Table of Contents

1 Introduction 1
  1.1 Aim and scope 3
  1.2 Outline of the thesis 5
2 Background 7
  2.1 Industrial decarbonization 7
  2.2 Comparative assessment of decarbonization pathways and their limitations 9
    2.2.1 Influence of system boundary selection 10
    2.2.2 Targeting minimal exergy losses toward net-zero CO_2 emissions plant configurations 11
    2.2.3 Site-specific techno-economic analysis 12
    2.2.4 Low-emissions hydrogen 16
3 Overview of the investigated processes and systems 19
  3.1 Process technologies 19
    3.1.1 Post-combustion CO_2 capture technologies 19
    3.1.2 Hydrogen production technologies 21
  3.2 Industrial case studies 25
    3.2.1 Combined heat and power plants 25
    3.2.2 Propane dehydrogenation plant 27
    3.2.3 Steam cracker plant 29
    3.2.4 Integrated hydrogen production system within petrochemical clusters 31
4 Methods 35
  4.1 Steady-state process modeling 35
  4.2 Process integration 36
  4.3 Combined exergy-pinch analysis 36
  4.4 Cost estimations 37
  4.5 Investment and dispatch optimization 38
5 Developed methodologies and case study applications 41
  5.1 Impact of system boundaries on the choice of decarbonization technology 43
    5.1.1 Impact of system boundaries on the choice of decarbonization technology 43
    5.1.2 The influence of system boundaries – BECCS in district heating systems 45
  5.2 Iterative combined exergy-pinch analysis 49

5.2.1 Identifying promising decarbonization process configurations using iterative combined exergy-pinch analysis 49

5.2.2 Targeting minimal exergy losses towards net-zero CO_2 emissions - Propane dehydrogenation plant 51

5.3 Site-specific techno-economic analysis 55

5.3.1 Methodological framework for incorporating site-specific factors 55

5.3.2 Impact of site-level constraints on the technology choice and CO_2 abatement costs – Steam cracker plant 63

5.4 Integrated hydrogen production systems 65

5.4.1 Methodological framework for cost-optimal design and operation of an integrated hydrogen production system under site constraints and energy market uncertainty 66

5.4.2 Techno-economic performance of integrated hydrogen production system and stepwise deployment strategy 68

6 Discussion 75

6.1 Summary of results 75

6.2 Implications 77

6.3 Methodological reflections 79

6.4 Limitations 80

7 Conclusions 83

8 Recommendations for future work 85

References 87

Nomenclature 99

Appendix A. 101

This page intentionally left blank.

1 Introduction

Global average temperature increases exceeded the 1.5°C threshold above pre-industrial levels for the first time in 2024 [1]. Despite the landmark Paris Agreement in 2015, global energy-related CO_2 emissions have steadily increased, reaching 36.8 $GtCO_2$/y in 2022. Of this, carbon-intensive industries accounted for about 9.2 $GtCO_2$/y, representing approximately 25% of the total global CO_2 emissions [2]. At the current rate of CO_2 emissions, global temperatures are projected to permanently surpass the 1.5°C threshold by 2032 and could approach 2°C before mid-century [2,3].

In the European context, ambitious targets have been set in recent years for reducing greenhouse gas (GHG) emissions. These targets include a 55% reduction by 2030 and a 90% reduction by 2040 relative to 1990 levels, aligning with the aim of achieving climate neutrality by 2050 [4,5]. A series of policy initiatives has been introduced under the European Green Deal [6], notably emphasizing the role of industries in leading the transition towards climate neutrality and promoting circular production and consumption systems. Carbon-intensive industries such as cement, iron and steel, refineries, petrochemicals, and pulp and paper collectively contribute approximately 94% of total industrial emissions in the EU [7]. These industries face significant challenges in meeting the stringent CO_2 mitigation targets within a rapidly evolving policy landscape. The challenges arise from technical, economic, market, and policy uncertainties [8].

Notably, the *polluter-pays* approach under the EU Emissions Trading Scheme (EU ETS) and the upcoming Carbon Border Adjustment Mechanism[1] (CBAM) have put increased pressure on these industries to undergo a complete transformation of their operations to achieve sustainable and emissions-free production. Currently, the aforementioned industries are considered at risk of carbon leakage and, therefore, benefit from free allowances under the EU ETS [9,10]. However, this free allocation[2] will gradually be phased out as CBAM is phased in during the period 2026–2034 [11], significantly increasing their compliance costs and, thus, the urgency to decarbonize.

Considering these timelines, most carbon-intensive industries in the EU face a narrow implementation window of less than a decade, until 2034, to assess, choose, and deploy enabling process technologies to transform existing industrial sites. Throughout this period, they will have to concurrently adopt energy efficiency and other decarbonization measures (e.g., direct electrification or fuel switching) as transitional solutions toward net-zero CO_2 emissions. Such transformations are particularly challenging in fossil-dependent sectors such as oil refining and petrochemicals.

---

[1] To prevent potential carbon leakage, i.e., relocation of industries to regions with less stringent climate regulations, imports of materials and goods into the EU from these regions are penalized. This supports the EU's climate mitigation actions and the competitiveness of European industry [152].

[2] The existing policy instrument under the EU ETS that grants emission allowances at no cost to regulated industries to safeguard competitiveness and address carbon leakage risks [7].

In these industries, achieving sustainable production of carbon-based fuels and materials will require the elimination of direct CO_2 emissions from the combustion of fuel-grade by-products (*decarbonization*) and the replacement of fossil feedstock with alternative carbon sources (CO_2, biomass, and waste), in order to avoid end-of-life indirect CO_2 emissions (*defossilization*). These industries are, therefore, expected to transition into more circular and electrified systems, driven by the increasing need to decouple from fossil-resource extraction and the diminishing carbon footprint of electricity as the share of variable renewable energy sources, such as wind power, grows. Furthermore, significant amounts of *low-emissions hydrogen*[3] will be required as feedstock, reductant, or fuel in hard-to-electrify industries [12].

Near-term investments in the transformation of existing industrial assets through retrofits and the installation of low-carbon technologies will ultimately determine the levels of emissions reductions achievable within these industries. Given that most of these installations will be first-of-their-kind, they are expected to incur significantly higher costs than installations deployed elsewhere in subsequent years. Therefore, the upcoming investment cycles will be critical with regard to the careful selection and implementation of decarbonization measures and technologies under these uncertainties. More importantly, these investment cycles will be essential to ensure that these industries comply with mandated policies and emissions reduction trajectories while retaining their competitive advantage.

In this context, the selection of appropriate measures and technologies within specific industries often poses a paradox of choice or, conversely, a lack thereof, which would ultimately induce decision paralysis. Many emerging[4] low-carbon technologies currently remain unproven at industrially relevant scales and will, therefore, require several years of development before they can be commercialized. Depending on their levels of technological maturity, these technologies may remain unavailable during the targeted deployment timeframe, thereby limiting their immediate role in curtailing industrial CO_2 emissions.

In contrast, the choice between mature[5] and emerging substitute technologies that are nearing commercialization remains unclear, considering the risk of technology lock-in, the limited time for near-term implementation, and the associated deployment barriers. The timing of their deployment will also depend on resource availability (e.g., low-cost renewable electricity) and on the availability of and access to critical infrastructure, such as CO_2 transport and storage facilities, hydrogen networks, and grid transmission capacity. These uncertainties are further compounded by limitations linked to incumbent methods used for evaluating decarbonization measures and comparing competing technologies at an early stage of assessment.

First, the choice of system boundaries during the evaluation can significantly influence technology selection, and the optimal solution may vary depending on whether the assessment is approached from the perspective of a plant owner or end-users[6]. This highlights the need for careful consideration of system boundaries in the evaluation process.

---

[3] *Low-emissions hydrogen* refers to both renewable hydrogen (produced by electrolysis using renewable electricity) and low-carbon hydrogen ($\geq 70\%$ GHG emissions savings compared to fossil-derived hydrogen) [68,153].

[4] Refers to technologies with technology readiness levels (TRL) 3–7 [36,154].

[5] Refers to technologies with TRL >7. For example, end-of-pipe CO_2 capture based on chemical absorption [89].

[6] *End-users* refer to the consumers of end-products and services in the value chain, who may eventually bear the additional costs and environmental benefits of decarbonization at an unabated plant [26,155].

Second, while traditional process integration methods effectively minimize external thermal energy use in integrated industrial processes, they are not suitable for identifying innovative configurations that involve unconventional integration measures. Given the projected increase in the availability of pure exergy, i.e., electricity, and the anticipated convergence of gas and electricity prices, unconventional integration measures, including process electrification and modifications to the core production units, will become more prevalent. Nonetheless, the ability to identify unique integration possibilities depends on the tools and methods that are available to the process designer. Therefore, there is a need for exergy-based methods to assess retrofit designs and develop novel integrated processes that achieve high CO_2 avoidance with minimal exergy losses.

Third, site-level factors, such as the availability of space for new installations, interconnection costs, and other unaccounted site-level costs not captured in incumbent early-stage techno-economic assessment (TEA) methods, could alter the indication of the optimal decarbonization technology for a specific site, limiting the effectiveness of such methods.

Fourth, isolated technology comparisons risk overlooking potential synergies from integrating distinct technologies with varied operational constraints, resources, and infrastructure requirements. Such integration could mitigate individual deployment barriers, enhance operational flexibility, and reduce investment risks. These limitations associated with the incumbent assessment methods not only risk delaying the implementation of decarbonization measures but also increase the likelihood of deploying sub-optimal technologies at existing industrial sites. Consequently, establishing robust early-stage assessment methods becomes crucial to prevent decision paralysis, facilitate optimal technology selection, and provide practical guidance on when, where, how, and which set of decarbonization solutions should be implemented.

1.1 Aim and scope

This work presents methodological frameworks for the early-stage assessment of competing *decarbonization technologies*[7] and strategies for carbon-intensive industries. The overarching goal is to facilitate enhanced identification of cost-effective *decarbonization pathways*[8], providing valuable insights to support decision-making toward practical implementation as these industries transition to net-zero or negative emissions. The specific aims of this thesis are to develop generalized assessment methods that enhance technology comparisons and propose novel process configurations for industries facing practical retrofit challenges or systemic barriers to deployment. To this end, this work addresses the limitations of incumbent process integration and techno-economic assessment methods, as well as deployment barriers, by considering relevant technical, economic, and policy factors across site-, plant-, and system levels. The individual frameworks developed in **Papers I–IV** are synthesized into a generalized assessment framework (Figure 1-1), representing the following key contributions of this thesis:

---

[7] Set of process equipment required to enable a specific decarbonization pathway. For example, post-combustion CO_2 capture would require a CO_2 capture technology (chemical/physical/cryogenic) in combination with compressors and CO_2 purification or liquefaction units, depending on the mode of CO_2 transportation. Together, these sets of process equipment enable the post-combustion CCS pathway.

[8] Pathways or options arising from different technological alternatives (e.g., pre-combustion, post-combustion, or oxyfuel combustion) and measures (e.g., fuel switching, direct or indirect process electrification) that can be implemented to achieve net-zero CO_2 emissions at an unabated process plant.

- A methodology for comparing competing decarbonization technologies, using exergy as a figure of merit, with the appropriate selection of system boundaries to highlight potential inconsistencies between the perspectives of the plant owner and those of the end-users in the local energy system concerning the optimal decarbonization technology.
- An iterative combined exergy-pinch analysis with techno-economic analysis that enables the identification of promising process modifications designed to maximize exergy utilization and CO_2 avoidance within industrial processes with the retrofit of decarbonization technologies.
- A site-specific techno-economic analysis method that builds upon *standardized*[9] approaches by enabling early quantification of the site-level factors that influence the feasibility of deploying decarbonization technologies at a specific site. This approach facilitates the rapid screening of competing technologies, allowing for an estimation of retrofitability costs with limited site information and subsequently determining their CO_2 avoidance cost (CAC) at the site level.
- A modeling framework that integrates process and cost-optimization models to assess the value of co-location, integration, and flexible operation of multiple low-emissions hydrogen production technologies. The framework facilitates the identification of cost-optimal system configurations and operational strategies under site-specific constraints and varying economic conditions.

The developed frameworks are demonstrated through case studies of selected carbon-intensive industries, evaluating decarbonization technologies available to them for near-term implementation. Within the context of each case study plant, the following questions are addressed:

- What is the optimal CO_2 capture technology for large-scale BECCS deployment in bio-CHP plants operating within district heating (DH) systems, considering both the plant owner's and the end-users' perspectives on CO_2 capture technologies with inherently different exergy requirements per unit of CO_2 captured?
- How can a widely adopted propylene production technology be cost-effectively decarbonized, given the significant challenges posed by low CO_2 concentrations in its highly diluted flue gases?
- How do site-specific factors influence the choice of decarbonization technology for a steam cracker plant, considering the potential cost escalation associated with these factors?
- How do site-specific constraints and energy market uncertainties affect the optimal technology mix and hydrogen production costs in an *integrated hydrogen production system*[10], and to what extent can flexible operation with energy exports reduce on-site hydrogen supply costs?

---

[9] *Standardized* refers to an an established CCS costing methodology with common nomenclature and consistent cost escalation guidelines. More information on these methods can be found in Ref. [36].

[10] *Integrated hydrogen production system* refers to a set of hydrogen production technologies that are integrated and operated in coordination to supply hydrogen to potential off-takers.

1.2 Outline of the thesis

The thesis consists of a summarizing essay and four appended papers. The summary is divided into eight chapters. Chapter 1 introduces and contextualizes the appended papers, outlining the objectives of the undertaken work. Chapter 2 provides background information, including a review of existing methods for evaluating decarbonization pathways and their limitations. Chapter 3 describes the process technologies and industrial systems investigated. Chapter 4 presents the applied methods. Chapter 5 presents the developed frameworks and summarizes the key results obtained from applying these frameworks to selected industrial case studies. Chapter 6 discusses the potentials and implications of the proposed process designs and frameworks. Chapter 7 concludes the thesis by presenting the overall findings, and Chapter 8 provides recommendations for future research directions. The scope of the appended papers is outlined below.

- **Paper I** investigates the performance of two inherently different CO_2 capture technologies in the context of a large-scale biomass-fired combined heat and power (CHP) plant within a district heating system. The study focuses on using exergy as a figure of merit for technology comparisons while expanding the system boundaries from the plant to the end-users to highlight diverging perspectives on the optimal decarbonization solution.

- **Paper II** demonstrates the iterative combined-exergy pinch (CEP) method for stepwise process modifications to a propane dehydrogenation process. The study derives process modification options from the CEP analysis, conducts a techno-economic analysis to assess economic viability, and identifies a novel decarbonized process configuration. The potential and implications of the proposed configuration are discussed and compared with those of alternative decarbonization strategies.

- **Paper III** demonstrates the application of site-specific techno-economic analysis at a steam cracker plant, highlighting spatial, operational, and temporal factors relevant to large industrial sites, such as pulp and paper, cement, and petroleum refining. This study considers spatial factors such as site-layout-dependent CO_2 interconnections and the value and opportunity cost of available space for new installations. This study also examines operational factors, including the cost and emissions intensity associated with energy supply options. Temporal factors, including forced downtimes during retrofits and the timing of deployment relative to the residual plant lifetime, are also analyzed. Qualitative site-specific factors and technology-specific attributes are assessed through expert elicitation using a retrofitability assessment matrix, which is generalizable to other process industries considering their site-level conditions.

- **Paper IV** evaluates integrated hydrogen supply systems comprising solid oxide electrolyzers (SOECs), ammonia crackers (AC), and autothermal reformers with carbon capture and storage (ATR-CCS). This study accounts for site-level constraints such as grid transmission and ammonia storage capacities, as well as the availability of methane-rich fuel gas. A mixed-integer linear programming (MILP) model is used to determine cost-optimal hydrogen supply configurations and dispatch strategies under varying price conditions. Building on the results from **Paper III**, low-emissions hydrogen is considered for use as cracker fuel to decarbonize the steam cracker plant. The study also proposes a stepwise implementation strategy that leverages the inherent redundancies and operational flexibilities offered by the plant, together with short-term policy incentives to overcome barriers to large-scale standalone hydrogen deployment.

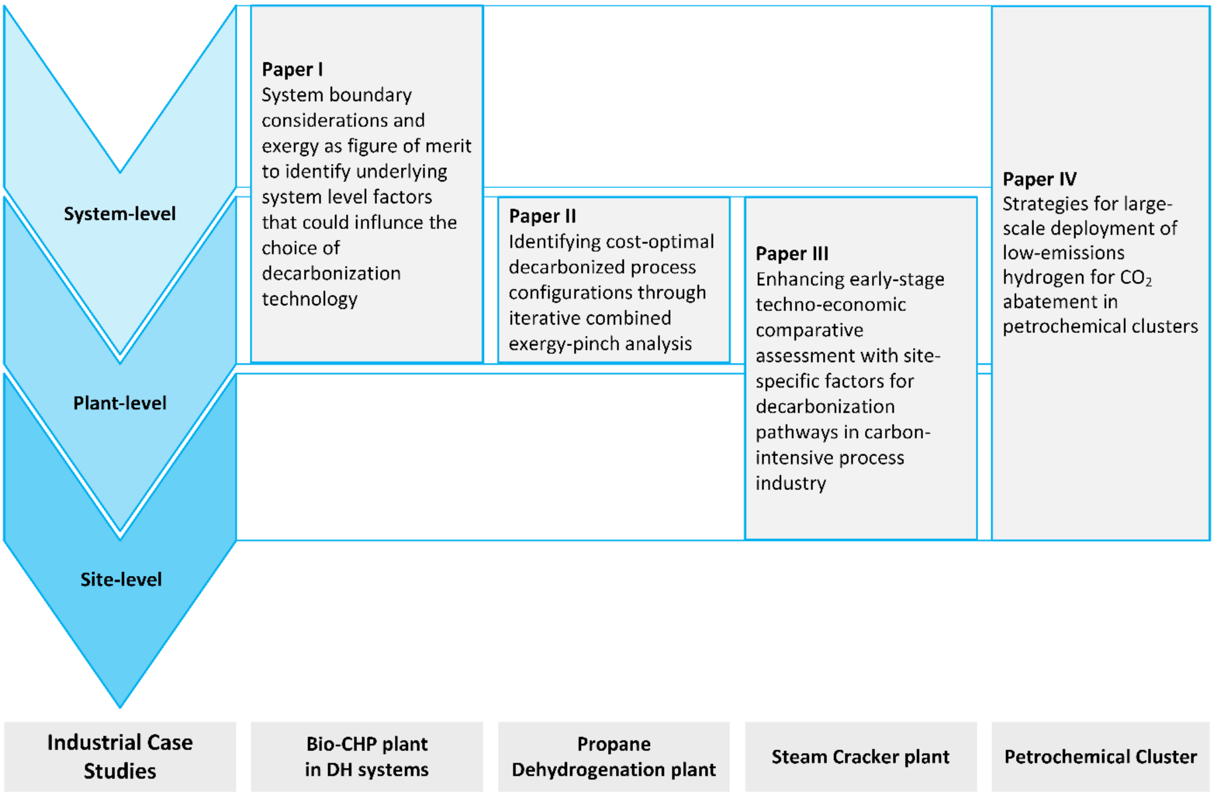

Figure 1-1: Overview of the generalized assessment framework, combining individual frameworks and industrial case studies from Papers I–IV. The framework addresses limitations in incumbent process integration and techno-economic methods, as well as deployment barriers, at different evaluation levels.

2 Background

This chapter presents background information relevant to the thesis, with a focus on incumbent methods and their limitations in identifying optimal decarbonization technologies for different carbon-intensive industries. The theoretical backgrounds for the developed frameworks in this thesis are detailed in the appended papers, ***Papers I–IV.***

2.1 Industrial decarbonization

Decarbonizing carbon-intensive industries is central to the European Union's goal of achieving climate neutrality by 2050 [13]. However, transforming these sectors requires balancing competing priorities such as emission reduction, circularity, self-sufficiency, resilience, and competitiveness [14]. In recent years, this challenge has been further exacerbated by global supply–demand disruptions during the COVID-19 pandemic in 2020, surging energy prices driven by geopolitical instability since 2022, persistent uncertainty over renewable electricity deployment, and escalating trade tensions in 2025.

Figure 2-1 illustrates the development of announced carbon capture and storage (CCS) and green hydrogen projects to date, along with future projections, highlighting the ambition and implementation gaps for these two key decarbonization technologies. The *ambition gap*, as defined by Odenweller et al. [15], is the difference between the capacity required to meet climate targets and that of announced projects. In contrast, the *implementation gap* refers to the difference between project announcements and the actual operational facilities.

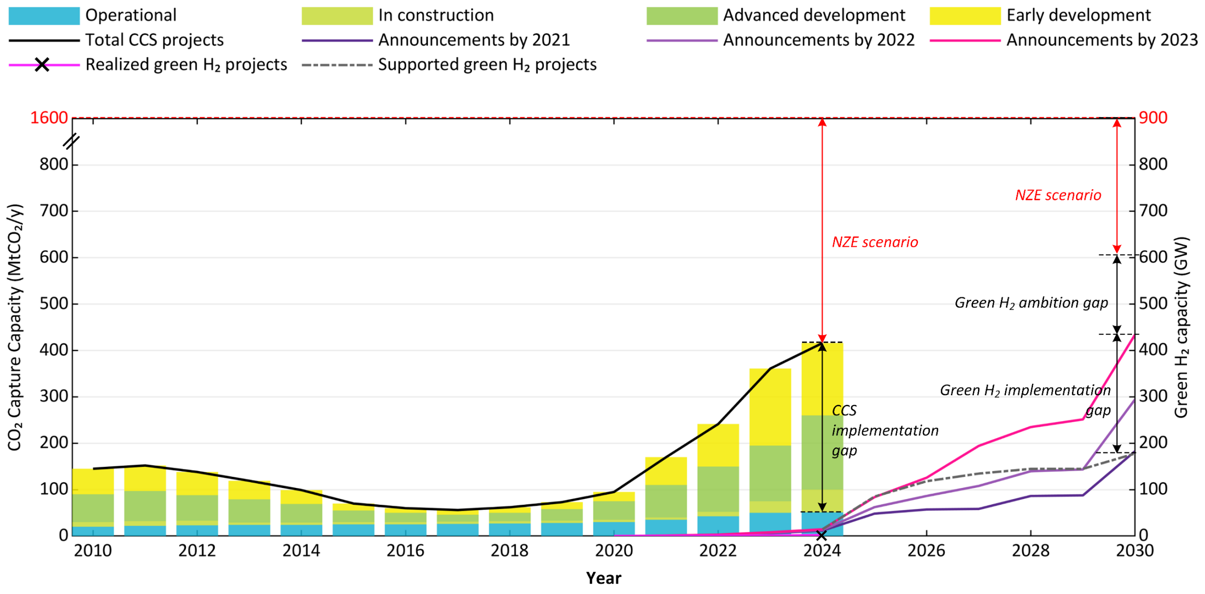

Figure 2-1: The development of announced (i.e., in construction, early, or advanced development) and operational CCS facilities (MtCO$_2$ yr^{-1}) is adopted from [16]. The trajectories of announced and realized green hydrogen projects until 2024, together with projections of electrolyzer capacity (GW) based on announcements in 2021–2023, are derived from Odenweller et al. [15]. The grey dashed line indicates the subset of projects estimated by Odenweller et al. [15] that are supported by either implemented demand-side policies or subsidies. The upper limits of the y axes (1600 MtCO$_2$ yr^{-1} and 900 GW electrolyzer capacity) represent the scale of CO$_2$ sequestration and electrolyzer deployment required under a Net-Zero Emissions scenario by the IEA [17,18]. Note: stacked bar values before 2022 were approximated from [16], and therefore carry an uncertainty of ±5–10 MtCO$_2$ yr^{-1}.

Figure 2-1 shows that the number of CCS facilities in the pipeline has increased gradually since 2020, despite the aforementioned challenges. As of 2024, there are nearly 578 CCS in total, either under construction or at different stages of development, representing an annual capture capacity of 365 $MtCO_2$ [16]. However, the number of operational facilities remains substantially lower, with an annual capture capacity of 51 $MtCO_2$ [16]. Similarly, as of 2023, only about 7% of the total announced green hydrogen projects, representing 4.3 GW of electrolyzer capacity, had become operational [15].

From Figure 2-1, it is clear that even if all announced CCS projects were realized within the next five years by 2030, the total capture capacity would still fall substantially short of the 1.6 $GtCO_2$ target for permanently stored CO_2 required under the IEA's Net Zero Emissions (NZE) scenario [17–19]. Similarly, despite the sharp increase in hydrogen project announcements over the past 1–3 years, the projected capacity still falls short of the green hydrogen requirements under the NZE scenario, highlighting the future ambition gap, while the gap between projects estimated to be supported by demand-side policies and subsidies and those announced illustrates the future implementation gap [15]. Although these are global trends, similar patterns can be expected in the EU, where a wide gap remains between project announcements and actual deployment.

The EU has introduced major policy initiatives to accelerate industrial transformation. The Clean Industrial Deal, announced in 2025, will mobilize over €100 billion to support industrial decarbonization and enhance competitiveness [14]. In parallel, the EU Innovation Fund, financed through ETS revenues, supports first-of-a-kind industrial-scale projects in energy-intensive sectors. With this financial support, several flagship projects have progressed from planning to the implementation phase. Notable examples include the Brevik cement plant in Norway and the Northern Lights project, which became operational in August 2025 as the first full-scale CCS chain to transport CO_2 from Brevik for offshore storage in the North Sea [20].

Another example is Stockholm Exergi's BECCS project, which aims to capture and store up to 900 kt of biogenic CO_2 annually from its biomass-fired combined heat and power plant [21]. In addition, projects such as Greensand in Denmark [22], Porthos in the Netherlands [23], and Antwerp@C in Belgium [24] are developing shared infrastructure for CO_2 transport and storage, with potential for cross-border CO_2 transport. Similarly, the European Hydrogen Backbone initiative aims to connect industrial regions through a dedicated pipeline network for low-carbon hydrogen [25].

While these initiatives mark important progress, the core challenge of decarbonization remains at individual industrial sites. As industries approach the phase-out of free EU ETS allowances by 2034, they face three possible options: i) deploying best-available technologies in the near term, often through retrofit measures such as end-of-pipe CO_2 capture; ii) delaying investment in anticipation of emerging process technologies that may substitute the existing technologies[11] or iii) continuing operations without abatement, which in some cases may remain cheaper than the least-cost decarbonization option in the short to medium term. These industries, therefore, face a closing window of opportunity to evaluate, select, and deploy suitable retrofit technologies before 2034, beyond which retrofit and substitution options will likely compete for investment amid policy, economic, and technological uncertainties.

---

[11] For example, electrified steam crackers [117,156], Coolbrook's RotoDynamic reactor technology [157] or advanced thermochemical recycling technologies [158], could be substitutes for conventional steam cracking technology for olefins production.

2.2 Comparative assessment of decarbonization pathways and their limitations

Identifying optimal decarbonization technologies in the context of a specific industry or industrial cluster is often addressed through a comparative assessment of decarbonization pathways incorporating various best-available technologies or alternative process routes utilizing emerging process technologies. The objective of such assessments is to provide an *industry-specific indication*[12] of the most cost-effective decarbonization pathway, considering both retrofit and substitute process technologies.

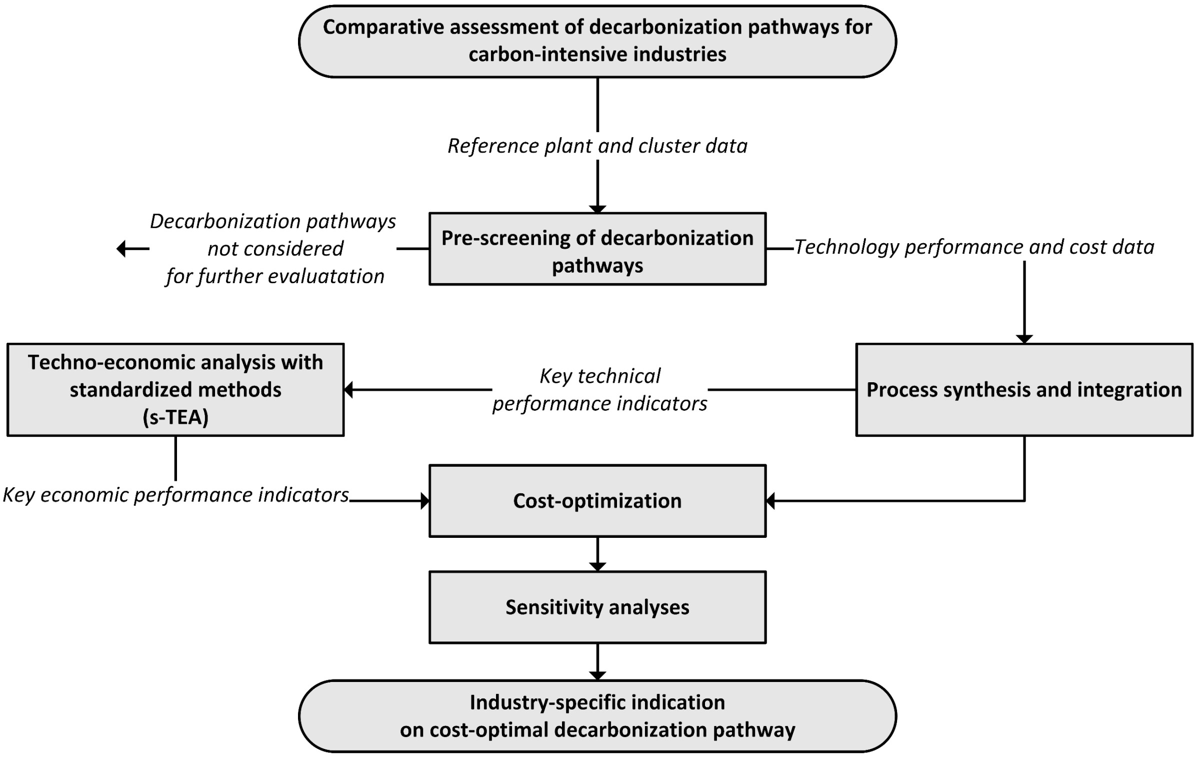

Figure 2-2: Overview of methodological steps in comparative assessment of decarbonization pathways for carbon-intensive industries and clusters. The oval symbol indicates the start/end of the framework methodology and rectangles indicate methods.

As illustrated in Figure 2-2, the method typically begins by selecting a case study plant or cluster and extracting key performance data such as material and energy flows (interconnections), flue gas compositions, and site-energy systems (steam and fuel gas networks). Decarbonization pathways are then pre-screened by selecting a comparable set of technologies and compiling their key technical and cost data for further evaluation. Next, system boundaries and performance indicators are defined to ensure fair comparison of the shortlisted technologies. This is followed by developing process models of the reference plant and associated decarbonization technologies to establish mass and energy balances of the integrated system. Finally, key technical performance indicators from the integrated processes are extracted to evaluate economic performance using standardized techno-economic analysis methods, typically complemented by sensitivity analyses on key economic parameters. In some cases, this methodological framework is extended by applying cost-optimization tools to determine optimal installed capacities and operation under varying

---

[12] *Industry-specific indication* refers to the outcome of s-TEA studies in which cost estimates are derived for a reference industry based on its process characteristics (e.g., flue gas properties) which are then generalized and presented across the entire sector, inherently assuming that all plants have similar conditions.

energy market conditions. The following subsections (2.1.1–2.1.4) present the identified limitations in existing comparative assessment methods.

2.2.1 Influence of system boundary selection

System boundaries delineate the scope of a study by specifying what is included and excluded from the evaluation. They are particularly important for selecting technologies for decarbonization in existing industries, as the choice of system boundaries influences how technology alternatives are perceived in terms of their cost, net CO_2 abatement, and technical feasibility, which in turn affects the early-stage indications of the optimal decarbonization solution.

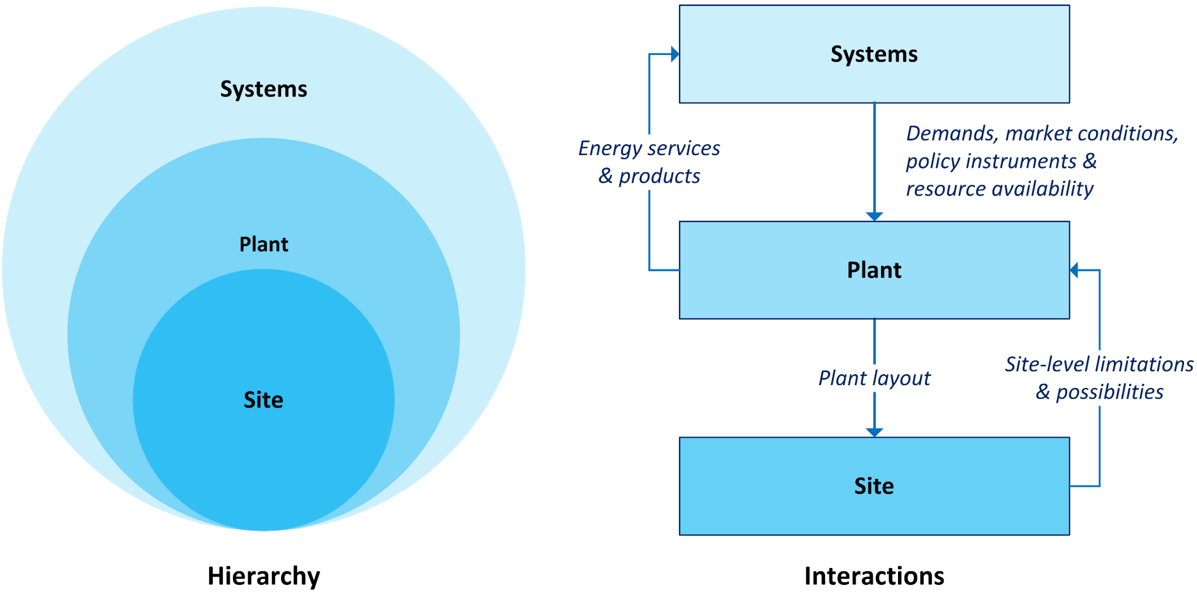

Figure 2-3: Hierarchy and interaction of the system boundaries for the evaluation of decarbonized industrial systems

Figure 2-2 illustrates the hierarchy and interactions among the various system boundaries of a typical unabated process plant. This framework helps explain how decarbonization measures will affect not only the plant but also its interactions with surrounding energy systems through changes in material and energy flows. For example, single-product industries, such as cement and steel, when equipped with CCS, would evolve into multi-product sites, generating concentrated streams of CO_2 alongside existing co-products such as excess heat and electricity. As a result, decarbonized industries would interact more closely with their local energy system compared to unabated ones. Moreover, given that different decarbonization technologies have distinct energy and material requirements, their interactions with the local energy system would also vary significantly.

Several recent studies across different industrial sectors have highlighted the importance of expanding system boundaries in comparative assessments. For example, while CCS is often perceived as too expensive by plant owners, these studies show that when system boundaries are expanded to include the entire value chain, the resulting cost increase in the final product or service is insignificant (1–2%) [26–29]. They also show that, when accounting for value-chain emissions, a considerable reduction (>50%) can still be achieved, albeit lower than what is reported at the plant level (~90%).

Such expansion of system boundaries is particularly important for emissions accounting in carbon removal technologies to accurately estimate the net CO_2 removal achieved [30]. Moreover, expanding system boundaries in the early design phase is crucial to capture the complexity of interconnected processes as well as the cascading effects of integrating new processes at existing sites [31].

In addition to these aspects, inconsistencies between stakeholders, such as the plant owner and the end-user of energy services and products, may arise regarding which technology is considered optimal. For example, plant owners are likely to initiate investments in decarbonization technologies. Plant-level evaluation is, therefore, justifiable as the economic viability of these investments hinges on maximizing profits (or minimizing costs) through profitable transactions involving all possible main products and co-products. Consequently, from the plant owner's perspective, the choice of technology is intricately tied to economic considerations.

In contrast, the end-users are likely to prefer a technology that maximizes overall CO_2 avoidance while incurring minimal cost increases in the final product. This divergence in perspective is expected to be aggravated in industrial energy systems, where incumbent market or policy conditions favor the installation of a sub-optimal CCS technology at a specific site, which may maximize profit for the plant owner but, consequently, increase the end-users' cost of consumption.

Therefore, careful selection of optimal decarbonization technologies must account for changes in energy and material flows, systematically differentiate between technology options, and distinguish between the perspectives of plant owners and the wider system, especially at an early stage of evaluation. These aspects were addressed in **Paper I**, where a framework was developed to demonstrate how system boundary choices and the figure of merit influence the indication of the optimal solution.

2.2.2 Targeting minimal exergy losses toward net-zero CO_2 emissions plant configurations

Process integration methods such as pinch analysis are widely used in early-stage TEA studies with conceptual process designs to quantify minimum heating and cooling demands as well as the theoretical potential for maximum process heat recovery. Traditionally, these methods have been applied to identify energy-saving measures in the process industries to minimize overall thermal energy losses in existing processes, thereby reducing primary energy use and operational costs. Energy savings of up to 20–40% in the process industry have been achieved in the past using pinch analysis tools [28,29].

More recently, these methods have been extensively used to evaluate the impact of integrating new decarbonization technologies into existing industries and conceptual process designs, such as integrated oil refinery concepts [18,30–32], biomass-based processes for the production of synthetic natural gas [33,34], platform chemicals [34–36], pulp mills [37], and steelmaking [38]. In these studies, pinch analysis was primarily applied to improve the overall energy efficiency of the integrated processes and thereby reduce their primary energy use, resulting in avoided CO_2 emissions. These examples reveal a shift in focus from minimizing operational costs to reducing overall CO_2 emissions, where the applications of pinch-based targeting methods have expanded from evaluating retrofit designs (i.e., adding new equipment to existing plants [9]) to evaluating grassroots designs of integrated processes.

However, one of the limitations of conventional pinch analysis is that it analyses only heat flows in industrial energy systems. This approach inherently neglects the evaluation of electricity-driven process equipment in these systems. Inefficient electrically driven processes are only identified when a value is ascribed to them in economic or exergy terms at a later stage of the assessment. Here, inefficient electrically driven processes refer to the use of electricity, a high-quality energy carrier, in process equipment that causes significant exergy destruction, resulting from either process heating at relatively lower temperatures or motor-driven units with poor mechanical efficiencies.

Consequently, pinch-based energy targeting methods are expected to be inadequate when designing decarbonized industrial systems with increased process electrification [32]. Process electrification has not been widely considered a decarbonization measure in the past due to the high cost and high carbon intensity of the power sector. Nonetheless, with the anticipated decline in grid carbon intensity, process electrification provides the possibility of both improving plant performance and reducing CO_2 emissions.

These limitations have been addressed, to some extent, through both variants of pinch-based methods and other process integration approaches. For example, Umeda et al. [33] introduced the so-called shaft work targeting method, which used a heat cascade diagram where heat flows were plotted against Carnot efficiency corrected temperatures to determine the maximum theoretical work that can be produced by a given system. This method was primarily adopted in studies evaluating the performance of low-temperature processes.

Another example is *process change analysis* [34], also known as background-foreground analysis, which relates the performance of a specific unit to the overall plant. Wiertzema et al. [32] developed a bottom-up framework using this method to evaluate electrification options in energy-intensive industries. Similarly, de Raad et al. [35] applied this method to identify heat extraction strategies to improve heat pump integration and performance. These methods remained restricted to heat recovery, limiting their ability to identify broader process modifications that minimize exergy losses. This points to a need for exergy-based targeting methods that depart from the traditional pinch-based methods of minimizing thermal energy consumption, and to methods that maximize exergy utilization through process modifications. These aspects were addressed in **Paper II**, where the CEP method is applied to systematically identify process modifications that minimize exergy losses while enhancing CO_2 avoidance.

2.2.3 Site-specific techno-economic analysis

Early-stage techno-economic assessments (TEA) serve as crucial inputs for various stakeholders, including governmental organizations, funding agencies, industry, and academia [36,37]. The term *early-stage* implies that these studies are conducted in the initial stages of a project[13]. Within industries, the results from these studies provide the basis for a more detailed evaluation of the selected technology. This involves increased engineering detail and project definition, which in turn enables more detailed cost estimates before securing project commitment through a final investment decision. However, given that these subsequent stages involve substantial investment of time and capital, early-stage TEA is particularly critical for guiding technology selection, often framed around the questions: what could it be?, what should it be?, and what will it be? [38]. In doing so, early-stage TEA aims to reduce uncertainty before such commitments are made.

---

[13] A project typically progresses through the following; scoping, pre-feasibility and feasibility studies, front-end engineering design (FEED), the final investment decision (FID), detailed engineering, construction, commissioning, start-up, and operation [38].

Table 2-1 presents a non-exhaustive list of early-stage TEA studies that have compared a wide range of decarbonization pathways in carbon-intensive industries, often using the method illustrated in Figure 2-2. Although comparing reported CO_2 avoidance cost estimates across studies is generally not recommended due to differences in cost basis, the estimates have been levelized to the year 2023 to enable general comparisons. Three observations can be drawn from this literature.

First, there is a wide variability in levelized CAC estimates across studies evaluating the same decarbonization technology within a given industry sector. The variability stems from differences in plant and site characteristics, data sources from different locations and time periods, and underlying economic assumptions, which together limit the comparability of other reported results across the same industry.

Second, most studies draw system boundaries at the plant level and therefore report CO_2 avoidance cost estimates without accounting for the additional costs along the full value chain, such as interim storage, transportation, and final geological storage. These downstream costs could add about 35–300 €/tCO_2 [39–44], depending on transport mode and specifications, as well as the location and distance to final storage. For more information on costs associated with carbon capture, transport, and storage (CCTS) supply chains, the reader is referred to the works of Becattini et al. [41,43] and Karlsson et al. [42].

Third, the CAC estimates in studies comparing multiple decarbonization pathways consistently fall within a narrow range, well within the accuracy range (-15% to +50%, Class 4 Estimate [45]) expected from the cost estimation methods applied in these studies. Consequently, these studies generally fall short of drawing concrete conclusions on the optimal decarbonization technology for the studied industry, indicating no standout winners in the compared set of decarbonization technologies.

This inconclusiveness leads to two possible implications. First, if the differences in CAC estimates across a wide range of available decarbonization technologies prove negligible, the process of selecting and deploying technology becomes less dependent on cost considerations. Consequently, ongoing research and development in emerging decarbonization technologies are only justified if potential cost reductions are proven to be substantial, assuming realistic market conditions, in comparison to the best available technologies. Second, if the comparative TEA studies reveal a clear differentiation, indicating the optimal decarbonization solution, the *technology-specific attributes* that might impede their direct integration or retrofit into these industries are seldom addressed.

For example, Table 2-1 shows that oxyfuel combustion incurs the lowest CAC for refineries, cement, and the petrochemical industry, suggesting it could be considered the most cost-effective decarbonization solution. However, as highlighted by Hills et al. [46] in the context of retrofitting a cement plant, factors such as the impact on product quality, shutdown periods during installation, operational complexity, and the process changes required in the host plant to minimize gas ingress and leakage, along with other retrofitability aspects, must be considered at an early stage of assessment. Taken together, these aspects raise questions about the efficacy and reliability of existing TEA methods in clearly identifying a cost-optimal decarbonization technology that can be selected for actual implementation at specific industrial sites.

Substantial efforts have been made in the past to standardize costing methods, which entailed harmonizing cost escalation factors and economic assumptions to ensure reliable and comparable results [36,47]. Here, the term *standardized* implies an established CCS costing methodology with common nomenclature and consistent cost escalation guidelines. Other contributions in this field of research include the development of frameworks for differentiating between emerging and mature technologies [48] and the application of uncertainty analysis methods to better understand the source of uncertainties in early-stage TEA studies [37].

While these studies addressed the specific limitations within the costing methods, numerous other studies, some of which are listed in Table 1, that applied these standardized methods have overlooked site-related constraints and opportunities in order to provide a fair comparison between different technological options. This approach inherently assumes that all plants within an industry sector have similar site conditions, while disregarding the fact that different decarbonization technologies have different resource and siting requirements. In reality, both site-specific characteristics and technology requirements can vary significantly across sites, even within the same industry. Therefore, the results of these comparisons may be misleading and could potentially lead to severe disparity between the early-stage indication of cost-optimal decarbonization technology for a specific industry and its actual (post-deployment) economic performance at a specific plant.

Roussanaly et al. [36] addressed these aspects with guidelines for estimating costs for CCS in the process industry, which inherently have varying site-specific conditions. They also presented different CO_2 interconnection configurations that may result from site layout constraints, such as limited space availability and multiple emission point sources within plant boundaries. Martorell et al. [49] compared detailed cost estimates from front-end engineering design studies for CO_2 capture via amine scrubbing for two natural gas combined-cycle power plants, and identified site-specific factors such as site layout, determining the extent of flue gas conveying equipment, resource availability (e.g., water), and steam supply alternatives as key contributors to capital cost escalation relative to early-stage standardized TEA estimates.

Stepchuk et al. [50] explored the integration of a bio-based isobutene process into an existing petrochemical cluster and found that it would require 90 times the land occupied by its fossil-based counterpart, effectively doubling the cluster's land footprint. Other recent studies have also highlighted the increasing demand for space at existing clusters to accommodate new infrastructure (renewable power, hydrogen, and CO_2 infrastructure), which competes with space requirements for the transition to sustainable feedstocks, which could range from 1.4–4 times the space that is currently occupied [51,52]. This underscores spatial limitations as a critical constraint in transforming existing clusters.

Therefore, transforming existing industries or industrial clusters necessitates a thorough evaluation of technology options tailored to the site-specific characteristics of each plant within an industrial sector, especially at an early stage of assessment. These aspects were addressed in **Paper III**, where a *site-specific TEA method* was developed, with generalized tools, to improve early-stage technology selection and thereby accelerate deployment of decarbonization technologies in these industries.

Table 2-1: Overview of early-stage techno-economic studies that have applied process modeling and integration methods with ex-ante techno-economic analysis with varied levels of detail to compare the overall economic viability of decarbonization via CO_2 capture pathways in different carbon-intensive industries.

Carbon-intensive industries	Refs.	CO_2 capture pathways	Estimated CO_2 Avoidance Costs (€/tCO_2)	Levelized CO_2 Avoidance Cost (€$_{2023}$/tCO_2)
Iron & Steel	[53]	Post-combustion (MEA)	64	92
		Post-combustion (advanced amines)	41	59
		Overall reported CAC range for a set of decarbonization pathways	30–75	43–107
	[54]	Post-combustion (MEA), CO_2 captured from hot stoves and CHP	86–116	109–147
	[55]	Post-combustion (MEA), CO_2 captured from hot stoves, coke ovens, lime kilns, and CHP	100–150	127–190
	[56]	Post-combustion (MEA) CO_2 captured from hot stoves, coke ovens, lime kilns, and sinter	56–72	71–91
Refineries	[53]	Post-combustion (MEA)	72–118	103–169
		Oxyfuel combustion	54–55	77–79
	[57]	Post-combustion (MEA), CO_2 captured from the hydrogen production unit stack	35–60	43–73
		Post-combustion (MEA), CO_2 captured from all stacks	59–101	72–123
	[58][a]	Post-combustion (MEA)	76–80 (69)	94–109
		Oxyfuel combustion with cryogenic air separation	59–62 (33–38)	45–84
		Oxyfuel combustion -membranes for air separation	52–57 (24–31)	33–77
		Pre-combustion	73–84 (87–90)	99–122
	[59]	Post-combustion (MEA), (T_{reb} = 90°C)	41–57	52–73
		Post-combustion (MEA), (T_{reb} = 120°C)	39–44	50–56
Cement	[60]	Post-combustion (MEA)	80	101
		Oxyfuel combustion	42	53
		Membrane-assisted CO_2 liquefaction	83	106
		Chilled ammonia process	66.2	84
		Calcium looping	52–59	66–75
	[61]	Post-combustion (MEA)	118	137
		Calcium looping	82	95
		CO_2 selective membrane	70	81
		Partial oxyfuel combustion	85	99
		Full oxyfuel combustion[b]	61	71
	[53]	Post-combustion (MEA)	66–131	94–187
		Post-combustion (advanced amines)	37–52	53–74
		Partial oxyfuel combustion	43	62
		Full oxyfuel combustion	44	63
Petrochemical	[53]	Post-combustion (MEA)	118	169
		Pre-combustion (H_2-fired furnaces)	81	116
		Oxyfuel combustion	50–60	72–86
	[62][c]	Post-combustion (MEA), standalone NG combined cycle	58–129	79–175
		Post-combustion (MEA), standalone NG boiler	35–47	48–64
		Post-combustion (MEA), standalone biomass boiler	41–59	56–80
		Post-combustion (MEA) use of current excess heat with industrial heat pumps	26–27	35–37

[a] Cost estimates in brackets indicate long-term CAC estimates. The lower bound and upper bound CAC estimates correspond to two different refineries, with annual CO_2 emissions of 4.1 Mt/y and 2.2 Mt/y, respectively.

[b] Full oxyfuel combustion includes the kiln and pre-calciner. Partial oxyfuel combustion is considered the pre-calciner alone.

[c] Energy supply options for an amine-based CO_2 capture technology were compared. The lower and upper bound estimates correspond to an assumed specific reboiler duty range of 2.8–4.7 MJ/kgCO_2.

2.2.4 Low-emissions hydrogen

Low-emissions hydrogen is essential for achieving deep reductions in CO_2 emissions in carbon-intensive industries and is particularly important for enabling circularity in sectors such as petrochemicals and transport fuels [63]. It can be produced via electrolysis using renewable electricity (green), nuclear power (pink), or low-carbon grid electricity, as well as through steam methane reforming with carbon capture and storage (blue hydrogen). Compared to fossil-derived (gray) hydrogen, these production routes result in hydrogen that has a substantially lower emissions intensity [64].

One of the main challenges for the large-scale deployment of low-emissions hydrogen is the so-called *chicken-and-egg* problem, where a coordinated scale-up of supply, demand, and supporting infrastructure is required [65]. However, in practice, this coordination is difficult to achieve due to a combination of cost-related and implementation prerequisites. First, there is a persistent cost gap between low-emissions and grey hydrogen, primarily due to higher production costs and the low cost of emitting CO_2 [15]. For example, although end-of-pipe CO_2 capture technologies are technically mature, their adoption in existing steam methane reformers (SMR-CCS) for blue hydrogen production remains limited. This can partly be explained by the fact that the *emit-and-pay* approach remains a viable alternative to producing low-emissions hydrogen in the foreseeable future, as even CO_2 allowance prices of 100–200 €/tCO_2 would only translate to a cost penalty of about 20–40 €/MWh (~0.7–1.3 €/kgH_2) for gray hydrogen.

On the other hand, green hydrogen faces additional deployment barriers, as reflected in the widening implementation gap in recent years [15]. This can be attributed to the rising costs of electrolyzers [15,66], limitations in their scalability [66], the failure to account for hydrogen storage and transport costs [67], and the focus on sub-optimal end-use sectors (e.g., domestic heating) where more competitive alternatives are available. In addition to these cost uncertainties, recent EU regulations require power purchase agreements (PPAs) for hydrogen to qualify as renewable, subject to specific conditions and exceptions [68]. This requirement influences hydrogen production costs and limits the possibility of optimizing costs through flexible operation. Such cost optimization is possible only when procuring electricity on the spot market, albeit with greater uncertainty in both electricity prices and their associated emissions intensity.

Second, the availability of critical infrastructure determines when hydrogen production technologies can be deployed. For example, blue hydrogen production cannot be implemented until CO_2 transport and storage infrastructures are available. Similarly, the rollout of green hydrogen depends on access to reliable, low-cost renewable electricity, as well as critical infrastructure such as hydrogen networks and grid transmission capacity. The timing of such a rollout is also crucial, as diverting renewable electricity to green hydrogen production before decarbonizing the power sector entails an opportunity cost [69].

Third, the risk of technology lock-in exists for both blue hydrogen and green hydrogen, although the degree of this risk depends on whether the hydrogen plant is tied to an isolated host plant or integrated with a plant located in a cluster with multiple alternative off-takers [15,70]. These deployment barriers indicate the need for a more comprehensive and practical evaluation of when, where, how, and which hydrogen production technologies can and should be deployed.

Several systems-level studies have analyzed the cost-optimal design and rollout of hydrogen infrastructure, considering a wide range of hydrogen production technologies. Kountouris et al. [71] investigated plausible deployment scenarios for hydrogen production centers and cross-border hydrogen networks in the EU, highlighting the value of co-locating hydrogen production and demand regions to reduce the need for long-distance hydrogen transport infrastructure. Ganter et al. [72] evaluated mature hydrogen technologies under varied spatial resolutions and highlighted the importance of higher spatial and temporal resolution in supply chain modeling to avoid underestimating system costs and to capture variability in renewable electricity supply. Terlouw et al. [73] evaluated the techno-economic and environmental performance of large-scale green hydrogen production via electrolysis, considering operational constraints with high temporal resolution. However, their broader spatial resolution focused mainly on resource availability, overlooking site-specific constraints. Together, these system-level studies provide valuable insights into the challenges of scaling up low-emissions hydrogen production. However, they typically rely on aggregated spatial and technological representations and adopt a greenfield approach, which inadvertently overlooks technology-specific and site-specific constraints, as well as infrastructure requirements critical to deployment at existing industrial sites. There is, therefore, a need for site-specific studies to improve the robustness of system-level analyses.

Many studies have also focused on individual hydrogen production technologies, particularly their techno-economic performances. While SMR-CCS has been widely studied, the focus has largely been limited to evaluating the CO_2 capture performance [74,75]. The literature on electrolytic hydrogen encompasses a broad scope, including assessments of the technical and economic factors that influence production costs [76,77], integration within conceptual process designs [78–80], and the impact of electrolyzer deployment on the electricity system [81]. In addition, hydrogen carriers, such as ammonia and liquid organic hydrogen carriers, have been explored, particularly for transporting hydrogen from regions with favorable conditions for production to regions with high hydrogen demand [82–85]. However, these evaluations have often been conducted in isolation, based on differing assumptions and system boundaries, which limit their comparability. Consequently, the question of technology selection for specific sites remains unresolved, as site-specific conditions may warrant a combination of technologies. Furthermore, in such cases, determining their optimal installed capacities and operational flexibility levels is crucial, given the technology-specific limitations, such as operating envelopes, start-up and shutdown behaviors, and ramping constraints.

A few studies have explored the complexity of integrating multiple process technologies into industrial clusters, while simultaneously optimizing their installed capacities and their flexible operation under varying market conditions [86–88]. Tiggeloven et al. [87] optimized emissions reductions in existing petrochemical clusters, considering multiple process technologies and incorporating key constraints such as electricity price fluctuations, grid transmission and storage capacities, and access to CO_2 transport infrastructure. However, as noted by the authors, such cluster-level optimization assumes cooperation and the absence of competing interests among the industries within the cluster, which may overestimate the integration potential and limit the relevance to real-world conditions.

Together, these gaps underscore the need for site-specific evaluation of hydrogen production technologies as integrated systems, rather than standalone systems, which account for site constraints, technology-specific limitations, and energy market uncertainties. These aspects are addressed in **Paper IV**, where a framework was developed to evaluate cost-optimal system configurations, operational strategies, and deployment strategies for integrated hydrogen production within petrochemical clusters.

3 Overview of the investigated processes and systems

---

*This chapter describes the key process technologies and industrial case studies considered in Papers **I–IV** and provides the rationale for their selection to demonstrate the methodological frameworks developed in this work.*

3.1 Process technologies

3.1.1 Post-combustion CO_2 capture technologies

Technologies that can be used for bulk CO_2 removal from flue gases include chemical absorption, physical absorption, adsorption with solid sorbents, membrane separation, and cryogenic separation [89,90]. Among these, chemical absorption-based technologies are the most widely adopted, particularly for natural gas sweetening and syngas cleaning in the oil and gas and ammonia industries, respectively [89,90]. For end-of-pipe CO_2 capture at existing industrial sites, the choice of method depends on the flue gas properties such as composition, level of impurities, temperature, and pressure.

Two inherently different chemical absorption-based CO_2 capture processes, namely an amine-based process using the then-benchmark[14] monoethanolamine (MEA) and a hot potassium carbonate (HPC) process, were compared in **Paper I**. The MEA-based process was also considered in **Papers II–III**. Figure 3-1 presents the process flowsheets of the CO_2 capture technologies, along with an ammonia-cycle-based CO_2 compression and liquefaction unit, representing the full CCS chain evaluated in this work. Both processes utilize aqueous capture solvents that are brought into contact with CO_2-containing flue gas in a trayed or structured-packed column (absorber). The CO_2 chemically binds to the solvent in the liquid phase, resulting in a CO_2-lean gas that is vented from the top of the absorber. The CO_2-rich aqueous solution is then sent to a desorber (or stripper), where the CO_2 is released and the capture solvent is regenerated. The regenerated solvent is then recirculated to the absorber.

The fundamental difference between the two processes is that the MEA-based process is temperature-swing driven, relying on a temperature difference between the absorber and desorber. CO_2 is typically absorbed at near-ambient temperature and pressure and desorbed at higher temperatures (110–120 °C) and moderately increased pressure (~1.2 bar) using low-pressure steam that is supplied to a reboiler. In contrast, the HPC process is pressure-swing driven, relying on a pressure difference between the absorber and desorber. The process entails compressing the flue gas prior to the absorber, which operates at higher temperatures and pressures, while the desorber operates at close to ambient pressure or the desired CO_2 delivery pressure. As desorption is primarily pressure-driven, the steam demand for solvent regeneration is lower in the HPC process than in the MEA process [91]. Additional operational and modeling differences between the two processes are listed in **Paper I**.

---

[14] 2-amino-2-methyl-1-propanol (AMP) with piperazine (PZ), known as the AMP/PZ solvent, is regarded as the new benchmark solvent [159].

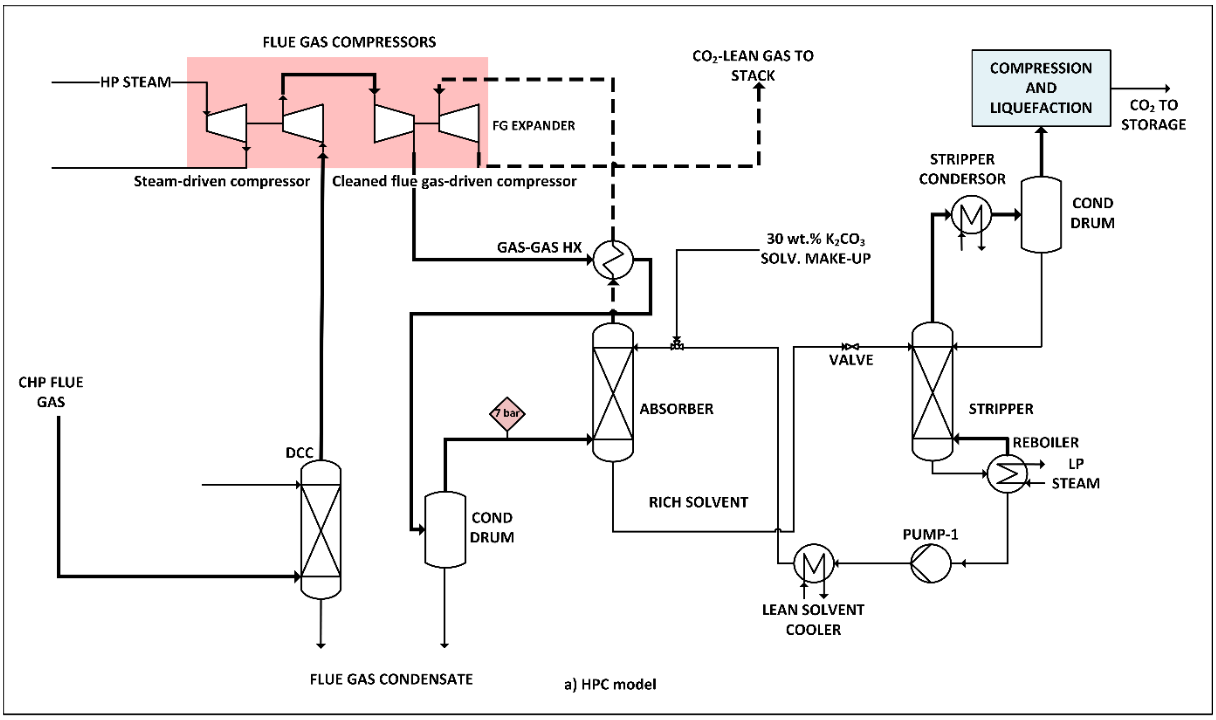

a) HPC model

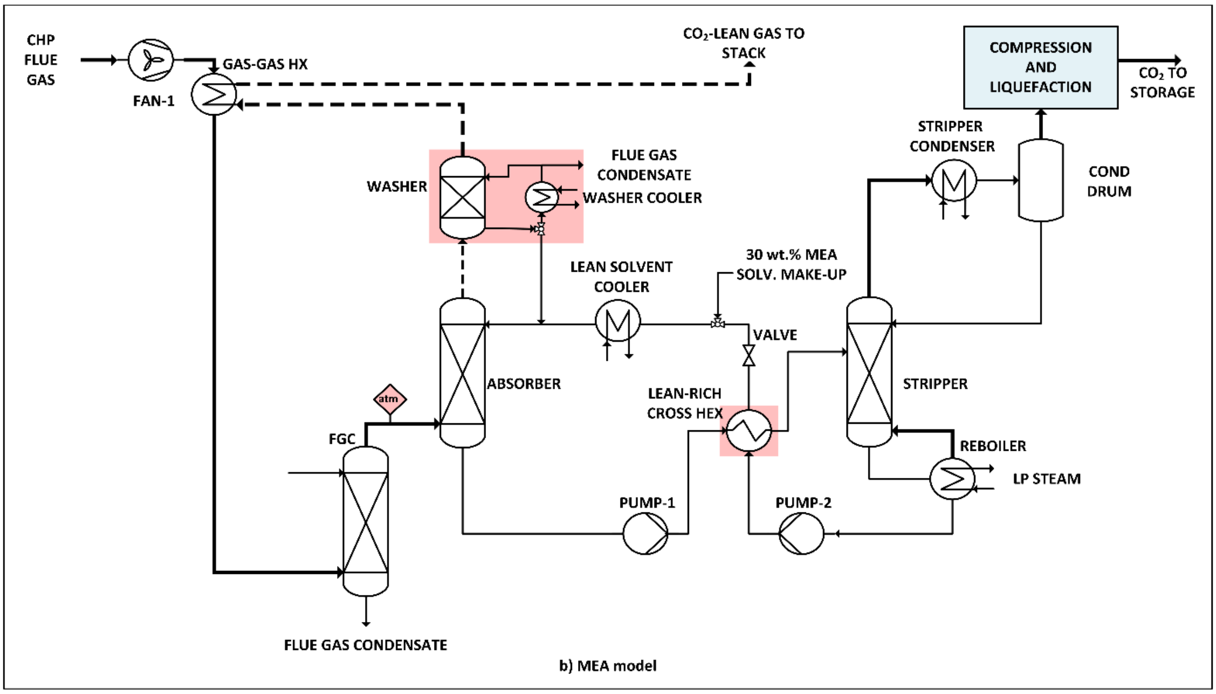

b) MEA model

Figure 3-1: Process flowsheet diagrams for a) the hot potassium carbonate (HPC) capture process; and b) the MEA capture process. The main differences between the two processes, i.e., the flue gas compression train in the HPC process and the cross-heat exchanger in the MEA process, are highlighted by red-shaded areas. The CO_2 compression and liquefaction processes are common to both carbon capture models and, therefore, are highlighted in blue. Dashed lines depict the CO_2-depleted flue gas streams. The thick and thin solid lines depict the gaseous and liquid (solvent and water) streams, respectively. (Abbreviations: Lean-Rich Cross HEX, heat exchanger for the CO_2-rich and lean solvents; cond drum, condensation drum; FGC, flue gas condenser; HP, high pressure; Solv., solvent).

3.1.2 Hydrogen production technologies

3.1.2.1 Methane reforming

Steam methane reforming (SMR) is one of the predominant methods for producing synthesis gas or hydrogen in industry. It involves converting a methane-rich hydrocarbon feedstock into synthesis gas in the presence of high-temperature steam and a nickel-based catalyst within tubular reactors. The synthesis gas is then conditioned in a water-gas shift (WGS) reactor to adjust the H_2/CO ratio or to maximize the hydrogen yield. The choice of reforming technology typically depends on the specific industrial application and operating conditions. The most widely used reforming technology is conventional SMR with fired tubular reactors, while other options include partial oxidation (POX), autothermal reforming (ATR), and the emerging electrically heated SMR (e-SMR).

In **Papers III and IV**, the ATR technology was considered for the case study of a steam cracker plant. This choice was based on three main advantages of ATR over conventional SMRs. First, it avoids external heating by using oxygen to carry out partial oxidation of the feedstock, which provides the heat required for the reforming reaction, resulting in higher energy efficiency [92,93]. Second, the partial oxidation within the same reactor also yields a synthesis gas with relatively higher CO_2 concentrations, enabling the separation and purification of hydrogen, as well as CO_2 capture, in a single step using pressure swing adsorption (PSA) units. Finally, this technology can achieve higher net CO_2 capture rates (~99%) [92,93], which is one of the key factors determining its cost-competitiveness compared to green hydrogen [94,95].

In the context of the steam cracker plant, an additional advantage of a co-located ATR is that, unlike blue hydrogen plants that rely on an external natural gas feedstock, it uses methane recovered from the fuel gas. Repurposing cracker fuel as feedstock for the reformers does not incur additional operating costs to the plant's operations, eliminating a major component of the blue hydrogen production costs and supporting its inclusion in the integrated hydrogen production system (see Section 3.2.4). A similar outcome to that of ATR, albeit with potentially improved performance, could be achieved with emerging technologies such as e-SMR. However, this technology was not considered in this work due to its lower technology readiness level and limited available cost data.

Figure 3-2 shows a simplified schematic of the pre-combustion pathway[15] integrated into the steam cracker plant, employing the ATR technology with PSA units for hydrogen separation from both the cracker fuel gas (H_2/CH_4) and the synthesis gas (H_2/CO_2). The fuel gas[16], typically composed of methane and hydrogen, is first compressed and sent to PSA units for hydrogen separation. The methane-rich tail gas, obtained as retentate, is then recompressed to pressures suitable for the ATR. A portion of the tail gas is combusted with pure oxygen to provide the heat required for the reforming reaction. The resulting synthesis gas passes through two-stage WGS reactors to convert CO into CO_2 and produce additional hydrogen. This hydrogen-rich syngas is then directed to another stage of hydrogen separation and purification for further hydrogen recovery. High-purity hydrogen from both PSAs is combined and sent to the steam cracker furnaces. The tail gas from this unit, referred to as depleted syngas containing mainly CO_2, CO, CH_4, and residual H_2, could either be directed to a utilization plant to recover the carbon with renewable hydrogen or conditioned to meet sea or pipeline transport specifications.

---

[15] This pathway is referred to as *Pre-CCS* in **Paper III** and as *ATR-CCS* in **Paper IV**.

[16] Approximately 50% methane and 50% hydrogen (by volume).

In both **Paper I** and **Paper III**, ship transport was assumed. Therefore, the depleted syngas was assumed to be combusted with oxygen in a catalytic incinerator to obtain a CO_2-rich flue gas, which could be cooled, dehydrated, and sent to a compression and liquefaction unit to produce liquefied CO_2 suitable for ship transport. A limitation of these technologies is that their deployment depends on the availability of CO_2 transport and storage infrastructure. In addition, significant capital cost reductions are achievable only through economies of scale [96]. They are also typically designed for continuous operation, resulting in a limited operational range and slow ramping capabilities [87]. These limitations could be mitigated by including electrolyzers in the integrated hydrogen production system.

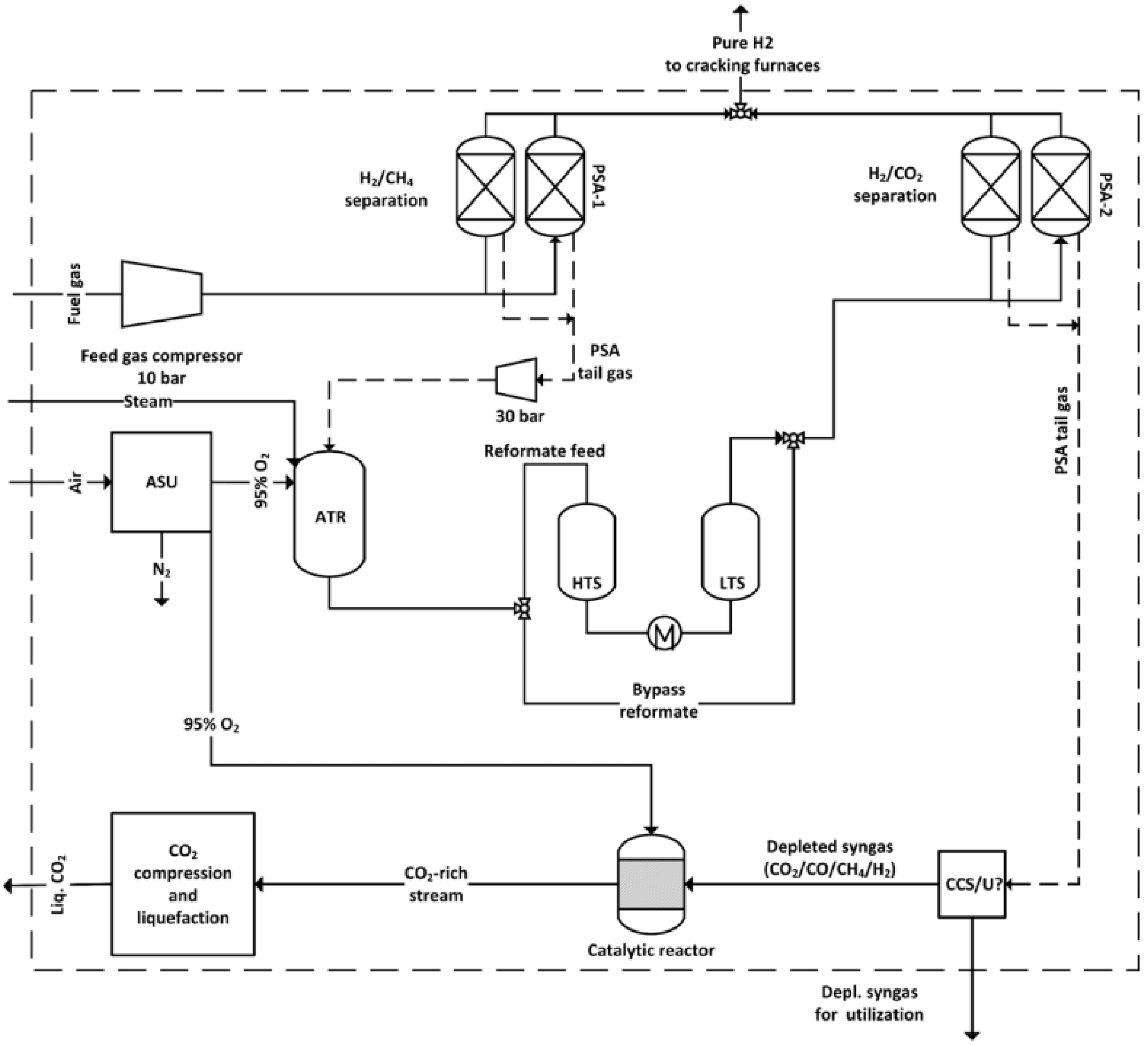

Figure 3-2: Process flowsheet of the pre-combustion process (Pre-CCS). Abbreviations: PSA, pressure swing adsorption unit; ASU, air separation unit; ATR, autothermal reformer; HTS, high-temperature shift reactors; LTS, low-temperature shift reactors.

3.1.2.2 Solid-oxide electrolyzers

Electrolyzer technologies, which include proton exchange membranes (PEMs), alkaline electrolyzers, and high-temperature technologies, such as solid-oxide electrolyzer cells (SOECs), can operate in a flexible manner, producing hydrogen when electricity prices are low and idling when they are high. In **Paper IV**, SOECs were the preferred electrolyzer type due to their high overall system efficiency[17] (~75%, LHV basis), given that they operate at the thermo-neutral voltage at high temperatures, enabling more efficient use of electricity. Unlike low-temperature water electrolyzers, SOECs can use steam directly as input, avoiding the need to supply the evaporation heat with electricity. Instead, about one-third of the required steam is generated through internal heat recuperation, while the remainder can be sourced from the host plant (e.g., steam cracker plant), or the surrounding cluster, or recovered from newly installed technologies such as the ATR, ammonia crackers, or other waste-heat-producing units. A detailed process flowsheet of an SOEC system integrated into the steam system of the steam cracker plant can be found in the Supplementary Materials of **Paper IV**.

Surplus steam available at the plant and from the surrounding cluster is used to evaporate demineralized water, which is supplied at a pressure of 5 barg. The resulting steam is heated to the stack operating temperature of 750°C through the internal heat exchanger network, before being supplied to the cathode side of the SOEC stacks. Within each SOEC cell, steam is split into hydrogen and oxide ions. The oxide ions move through the oxygen-conducting electrolyte to the anode, where they are oxidized into oxygen molecules. The anode side is typically fed with air (sweep gas), which results in dilution of the outgoing stream from the anode, where the oxygen concentrations could be anywhere between 30 and 50% [97]. Hydrogen from the cathode side is typically cooled, dehydrated, and compressed to the required specification for the downstream end-use. In **Paper IV**, it was assumed that the fuel gas used in the cracker furnaces was replaced with hydrogen from SOEC, with the same specifications as reported in [98]. A key limitation linked to deploying electrolyzer technologies is the availability of sufficient grid transmission capacity and low-cost renewable electricity. Therefore, the proposed integrated hydrogen production system in **Paper IV** included the ammonia cracker technology.

3.1.2.3 Ammonia Cracking

Ammonia cracking offers an alternative pathway to supply low-emissions hydrogen to the steam cracker plant (see Section 3.2.4) using ammonia imported from regions that have an abundance of renewable energy. This technology could help bridge the supply-demand gap for low-emissions hydrogen in areas with limited grid transmission capacity or limited availability of cheap renewable electricity. It offers the following additional advantages: i) importing ammonia ensures security of supply and cost certainty through long-term contracts; ii) ammonia cracking can be performed either on-site or on floating barges [99], making it geographically flexible and also a practical alternative at space-constrained sites; iii) using cracked gas (mainly 75% H_2 and 25% N_2 by volume) as the primary fuel in the ammonia crackers decouples blue hydrogen production from the need for CO_2 transport and storage infrastructures.

---

[17] Accounting for both electricity and steam demand [97,98].

Nevertheless, it is important to note that using ammonia as a hydrogen carrier is fundamentally inefficient, with a round-trip efficiency of below 20%, accounting for synthesis, transport, cracking, and subsequent end-use [39]. Therefore, its primary role in the integrated system in **Paper IV** was to complement other hydrogen production technologies by enhancing overall system flexibility and redundancy, particularly when site-specific constraints limited their deployment.

Figure 3-3 shows a simplified schematic of the ammonia cracking process. A more detailed process flow diagram of the ammonia cracking system, integrated with a steam cracker plant, can be found in [97]. The ammonia cracker consists of fired-catalytic tubular reactors, similar to commercially available steam-methane reforming reactors. Anhydrous liquid ammonia is evaporated, compressed, and preheated to around 500°C before entering the reactor. The ammonia decomposes to nitrogen and hydrogen under high pressure (20–50 barg) and at temperatures close to 800°C. The cracked product gas, which consists mainly of hydrogen, nitrogen, and unconverted ammonia, is subsequently used for preheating both the combustion air and ammonia feed.

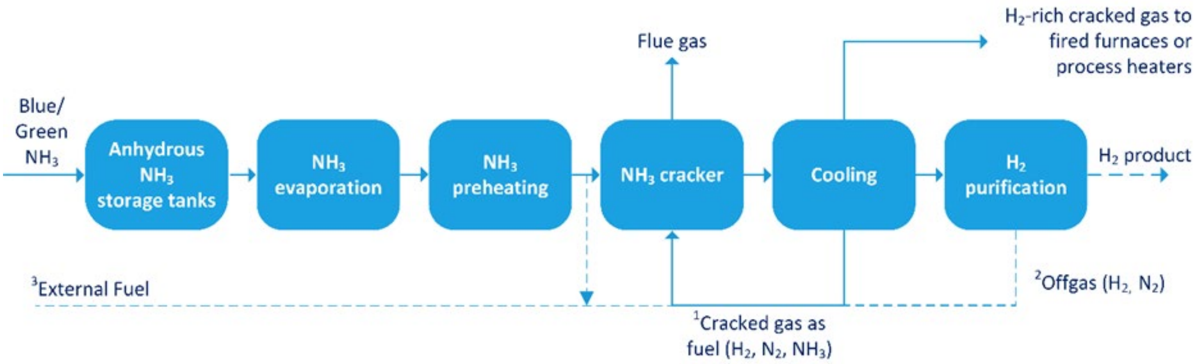

Figure 3-3: Process schematic of the ammonia cracking process. Source: [97]

The endothermic ammonia decomposition reaction can be driven by combustion of an externally provided fuel or by recycling a part of the cracked product as fuel, ensuring zero direct CO_2 emissions from the cracking process. The remaining cracked product gas is typically directed to separation and purification units (PSAs) downstream, for the production of high-purity hydrogen. The off-gases from these units are recycled as cracker fuel. Alternatively, the cracked product gas can be used directly as fuel in fired furnaces and process heaters. In such cases, the ammonia cracker offers fuel flexibility to the host plant, allowing the use of ammonia and hydrogen-blended fuels. Moreover, in the absence of separation and purification units, the operating pressure of the ammonia cracker can be adapted to reflect the required compositions and delivery pressures. More information on the ammonia cracking technology can be found elsewhere [100–103].

3.2 Industrial case studies

3.2.1 Combined heat and power plants

Context: Combined heat and power (CHP) plants comprise industrial CHP, biomass-fired CHP (bio-CHP), and waste-fired CHP plants. Among these, existing pulp and paper mills, bio-CHP plants, and, to some extent, waste-fired CHP plants, represent some of the largest point-source emissions of biogenic CO_2 in Sweden. These facilities could be converted into large-scale sites for CO_2 removal through the integration of end-of-pipe CO_2 capture technologies. In Sweden, the total biogenic capture potential is estimated to be around 30 $MtCO_2/y$[18], which represents more than 80% of Sweden's total fossil CO_2 emissions in 2023[19] [104]. BECCS represents a relatively low-cost pathway for achieving large-scale CO_2 removal[20], especially compared to other technology-based alternatives such as direct air capture. However, an important caveat is that BECCS systems must account for all GHG emissions throughout their lifecycle (cradle-to-grave) to accurately quantify the net CO_2 removal [30].

Rationale for case study selection: A bio-CHP plant was chosen as the case study in **Paper I** for three key reasons. First, most bio-CHP plants in Sweden operate within a district heating system and are typically the main providers of district heat in the region. Retrofitting CO_2 capture and conditioning units to these plants incurs a significant energy penalty, the magnitude and nature of which depend on the selected CO_2 capture technology. This energy penalty could be managed upstream by burning more fuel (in this case, biomass) or by reducing the energy service outputs (electricity and district heat) of the plant [105]. While the former option is undesirable from a sustainability perspective, the latter is more likely in practice. Therefore, the impact of the selected CO_2 capture technology on plant performance becomes a crucial consideration in technology selection.

Second, CHP plants operate in a closed DH market and are, therefore, regarded as local natural monopolies [106]. As a result, CHP plants prioritize district heat over electricity power production, as the generated electricity is traded in the power market and is subject to both competition and price volatility [107]. Furthermore, there are a few limitations (apart from operational limitations) on the CHP plant's electric power production levels, which are dependent upon the seasonal heating and cooling demands [108]. This operational profile makes bio-CHP plants particularly sensitive to the energy penalties associated with CO_2 capture, and underscores the need to evaluate various technology options in the contexts of plant-level and system-level performances.

Third, the selection was motivated by ongoing developments in BECCS in Sweden at the time of writing **Paper I**. Stockholm Exergi´s CHP8 plant, one of the world's largest bio-CHP plants, with a production capacity of 280 MW of district heat and 130 MW of electricity, supplies more than 80% of the DH demand in Stockholm [109]. This plant has been awarded funding by the EU Innovation Fund for the demonstration and full-scale implementation of BECCS using the HPC technology, with a planned capture capacity of approximately 800 kt of biogenic CO_2 per year [21].

---

[18] Assuming 90% capture rate. The total biogenic emissions were reported to be around 33 Mt/y [104].

[19] 36.56 $MtCO_2$ in the year 2023 [104].

[20] Capture costs from these plants are expected to vary substantially due to differences in flue gas composition, operational hours, location and other site-specific conditions. For example, a majority of the kraft pulp mills in Sweden could achieve capture costs below 70 €/tCO_2. However, these plants are geographically dispersed, with most located along the Swedish costs. Karlsson et al. [160] estimates the total cost of the BECCS chain could ranging between 150–300 €/tCO_2.

Since then, this bio-CHP plant has secured offtake agreements for carbon removal, as well as contracts for the maritime transport and final storage of the captured CO_2. A final investment decision was taken in March 2025, with the CO_2 capture plant slated to begin operations in 2028 [21]. Therefore, CHP8 was used to exemplify the framework developed in **Paper I** (Section 5.1).

Process description: Figure 3-4 presents a schematic of the main steam cycle components. The boiler generates live steam at a pressure of 136 bar and a temperature of 558 °C. The live steam is expanded in a steam turbine in six stages, with steam being extracted into feedwater preheaters, a deaerator, and two DH condensers. Steam is also extracted to meet specified extraction pressures and DH target temperatures. In the CHP-HPC plant, live steam is extracted to drive the flue gas compressor and to supply heat to the capture process (depicted with black dashed lines in Figure 3-4). In the CHP-MEA plant, low-pressure steam for powering the capture process is extracted from the turbine at the deaerator stage. The steam condensate from the capture process returns to the deaerator in both cases. The energy requirements of the capture process, including the reboiler duty and compressor power demand, are met using the internal steam and electricity supplies.

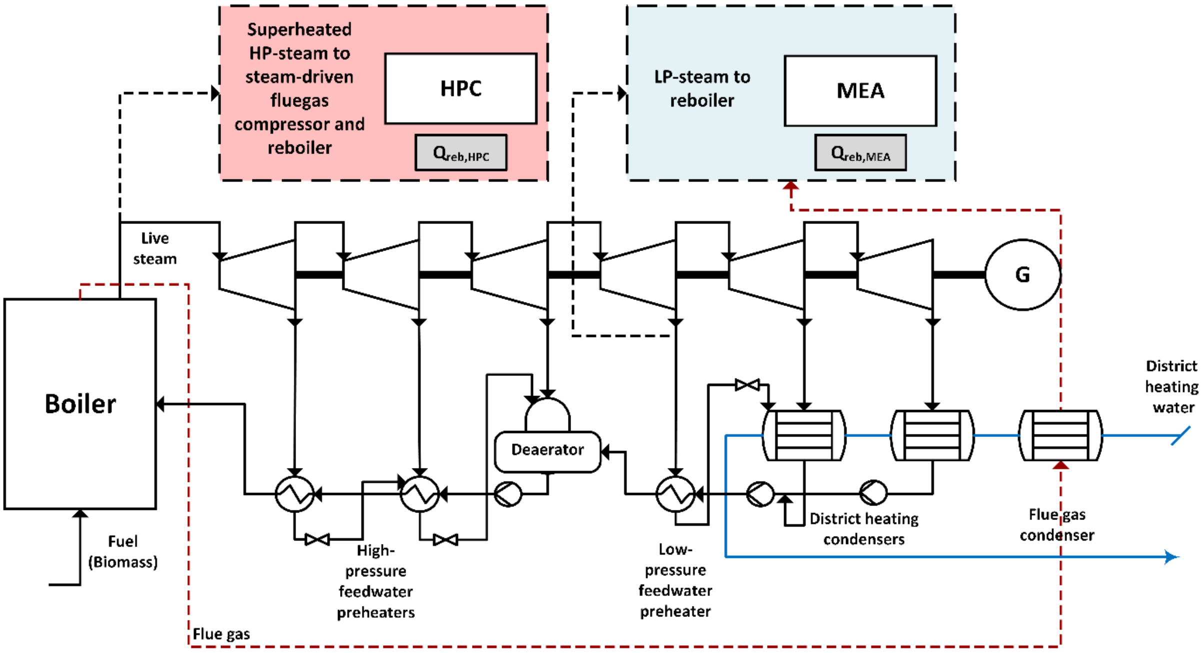

Figure 3-4: Process schematic of the CHP steam cycle modeled for the reference plant, adapted from Beiron et al. [3]. Note that only one of the two CCS units is considered when evaluating the CHP-MEA case or CHP-HPC case. Note also that the flue gas condenser (shown in Fig. 2) is now placed outside the CCS unit blocks, so as to represent more accurately the CHP steam cycle. Black dashed lines – steam extracted from the steam cycle to drive the corresponding CCS unit; Red dashed lines – flue gases from the boiler; Gray boxes – input data to the CHP steam cycle model. Source: Paper I

3.2.2 Propane dehydrogenation plant

Context: Propylene, which is a key chemical building block, has traditionally been produced as a co-product from steam cracking and fluid catalytic cracking (FCC) processes. However, over the past decade, a growing demand for polypropylene, combined with a shift in feedstock away from heavier hydrocarbons (e.g., naphtha) to lighter hydrocarbons (e.g., ethane), has reduced the supply from these traditional sources and created a so-called *propylene gap*. This shift in feedstocks was initially driven by the shale gas boom in the United States, and later driven by measures designed to improve energy efficiency and reduce emissions at existing steam cracker plants [110,111]. As a consequence, on-purpose propylene production technologies, such as propane dehydrogenation (PDH), have filled this gap and now account for approximately 22% of current global propylene production, a share that is expected to grow to 32% by 2027 [111].

Rationale for case study selection: A PDH plant using a state-of-the-art PDH process technology [112] (Figure 3-5) was selected as the industrial case study to demonstrate the framework developed in **Paper II** (Section 5.2). This selection was motivated by three key challenges. First, retrofitting end-of-pipe CO_2 capture is expected to be highly cost-intensive, due to the substantial volumes of flue gases to be handled that have extremely low concentrations of CO_2 (<3 vol.% CO_2, wet basis). Second, process-related constraints were found to limit the applicability of alternative decarbonization methods, such as oxyfuel combustion or hydrogen firing[21]. Third, this technology accounts for approximately 16 % of the global propylene production capacity (150 Mt/a) as of 2023 [113], and has been selected for implementation in more than 40 announced or planned projects since 2017, which represents an additional 24 Mt/a of capacity under development [114,115], corresponding to 23 Mt/y of CO_2 emissions in highly diluted flue gases[22]. Due to the complexity of this process technology and the lack of viable alternative decarbonization options, this plant served as an ideal case study in **Paper II** to demonstrate the developed framework and its effectiveness in identifying cost-effective decarbonization solutions.

Process description: This technology uses five to eight reactors in parallel to allow continuous operation that cycles between four reactor modes: dehydrogenation, steam purge, regeneration, and reduction. For a five-reactor setup, at any given time, two reactors are in dehydrogenation mode (on stream), two are in regeneration mode (on reheat), and one reactor is in an intermediate mode (either reduction[23] or steam purge[24]). Prior to the dehydrogenation step, a fresh propane feed is preheated in crossflow heat exchangers with reactor effluent from the onstream reactors, followed by a final heating to a temperature conducive to the dehydrogenation reaction (590°C) in the radiation section of the charge heater. For this, heavier liquid hydrocarbons (C_{4+}) and H_2-rich fuel gases recovered in the product recovery section are combusted in the charge heater, contributing roughly 26% of the total on-site CO_2 emissions (~256 $ktCO_2/a$). The remaining 74% (~188.8 $ktCO_2/a$) of the total on-site CO_2 emissions originate from the air-regeneration train(highlighted by the gray-dashed box in Figure 3-5).

---

[21] See Supplementary Material in **Paper II**.

[22] Overall, this process emits roughly 0.85 tCO_2 per tonne of propylene produced [161]

[23] In the reduction phase, recovered hydrocarbon off-gases are used to eliminate any remaining oxygen in the reactor after the regeneration mode, as well as to reduce the catalyst to its active form.

[24] Steam is used to eliminate any hydrocarbons remaining in the reactors after the dehydrogenation mode, before introducing hot air during the regeneration mode.

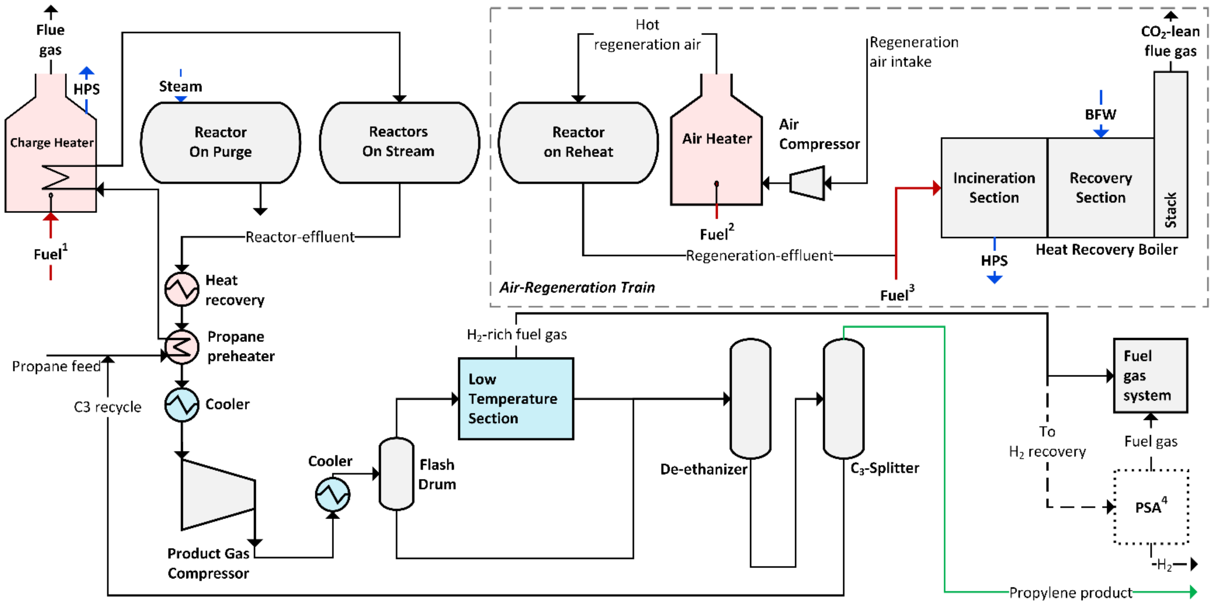

Figure 3-5: Simplified process flowsheet diagram of the propane dehydrogenation plant. The grey-dashed box indicates the system boundary of the air-regeneration train. Fuel inputs: ^{1} C_{4+}-liquid hydrocarbons and H_2-rich fuel gas. ^{2} H_2-rich fuel gas and natural gas at the main and pilot burners, respectively. ^{3} Volatile organic compounds in the reactor effluent are incinerated with natural gas supplied through the main burners. ^{4} Optional pressure-swing adsorption unit for hydrogen recovery; currently not in place at the reference plant. Source: Paper II.

The air-regeneration section in the PDH plant includes four major process units: the air compressor, air heater, reactors (on reheat), and the heat recovery boiler (HRB). In the regeneration mode, compressed air is fed to the air heater, where H_2-rich fuel gas is combusted to generate combustion products, at 565–650°C and 1.7 bar. The hot combustion products are then introduced into the regenerating reactors (on reheat), where the primary objective is to combust coke deposits to regenerate and reheat uniformly the catalyst bed to the desired reactor temperature before the dehydrogenation step.

Next, the regeneration effluent stream that is exiting the regenerating reactors is directed to the HRB, wherein additional firing in the incineration section reduces the CO and volatile organic compounds emissions and provides additional heat for steam production. Thus, the primary sources of CO_2 in the air-regeneration train are: (i) combustion of H_2-rich fuel gas, consisting predominantly of CH_4 and other hydrocarbons, in the air heater; (ii) coke combustion in the regenerating reactors, and (iii) additional firing in the heat recovery boiler. In addition, injection gases (de-ethanizer off-gases) are occasionally added during regeneration to create an exothermic reaction and provide additional heat to the catalyst bed. Therefore, the dilution of CO_2 in the flue gas stream at the HRB stack results from both the combustion of H_2-rich off-gases in the air heater and the large volumes of gases required during the regeneration step.

3.2.3 Steam cracker plant

Context: The steam cracker plants, which are typically located in proximity to oil refineries, use light hydrocarbons such as ethane, propane, and naphtha as feedstocks. The steam cracking process primarily produces olefins (e.g., ethylene and propylene) along with fuel-grade by-products (methane and hydrogen), which are used internally as fuel and exported to downstream chemical industries. Globally, steam cracker plants emit more than 300 $MtCO_2$/yr [116], while in the EU, these plants emit around 30 $MtCO_2$ annually [117]. These plants are among the most challenging to decarbonize due to their heavy reliance on fossil feedstocks and the end-of-life emissions of their products (plastics). These challenges are multifaceted.

First, transforming such sites to produce carbon-based materials in a sustainable manner is expected to require both substitute process technologies that enable decoupling from fossil feedstocks and retrofit technologies that abate CO_2 emissions. Substitute process technologies utilize alternative carbon sources such as biomass, CO_2, and plastic waste to produce olefins [50,118]. Retrofit measures include direct electrification of existing cracker furnaces, which in turn would eliminate combustion-related emissions on site, as well as CO_2 capture technologies that enable either permanent storage or subsequent utilization for the production of CO_2-based products (CCU). Consequently, a combination of measures and technologies may be required at a single site, increasing the complexity of the technology selection.

Second, these plants are often situated within large petrochemical clusters with complex material and energy flows to downstream chemical industries. In these settings, careful selection of technologies is critical, given the cascading effects on the interconnected processes within the cluster [31,118].

Third, these plants often have spatial constraints that limit the possibility of retrofitting new process technologies, especially those with large spatial footprints [50,51]. In such cases, the plants may be forced to either deploy a costlier alternative that can be accommodated at the existing site, or reduce production capacity to accommodate the selected technology, or proceed with plant closures.

Fourth, major revamps (turnarounds) in these plants typically occur on a 4–6 year cycle, entailing 3–4 weeks for performing maintenance, overhaul, and inspection, and the replacement of process equipment [119]. These periods also provide a window of opportunity to install and integrate new process technologies. Considering this, these plants have a finite number of opportunities to install decarbonization technologies before the target year set for achieving net-zero emissions.

Fifth, most steam cracker plants in the EU have limited residual lifetimes, which increases the risk of stranded assets from a mismatch between the host plant's residual lifetime and the newly installed technologies' economic lifetime, potentially leading to premature decommissioning. At the same time, these plants face growing competition due to overcapacity outside the EU [120,121], making even unabated operations increasingly unprofitable in recent years. Thus, the selection of appropriate decarbonization technologies becomes increasingly crucial, although this decision may have to contend with the possibility of full plant closure.

Rationale for case study selection: A steam cracker plant located on the west coast of Sweden was selected as the industrial case study to demonstrate the framework developed in **Paper III**. This plant operates within a large petrochemical cluster, is subject to spatial constraints, and has three remaining turnarounds before 2045. These conditions reflect the aforementioned challenges facing steam cracker plants in the EU, which makes this plant ideal for developing generalized methods and tools for early-stage assessment of the impacts of quantitative and qualitative site-specific factors on the cost of retrofitting different decarbonization technologies. Building on **Paper III**, this plant was also used as the case study in **Paper IV**, as discussed in Section 3.2.4.

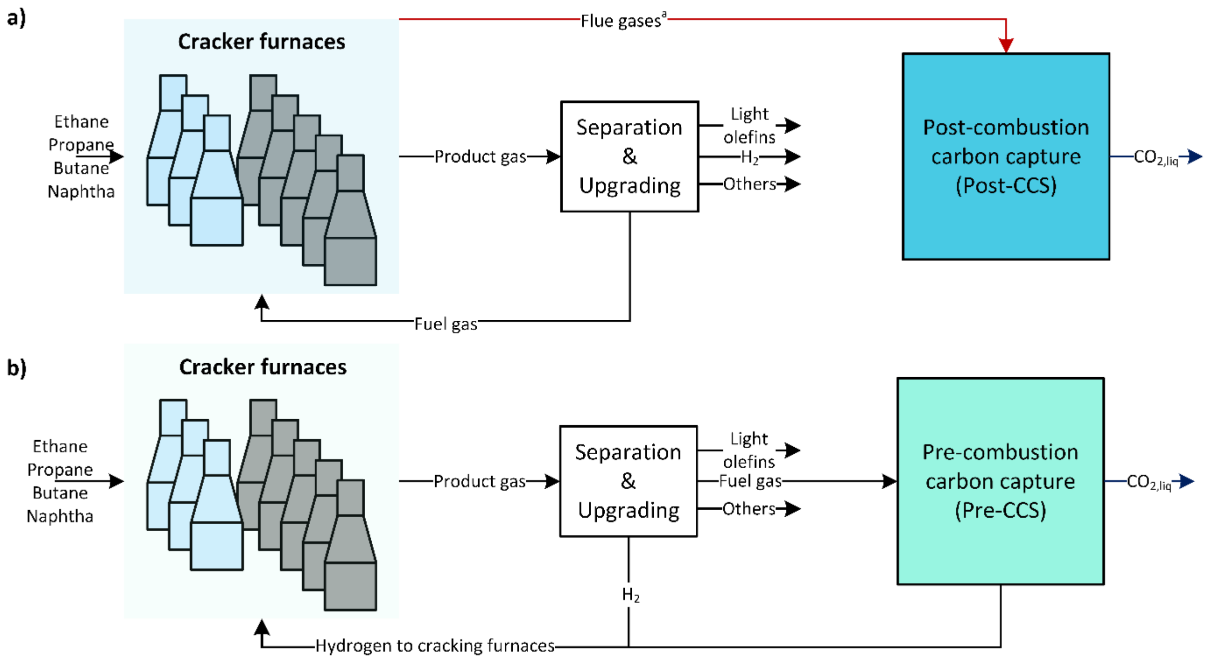

Figure 3-6: Overview of the main material flows in a steam cracker plant with (a) post-combustion (Post-CCS) and (b) pre-combustion (Pre-CCS) decarbonization pathways. ^{a} Flue gases include total plant CO_2 emissions. In Pre-CCS, CO_2 emissions from furnaces are entirely avoided, although the CO_2 emissions from NG-fired steam boilers remain (not shown in the Figure). Note that the output streams for both pathways are liquefied CO_2 at the liquid CO_2 transport specification reported in the Northern Lights project (-26.5°C, 15 barg [122,123]**). Source: Paper III.**

Process description: The plant consists of eight cracking furnaces that crack ethane and other mixed hydrocarbon feedstocks, corresponding to annual production capacities of up to 640 kt of ethylene and 200 kt of propylene [124]. It emits approximately 650 ktCO_2 annually, of which the cracker furnaces contribute 80%–85%, with the remaining emissions coming from three natural gas-fired steam boilers (12%–16%) and flaring (1%–3%) [124]. Figure 3-6 illustrates the main material flows in a steam cracker plant and the decarbonization pathways considered in Paper III. As shown in Figure 3-6a, the majority of the on-site CO_2 emissions originate from the combustion of fuel gases[25] in the cracker furnaces to provide energy for the endothermic cracking reaction. Two decarbonization pathways were compared in **Paper III**. The rationale for comparing these pathways and their implications for the steam cracker plant can be found in the Supplementary Materials in **Paper III**.

---

[25] Recovered from the cracker effluent (50 vol. % CH_4 and 50 vol.% H_2).

In the Post-CCS pathway (see Figure 3-6a), the CO_2 from the flue gases is captured using a benchmark amine-based solvent (MEA) in a CO_2 capture plant with an assumed capture rate of 90%, followed by compression and liquefaction to sea-transportation specifications [125]. In contrast, the Pre-CCS pathway entails valorizing the methane-rich fuel gas via steam-methane reforming to produce hydrogen, which is thereafter used as the primary cracker fuel, as shown in Figure 3-6b. The CO_2 generated from the steam-methane reforming reactions ends up in the tail gases (mainly containing CO_2, H_2, CH_4, and CO) from the hydrogen separation and purification units, which are oxidized with catalytic incinerators to obtain a pure gaseous CO_2 stream, prior to entry into the CO_2 liquefaction plant.

The scope of on-site decarbonization was limited to avoid CO_2 emissions from the cracker furnaces, with unchanged production capacities in both pathways. Therefore, at a CO_2 capture rate of 90% from the flue gas at the stack, the Post-CCS process captures roughly 585.5 kt/a, which is approximately 5% more CO_2 than the total cracker furnace emissions (552.9 kt/a). In contrast, the Pre-CCS process with hydrogen-firing in the cracker furnaces results in 100% avoidance of CO_2 emissions associated with the cracker furnaces. However, the CO_2 emissions associated with the steam boilers remain.

3.2.4 Integrated hydrogen production system within petrochemical clusters

Context: The global hydrogen demand is projected to reach 150 Mt/year by 2030, while the demand for hydrogen in the EU is expected to reach 45 Mt/year by 2050 [126]. The EU has set ambitious targets to produce 10 Mt/year of renewable hydrogen domestically and to import an additional 10 Mt/year by 2030 [127]. While no such targets are currently set for blue hydrogen, it is expected to play a crucial role in achieving the EU's decarbonization goals [127]. Despite the anticipated demand and urgency to reduce emissions, low-emissions hydrogen continues to face significant deployment barriers, as detailed in Section 2.3.4.

The deployment barriers and technology-specific limitations could be mitigated by combining inherently different hydrogen production technologies to enhance the overall system flexibility and redundancy, particularly when site-specific constraints limit their deployment. Such a system would reflect the general concept of a hydrogen hub, which is defined as a regional network consisting of hydrogen producers, connective infrastructure including storage, and cross-sectoral end-users [128]. However, since the scope of the proposed system in **Paper IV** was limited to the production technologies and their integration within a chemical cluster for a specific end-use sector, it is referred to as the *integrated hydrogen production system* or simply the *integrated system*.

Rationale for case study selection: The selection of the steam cracker plant as a case study was motivated by both the plant- and cluster-level benefits of hydrogen deployment within petrochemical clusters. Building on Paper III, hydrogen produced via the integrated hydrogen system was considered as cracker fuel, which also offered the following practical advantages: i) hydrogen firing is relatively straightforward at this plant, as existing burners can already handle hydrogen-rich blends and can, in some furnaces, use pure hydrogen; ii) unlike post-combustion CO_2 capture, the integrated hydrogen production system does not risk becoming a stranded asset at the end of the lifetime of the steam cracker plant. More importantly, it remains unaffected by potential changes at the host plant, such as alterations to the feedstock slate, and the installation of electrified crackers or advanced waste recycling technologies; and iii) methane recovered from steam cracker fuel gas could qualify as recycled carbon fuels[26] (RCF) under recent EU-delegated acts [28], as exporting this methane could directly displace natural gas imports and thereby reduce GHG emissions [29]. This would enable steam cracker plants to abate their Scope 1 emissions[27], while simultaneously reducing the EU's dependence on imported natural gas.

In contrast to hydrogen firing, direct electrification of cracker furnaces has been widely regarded as the preferred long-term solution due to its substantial CO_2 abatement potential and the anticipated availability of cheap renewable electricity. However, its demonstration at an industrial scale is still at an early stage, and commercial availability is not expected in the near term [12,67]. Moreover, retrofitting existing furnaces for direct electrification is expected to be relatively difficult, as compared to adapting burner systems for hydrogen firing. Finally, the availability of grid transmission capacity remains a key constraint for deploying electrified crackers at existing steam cracker plants. This makes hydrogen firing a more practical near-term solution for steam cracker plants.

Petrochemical clusters offer several advantages that make them ideal sites for large-scale hydrogen deployment. They provide access to multiple potential off-takers that have access to existing interconnections for transporting industrial gases, steam, and other material streams. Specifically, the geographic proximity of industries within the cluster, along with existing fuel gas networks that could be repurposed for hydrogen transport, reduces the need for new hydrogen distribution pipelines within the cluster. Furthermore, surplus steam from existing operations and newly installed processes can be used to lower the operating costs of high-temperature electrolyzers. These clusters typically have access to critical infrastructure, including ports, natural gas grids, power grids, and byproducts such as methane-rich fuel gas. They may also benefit from future infrastructure developments, including a shared CO_2 transportation infrastructure[28] and access to long-distance hydrogen pipelines [25].

---

[26] Recycled carbon fuels (RCFs) are liquid or gaseous fuels of non-renewable origin that are produced as unavoidable and unintentional by-product of industrial processes. To qualify, they must achieve at least a 70% reduction in GHG emissions compared to the fossil fuel comparator, as defined in the Commission Delegated Regulation (EU) 2023/1185 [162].

[27] Scope 1 emissions are direct GHG emissions from sources owned or controlled directly by an organization [163]. In this case, they are referring to direct CO_2 emissions from the cracker furnaces.

[28] This could include local CO_2 pipelines, shared CO_2 liquefaction plant, and intermediate CO_2 storage facilities, such as the one proposed at the Port of Antwerp [131].

Increased process electrification within the cluster would reduce the demand for fuel gas for combustion-related processes, enabling internal recovery of hydrogen from the fuel gas at the steam cracker plant. The resulting surplus methane could then be repurposed as feedstock for blue hydrogen production or exported to the natural gas grid. From the demand perspective, hydrogen use in these clusters is substantial and time-invariant, regardless of whether it is used as fuel or feedstock. This enables the supply of hydrogen on a use-as-produced basis across multiple off-takers. As a result, hydrogen production technologies can be sized for high-capacity utilization or overcapacity, so as to enhance operational flexibility. Moreover, unlike standalone systems, complementary technologies allow flexible operation without requiring costly hydrogen storage systems.

Finally, oil refineries and chemical industries within these clusters represent favorable end-use sectors for low-emissions hydrogen in the short term. As economic and regulatory conditions evolve to support their transition to a circular economy, the clusters will explore the possibility of redirecting hydrogen to other competing end-use sectors with greater CO_2 abatement potentials. Together, these cluster-level benefits motivate the development of a shared hydrogen infrastructure within clusters, which would help minimize investment risks and support phased deployment strategies.

Process description: Figure 3-7 shows the integrated hydrogen production system evaluated in **Paper IV**. Hydrogen demand in the cracker furnaces is met through a combination of autothermal reforming with carbon capture and storage (ATR CCS), solid oxide electrolysis cells (SOEC), ammonia cracking (AC), and hydrogen recovered from by-product fuel gas. The figure illustrates the integration of these technologies through the shared steam network and indicates the possibilities to export recovered methane and surplus hydrogen. It also highlights the key site-specific constraints relevant for deployment, including ammonia storage capacity, grid transmission limits, and the availability of on-site fuel gas.

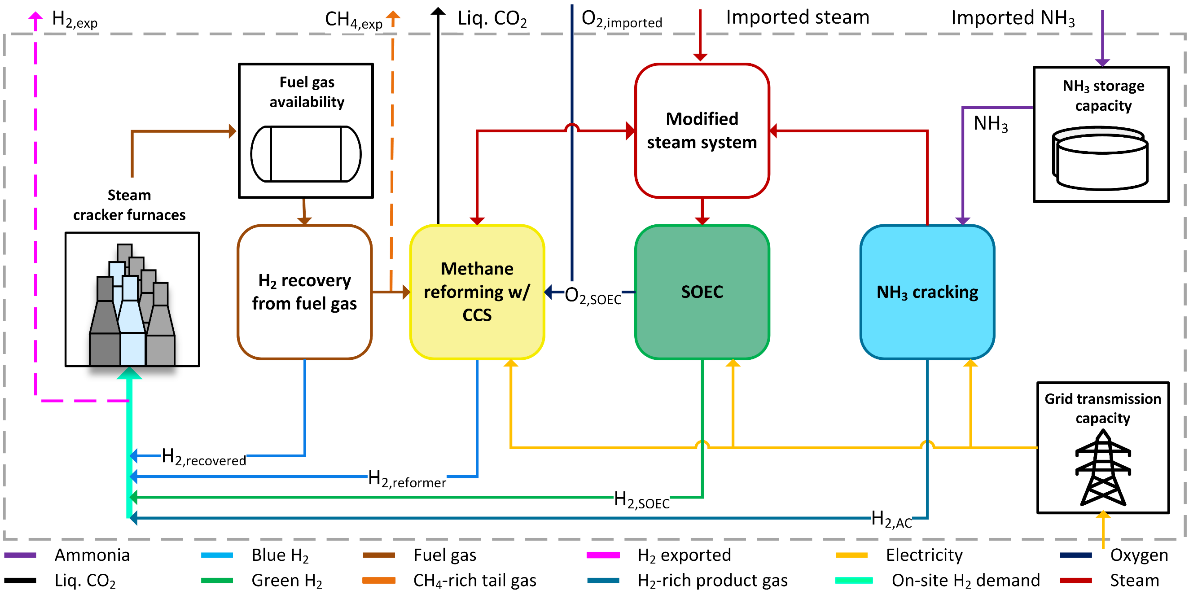

Figure 3-7: Simplified schematic of the integrated hydrogen production system, including the three hydrogen production technologies: (1) steam methane reforming with CCS; (2) solid oxide electrolyzer cells (SOEC); and (3) ammonia cracking. The potential end-use as a cracker fuel is shown, along with the possibility to export surplus hydrogen and recovered methane to the surrounding cluster. Key site-specific constraints, such as grid transmission capacity, ammonia storage, and fuel gas availability, are also indicated. For simplicity, the modified steam system is not shown here but is considered in the case study.

4 Methods

This chapter describes the methods upon which the developed frameworks were based. Figure 5-1 *provides an overview of these methods; some of these are established methods while others have been developed as part of this thesis.*

4.1 Steady-state process modeling

The process technologies and industrial case studies presented in Section 3 were modeled to establish the necessary mass and energy balances, including stream data and equipment specifications. These models served as the basis for the subsequent methods described in Sections 4.2–4.5, which are together applied within the frameworks presented in Section 5.

In **Paper I**, a process model of the reference bio-CHP plant was developed using the EBSILON Professional software with the available plant data. In addition, process simulation models of the MEA and HPC CO_2 capture processes were developed adopting rigorous rate-based models with detailed reaction kinetics. The MEA model, representing the amine-based capture process with an aqueous solution of monoethanolamine (30 wt.% MEA), and the HPC (30 wt.% K_2CO_3) process models were developed and validated based on data from Biermann et al. [58] and Gustafsson et al. [87], respectively.

In **Paper II**, the air-regeneration train of the PDH process was modeled and validated using the reference plant data. The MEA model in **Paper I** was adapted for the highly diluted flue gas of the air-regeneration train. Similarly, in **Paper III**, the Post-CCS process used an updated MEA model with the flue gas data from the reference steam cracker plant, while the Pre-CCS process employed an equilibrium-based model to simulate on-site hydrogen production by valorizing methane-rich fuel gas obtained from the steam cracking process, as described in Section 3.1.2.1.

Papers I–III used CO_2 compression and liquefaction models adapted from Eliasson et al. [129], developed based on the paper of Deng et al. [130]. The concentrated CO_2 stream from the capture models was assumed to contain CO_2, H_2O, N_2, and O_2, with trace MEA from the MEA model and no significant K_2CO_3 carryover from the HPC model. This stream was compressed in a three-stage intercooled system to 27.5 bar, as per Deng et al. [63], to account for potential impurities and ensure compatibility with downstream liquefaction. Downstream of the compression, a simple separator model mimicked the removal of excess oxygen and water. The liquefaction process employed an ammonia refrigeration cycle, with the outgoing liquid CO_2 stream at 16 bar and –26.5 °C, in line with the Northern Lights project specifications for ship transport and sub-seabed storage [123]. Note that in **Paper II**, the sea-transport option was compared with pipeline transport. The reference PDH plant is assumed to have access to a shared CO_2 transport infrastructure, similar to the one proposed at the Port of Antwerp [131], which includes a CO_2 backbone pipeline, a joint liquefaction facility, and intermediate storage. In this case, CO_2 emitters are only required to capture, compress, and purify the CO_2 stream within the plant boundaries to meet the pipeline export specification.

In **Paper IV**, the process models for the ammonia cracking process were developed and validated using reported process data [97]. The ammonia cracking model was primarily used to estimate the heat recovery potential for generating low-pressure steam, when the cracked product gas is used as fuel. Details of the modeling, key assumptions, and process parameters can be found in the respective papers.

4.2 Process integration

Grand composite curves (GCC) and a foreground–background analysis (also known as split-GCC analysis) were applied for energy targeting in Papers **I**–**IV**. The GCCs illustrate the net heat flows within a process at different temperature levels, including the minimum heat and cold utility demands of the process. In **Paper I**, energy targeting was performed to quantify and compare the heat recovery potentials for the two CO_2 capture technologies, including compression and liquefaction units, for the DH network. In Papers **II**–**IV**, these methods were applied to estimate the heat recovery potentials of different decarbonization technologies integrated into the case study plants, and thereby, estimate the on-site steam production capacity that would offset the steam production from existing utility steam boilers.

In **Paper IV**, the hydrogen production technologies were integrated via the steam network of the steam cracker plant. The SOEC required approximately 9 tH_2O/tH_2 of medium-pressure (MP) steam (5 barg), generated by a dedicated steam generator that was fed demineralized water owing to purity considerations [98]. The existing steam network was modified to include this generator and four potential MP steam sources: steam generated through heat recovery in process gas coolers in the ATR-CCS and AC processes; surplus low-pressure steam within the plant and imported steam from the cluster that was upgraded using a mechanical vapor recompression (MVR) unit; and a standby electric boiler, located within the SOEC subsystem, which was used during periods of MP steam deficit. An illustration of the modified system is provided in Supplementary Material S.2 of **Paper IV**, and detailed descriptions of both the existing and modified steam systems can be found elsewhere [132,133].

4.3 Combined exergy-pinch analysis

In **Paper II**, a combined exergy-pinch (CEP) analysis adapted from the work of Feng et al. [134] was modeled in MATLAB. The exergy-energy (Ω-H) diagram was used to visualize the total exergy losses in individual process equipment units. The energy level (Ω) for each unit was defined using a general expression (Equation 1), with detailed equations for steady-state flow systems, heat transfer, and work-driven equipment provided in **Paper II**. The total exergy loss (EX_{total}) in each item of equipment was calculated as the area between the respective hot and cold exergy composite curves. The inevitable exergy loss (INE_{EX}), defined as the theoretical minimum exergy destruction required to drive a given process [135], was used to determine the avoidable exergy loss (AVO_{EX}) in each component by calculating the difference between total and inevitable exergy losses (Equation 2).

Exergy efficiency, for a given process configuration, was calculated as the ratio of the useful exergy output to the total exergy input (Equation 3) or alternatively from the Ω-H diagram as the ratio of the total unshaded region to the total area[29] of the Ω-H diagram. Here, the $EX_{tot,area}$ term denotes the total exergy losses (shaded region[30], see Figure A1) of all the process equipment graphically assembled within the Ω-H diagram. The list of assumptions made in the CEP analysis can be found in **Paper II**.

$$\text{General definition}, \Omega = \frac{\text{exergy}}{\text{energy}} \tag{1}$$

$$AVO_{EX} = EX_{total} - INE_{EX} \tag{2}$$

$$\eta_{exergy} = \frac{\text{Useful exergy output}}{\text{Total exergy input}} = 1 - \frac{EX_{tot,area}}{\text{Total area of the } \Omega - \text{H diagram}} \tag{3}$$

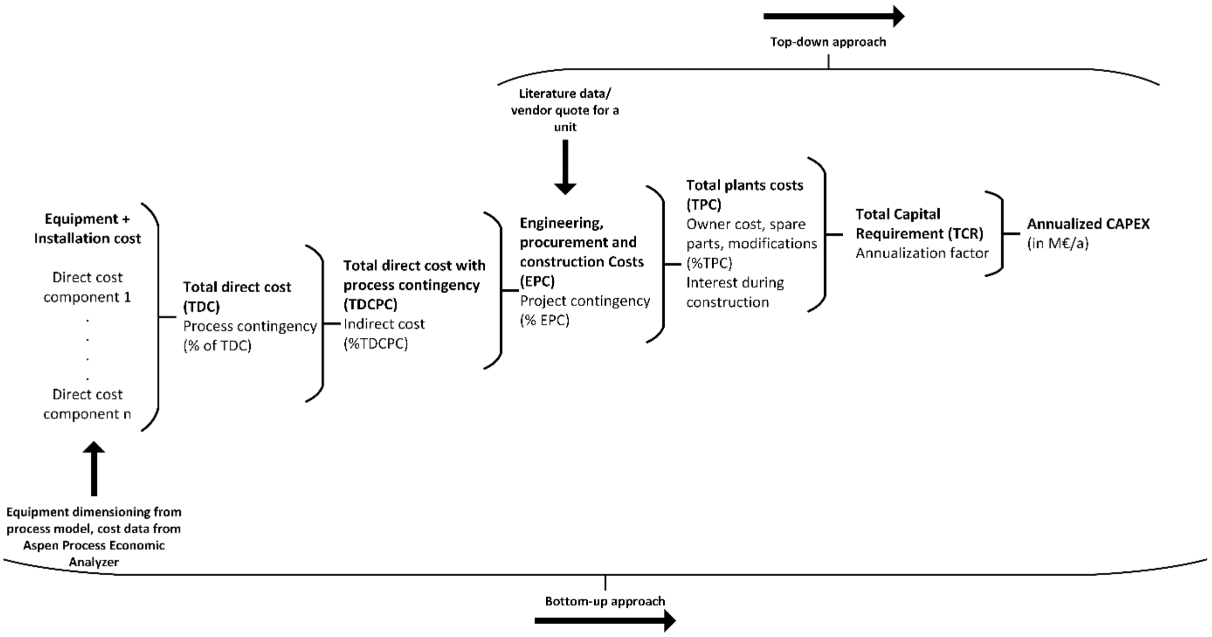

Figure 4-1: Capital cost estimation method. Arrows indicate the direction of cost escalation and input data from the Aspen Process Economic Analyzer. Adapted from [57,136].

4.4 Cost estimations

Figure 4-1 illustrates the hybrid[31] top-down/bottom-up capital cost estimation method, adapted from [57,136], applied in this work. A bottom-up approach involves using energy and material flow data from the developed process models to dimension each piece of equipment. The direct cost of each process equipment was obtained from direct cost data or regressed direct cost functions derived from the Aspen Process Economic Analyzer. The regressed direct cost functions presented by Biermann et al. [57] were used for all the major equipment sizes from the developed process models in Papers **II** and **III**.

---

[29] The product of the lengths of the x-axis and y-axis in the Ω-H diagram.

[30] The total exergy losses are differentiated as avoidable exergy losses, highlighted with diagonally-hatched lines, and inevitable exergy losses, highlighted with cross-hatched lines, respectively.

[31] Disambiguation: This approach should not be confused with the hybrid costing method, proposed by Roussanaly et al. [36], which combines a top-down modeling of technology learnings with a bottom-up engineering-economic analysis for emerging/advanced technologies.

The top-down approach entailed extracting data reported in the literature or using vendor data for a whole unit (including all associated equipment), which are typically reported as engineering procurement and construction costs. This approach was predominantly used for subsystems in the Pre-CCS configuration in **Paper III** and all the process technologies in **Paper IV**, for which ample cost data were available from the literature or technology providers. The total capital requirement estimated from the hybrid top-down/bottom-up capital cost estimation method was annualized over the assumed plant lifetime or the design lifetime of the process technology. The default economic parameters, assumptions, and cost escalation factors for the selected technologies can be found in the appended papers.

The CO_2 avoidance cost, as expressed by Equation 4, served as the key economic indicator for comparing different process configurations (**Paper II**), decarbonization pathways (**Paper III**), and hydrogen system configurations (**Paper IV**). It was defined as the ratio of the total annual system costs to the total CO_2 emissions ($\dot{m}_{CO2,avo}$) avoided annually by the individual production technologies. The total annual costs include the annualized capital investments and operational expenses, which include fixed (maintenance, insurance, and labor) and variable costs (fuel, electricity consumption, and other consumables).

In **Paper IV**, the total annual system costs of the optimized system configuration and the total CO_2 emissions avoided with ATR-CCS ($\dot{m}_{CO_{2,avo}}$) were used to estimate the CAC, as shown in Equation 4. As the differences in absolute CO_2 abatement across all three technologies were minor, for simplification, the total avoidance achieved with ATR-CCS was uniformly applied across all technologies. Detailed CO_2 avoidance calculations are provided in the Supplementary Material of **Paper IV**.

$$\mathrm{CAC} = \frac{\mathrm{CAPEX}_{\mathrm{annualized}} + \mathrm{OPEX}_{\mathrm{total}}}{\dot{m}_{\mathrm{CO2,avo}}} \left[\frac{€/\mathrm{a}}{\mathrm{tCO}_{2,\mathrm{avo}}/\mathrm{a}}\right] \tag{4}$$

4.5 Investment and dispatch optimization

A multi-period mixed-integer linear programming (MILP) model was developed in **Paper IV** to identify the cost-optimal technology mix and hydrogen dispatch strategy for the integrated hydrogen production system, as described in Section 3.2.4. The model was implemented in GAMS and simulated over 1 year of operation with hourly resolution. The model minimizes the total annual system costs of the integrated hydrogen production system by optimizing both investment (i.e., technology sizing) and operational decisions (i.e., hourly hydrogen dispatch and methane exports), while meeting a fixed hydrogen demand, as defined by Equation 5. Site-specific constraints such as grid transmission capacity, ammonia tank capacity, and fuel gas availability, as well as technology-specific constraints such as minimum load limits and ramp rate restrictions, were included to reflect practical deployment and operational limitations.

$$\min \mathrm{C}^{\mathrm{tot}} = \mathrm{C}_{\mathrm{inv,an}} + \mathrm{C}_{\mathrm{op,an}} - \mathrm{C}_{\mathrm{offset,an}} \tag{5}$$

where, c^{tot} is the total annual system costs, comprising the annualized investment costs ($C_{inv,an}$) the annual operational costs ($C_{op,an}$) and the total annual offsets ($C_{offset,an}$). These offsets represent cost reductions from methane export to the natural gas grid, hydrogen exports to the cluster, and avoided CO_2 emissions costs through surplus upgraded steam, which reduces natural gas use and associated on-site emissions. A complete model description, including input data and assumptions, can be found in **Paper IV**. Based on the cost-optimal system design, two cost metrics were calculated: the levelized cost of hydrogen (LCOH), representing the actual production cost, and the on-site hydrogen supply cost (OHSC). The LCOH represents the levelized hydrogen production cost and is defined as the ratio of total annual system costs to the total hydrogen produced by the individual production technologies (Equation 6). It includes annualized capital investments and operational expenses, such as those for energy, maintenance, and emissions. The OHSC, which reflects the net cost of supplying hydrogen to the steam cracker plant and is calculated as the ratio of the minimized total system costs (C_{tot}), which includes revenues from methane and hydrogen exports, to the total amount of hydrogen produced (Equation 7).

$$\mathrm{LCOH} = \frac{\mathrm{CAPEX_{annualized}} + \mathrm{OPEX_{yearly}}}{\sum_{t\in T}\left(p_{SOEC,t} + p_{NH_3,t} + p_{ATR-CCS,t}\right)} \quad \left[\frac{€}{\mathrm{kgH_2}}\right] \tag{6}$$

$$\begin{aligned}\mathrm{OHSC} &= \frac{\sum_{n\in N_{H_2}}\left(\mathrm{CAPEX_{annualized}} + \mathrm{OPEX_{yearly}}\right) - \sum_{t\in T} q_t^{CH_4,export} \cdot c_t^{CH_4} - \sum_{t\in T} q_t^{H_2} \cdot c_n^{H_2,exp}}{\sum_{t\in T}\left(p_{SOEC,t} + p_{NH_3,t} + p_{ATR-CCS,t}\right)} \\ &= \frac{C_{tot}}{\sum_{t\in T}\left(p_{SOEC} + p_{NH_3} + p_{,ATR-CCS}\right)} \left[\frac{€/y}{\mathrm{kgH_2}/y}\right]\end{aligned} \tag{7}$$

5 Developed methodologies and case study applications

This chapter presents the framework methodologies developed in **Papers I–IV***, each addressing the limitations discussed in Section 2.2. These frameworks combine methods described in Chapter 4 and are presented, progressing from systems-level to the site-level (see Figure 1-1). Figure 5-1 provides an overview of the applied methods and their linkages to the appended papers. This chapter also summarizes the key results obtained from applying these frameworks to the industrial case studies introduced in Section 3.2.*

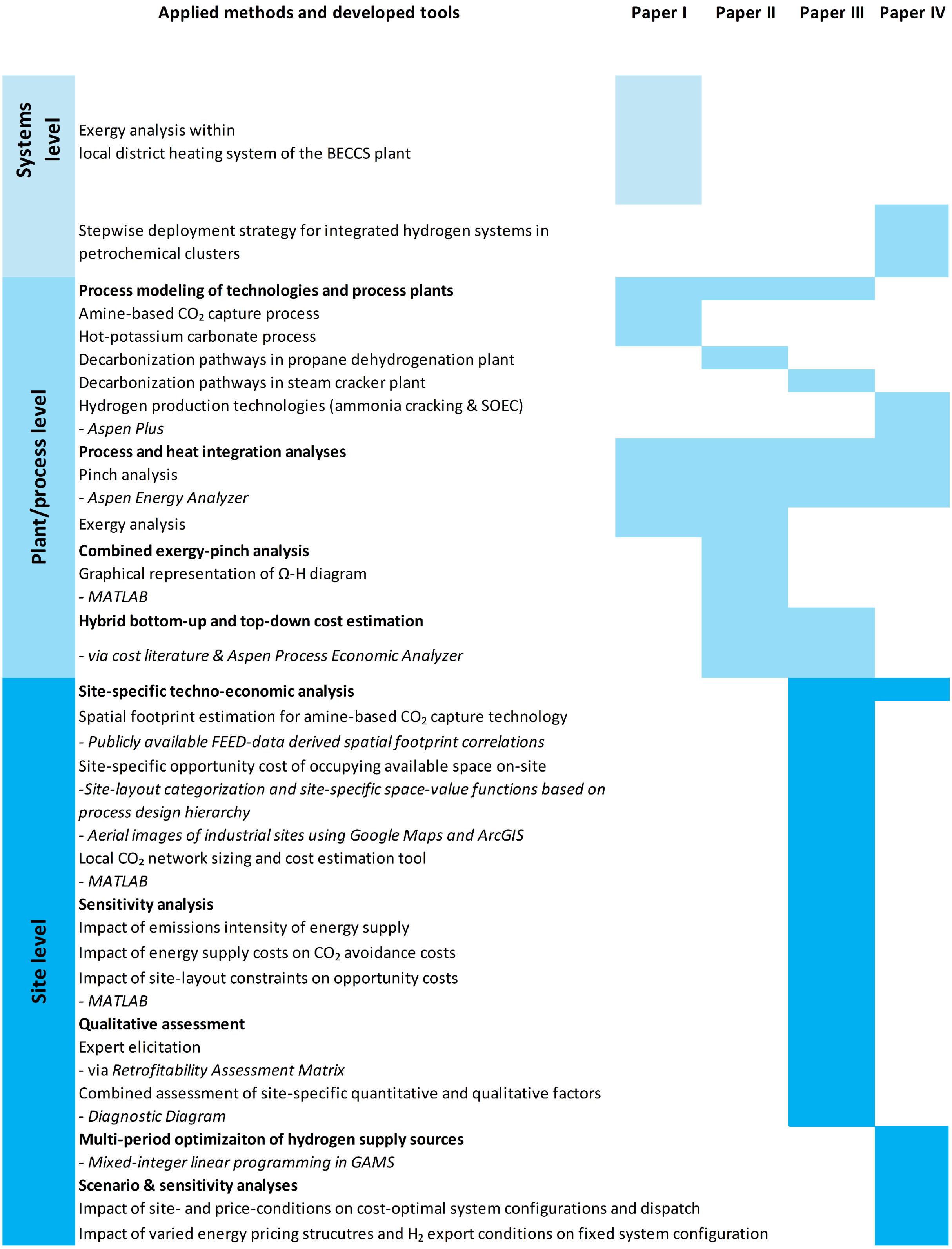

	Applied methods and developed tools	Paper I	Paper II	Paper III	Paper IV
Systems level	Exergy analysis within local district heating system of the BECCS plant	●			
	Stepwise deployment strategy for integrated hydrogen systems in petrochemical clusters				●
Plant/process level	**Process modeling of technologies and process plants**	●	●	●	
	Amine-based CO_2 capture process	●			
	Hot-potassium carbonate process	●			
	Decarbonization pathways in propane dehydrogenation plant		●		
	Decarbonization pathways in steam cracker plant			●	
	Hydrogen production technologies (ammonia cracking & SOEC)				●
	- *Aspen Plus*				●
	Process and heat integration analyses	●	●	●	●
	Pinch analysis	●	●	●	●
	- *Aspen Energy Analyzer*	●	●	●	●
	Exergy analysis	●	●		
	Combined exergy-pinch analysis		●		
	Graphical representation of Ω-H diagram		●		
	- *MATLAB*		●		
	Hybrid bottom-up and top-down cost estimation		●	●	
	- *via cost literature & Aspen Process Economic Analyzer*		●	●	
Site level	**Site-specific techno-economic analysis**			●	●
	Spatial footprint estimation for amine-based CO_2 capture technology			●	
	- *Publicly available FEED-data derived spatial footprint correlations*			●	
	Site-specific opportunity cost of occupying available space on-site			●	
	-Site-layout categorization and site-specific space-value functions based on process design hierarchy			●	
	- *Aerial images of industrial sites using Google Maps and ArcGIS*			●	
	Local CO_2 network sizing and cost estimation tool			●	
	- *MATLAB*			●	
	Sensitivity analysis			●	
	Impact of emissions intensity of energy supply			●	
	Impact of energy supply costs on CO_2 avoidance costs			●	
	Impact of site-layout constraints on opportunity costs			●	
	- *MATLAB*			●	
	Qualitative assessment			●	
	Expert elicitation			●	
	- via *Retrofitability Assessment Matrix*			●	
	Combined assessment of site-specific quantitative and qualitative factors			●	
	- *Diagnostic Diagram*			●	
	Multi-period optimizaiton of hydrogen supply sources				●
	- *Mixed-integer linear programming in GAMS*				●
	Scenario & sensitivity analyses				●
	Impact of site- and price-conditions on cost-optimal system configurations and dispatch				●
	Impact of varied energy pricing strucutres and H_2 export conditions on fixed system configuration				●

Figure 5-1: Overview of applied methods and developed tools and their links to the appended papers. The tools used are indicated in italics.

5.1 Impact of system boundaries on the choice of decarbonization technology

This section presents the framework developed in **Paper I** and its application to a bio-CHP plant, described in Section 3.2.1. Section 5.1.1 outlines how system boundaries influence the choice of decarbonization technologies for a specific industry. Section 5.1.2 applies this framework to the bio-CHP plant within a district heating system and presents the key results from the case study.

5.1.1 Impact of system boundaries on the choice of decarbonization technology

Discrepancies between the perspectives of plant and end-users arise because plant owners typically prefer decarbonization technologies that minimize the impact on production costs and have the lowest specific CO_2 capture cost[32], assuming that emitting CO_2 into the atmosphere is no longer cost-free. Conversely, from the end-users' perspective, technologies that maximize CO_2 avoidance with a minimal increase in the marginal cost of the final product would be preferable, assuming that the plant owners pass on the costs to their consumers.

Three key aspects must be considered to observe these different perspectives. First, the core functionality of the unabated process plant must be assessed and preserved, regardless of whether it involves delivering energy services or producing a primary product. This enables the identification of alternative means for delivering the same energy service or product before integrating decarbonization technologies. Second, the use of exergy as a figure of merit is crucial when comparing different decarbonization options and for evaluating how the integration of a decarbonization technology will affect the plant's performance in terms of both energy and exergy, particularly when these options entail inherently different exergy requirements. Third, it is important to account for pre-existing market or policy conditions that influence what is perceived as cost-optimal from the plant owner's perspective. Consequently, it is necessary to expand the system boundary to include the immediate consumers of energy services and products from the now-decarbonized plant. This expansion allows for the determination of which technology or process configuration retains the highest exergy efficiency within the broader system, considering that the end-user may assign a higher value to high-exergy energy carriers, such as electricity.

Figure 5-2 depicts this system boundary expansion in the context of a bio-CHP plant operating within a DH system. Figure 1 presents an overview of the method used in this work, together with: 1) the *CHP-CCS plant boundary*, which includes the bio-CHP plant fitted with CO_2 capture and conditioning (CO_2 compression and liquefaction for ship transport) units; and 2) *the extended system boundary*, which includes the local DH system, where it is assumed that the electric power delivered by the bio-CHP plant is consumed by decentralized ground-source heat pumps (GSHPs) that have been installed to meet the indoor-climate needs of end-users in residential buildings. The two system boundaries are chosen to enable evaluation of the plant- and system-level performances of a reference bio-CHP plant that is retrofitted with different carbon capture technologies (described in Section 3.1.1).

---

[32] Using CO_2 capture costs as a metric for technology comparison is also flawed, as it may favor technologies that capture higher levels of on-site emissions.

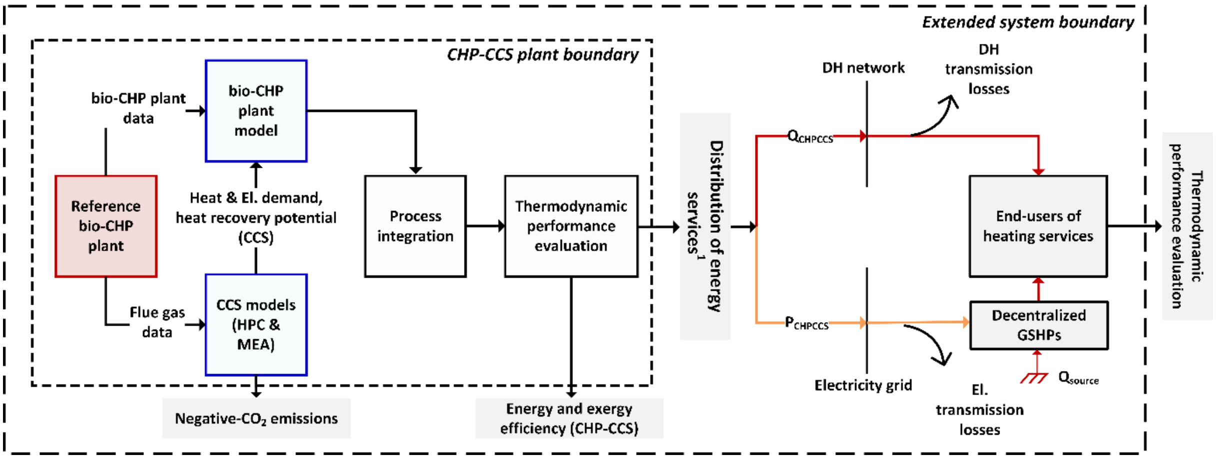

Figure 5-2: Overview of the methods and models used with the two system boundaries: bio-CHP plant boundary and the extended system boundary (the local DH system). The data from the reference bio-CHP plant (indicated in red) are fed to the developed numeric models, indicated in blue. Finally, the applied methods and results obtained are highlighted in gray. [1]Delivered energy services of the bio-CHP plant equipped with CCS units (CHP-CCS), which include the net district heating (DH) and power delivered to the bio-CHP plant's local DH system. Note that the electricity delivered to the grid is assumed to be consumed in decentralized ground-source heat pumps (GSHPs) to meet indoor climate needs, i.e., domestic hot water and space heating demands. Source: Paper I.

As mentioned previously, CHP plants prioritize the delivery of district heat over electricity power production, as generated electric power is traded in the competitive power market and is subject to competition and price volatility, whereas the DH market is closed and the price is typically set by the DH supplier in the city. On the other hand, the immediate energy consumers in the DH network naturally assign a higher value to a high-exergy energy carrier, i.e., the low-carbon electricity generated by the CHP-CCS plant, as it can be utilized for various purposes (heating, cooling, and other power demands in households or industrial applications) within the local energy system. Moreover, electricity transmission losses are expected to be minimal compared to the transmission losses incurred when DH is supplied over long distances. Therefore, the values assigned to the different energy services/carriers of an existing bio-CHP plant, i.e., heat and electricity, differ at the plant level than at the system level (energy consumers).

Considering that the different CO_2 capture technologies have varying exergy demands and, thereby, exert different impacts on the outputs of the host plant, the technology deemed optimal by the plant owner may be the same as that preferred by the end-users in the local energy system. For example, a bio-CHP plant in a DH system may favor a CO_2 capture technology (e.g., HPC) that minimizes the loss of heat sales at the expense of electric power output over an alternate technology (e.g., MEA) that can retain this output, which could be either be used within the plant (e.g., to power heat pumps that can restore lost DH output) or exported to the grid. Herein lies the underlying systems-level factor for this selected case study industry, which could alter the optimal choice of decarbonization technology. Specifically, it pertains to the difference in the value assigned to electricity and heat, driving the bio-CHP plant operator in a DH system to opt for a carbon capture technology that minimizes the loss of heat sales. This observation can be confirmed using exergy efficiency as the key performance indicator for comparing different CO_2 capture technologies within the bio-CHP plant boundary and, subsequently, within the local DH system.

5.1.2 The influence of system boundaries – BECCS in district heating systems

The choice of CO_2 capture technology from the plant owner's perspective: A detailed comparison of the CO_2 capture technologies can be found in **Paper I**. In general, the amine-based CO_2 capture technology using benchmark MEA solvent is inherently different from the HPC process in that flue gas compression is not required in the former, and the heat demand per tonne of captured CO_2 to regenerate the rich-amine solvent[33] is higher.

Figure 5-3 visualizes these technology-specific characteristics, and their impacts on the performance of the reference bio-CHP plant for the two investigated BECCS systems, namely, CHP-MEA and CHP-HPC plants. From an energy perspective, the CHP-HPC plant case incurs an energy penalty[34] of 9 percentage points, while the CHP-MEA plant incurs a significantly larger energy penalty of 15 percentage points. Although the total energy outputs of the CHP-MEA and CHP-HPC plants are similar[35], they exhibit different power-to-heat ratios.

More specifically, considering the turbine condensers, flue gas condensers, and recovered heat from the CO_2 capture and compression units, the CHP-HPC plant has the potential to deliver more heat (319 MW_{th}) than either the CHP-MEA plant (256 MW_{th}) or the reference plant (296 MW_{th}), as shown in Figure 5-3a. A significantly higher power preservation[36] of 81% was estimated for the CHP-MEA plant, which is roughly twice that of the electric power output preserved by the CHP-HPC plant (43.2%), as shown in Figure 5-3b. Using these energy performance indicators for technology comparisons within the plant boundaries indicates that the HPC process is more favorable for a bio-CHP plant operating as a baseload unit in a DH system. This conclusion holds true because the excess heat recovered at a relatively higher temperature from the flue gas compression could be utilized to increase the plant's DH delivery potential.

Therefore, from a plant owner's perspective, the choice of CO_2 capture technology comes down to selecting between the loss of power production with the integration of the HPC capture process and the increased heat losses associated with the MEA capture process. Considering the pre-existing DH market conditions of the case study plant, a compelling argument can be made in favor of the HPC capture technology as the optimal decarbonization technology.

Figure 5-3 presents a modified process configuration, the CHP-MEA-HP plant, which considers that the retained electric power output in the CHP-MEA plant, roughly 80% compared to the reference plant (Figure 5-3b), could be consumed on-site in large-scale heat pumps to increase DH delivery. Here, to ensure a fair comparison, the difference[37] in electric power output between the CHP-MEA and CHP-HPC plants was assumed to be utilized by large-scale centralized heat pumps on-site (COP ~2.5), so as to recover low-temperature heat within the CHP-MEA plant. In other words, both the CHP-MEA-HP and the CHP-HPC plant each have an equivalent electric power output of 47.5 MW, as shown in Figure 5-3a.

---

[33] Low-pressure steam for driving the MEA capture process is extracted from the turbine at the deaerator stage, while live steam is extracted from the boiler to drive the flue gas compressor and to supply heat to the HPC capture process.

[34] The percentage difference in the energy efficiency of the reference CHP plant following integration of the carbon capture and liquefaction processes.

[35] Estimated to fall within a narrow range of 345–366 MW_{th}.

[36] The ratio of the electric power output retained (or preserved) by the CHP plant following the integration of the carbon capture and liquefaction processes.

[37] Note that, for this assumption, the preservation of electric power is equal (43.2%) in the CHP-HPC and CHP-MEA-HP cases, as shown in Figure 5-3b.

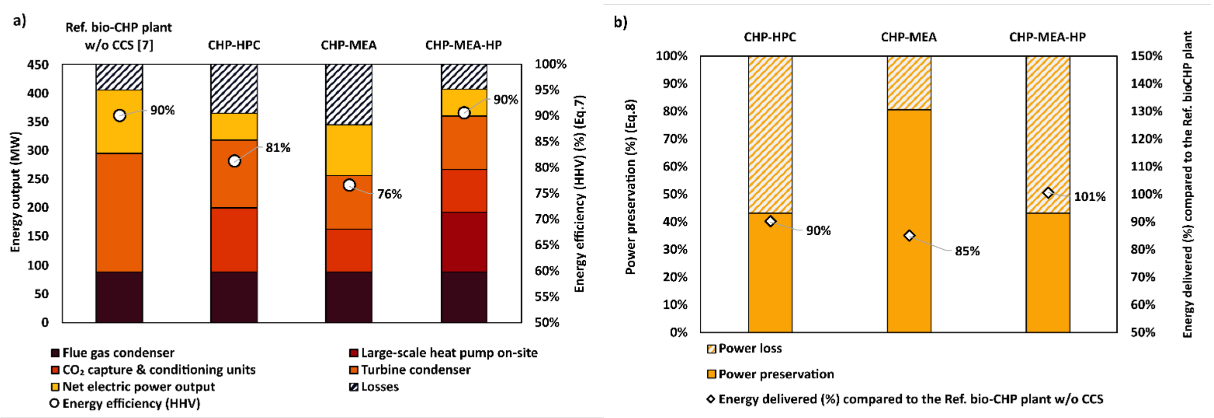

Figure 5-3: a) Comparisons of net electric power outputs, shares of the net heat outputs from different heat recovery units, and energy efficiencies between the different studied BECCS configurations and the reference bio-CHP plant without CCS units. b) Power preservation and energy delivered in the studied BECCS configurations relative to the reference bio-CHP plant without CCS units. The equations indicated in the figure can be found in Paper I.

Consequently, the integration of large-scale heat pumps resulted in a significantly higher heat output (361 MW_{th}), which represented approximately 21% more district heat delivery compared to the reference plant. This illustrates that the choice is not simply between power or heat losses due to CCS integration, but rather how the retained electricity is utilized within the plant. In this case, it is a choice between using electricity for flue gas compression in the HPC technology or in heat pumps for recovering heat from the newly installed MEA-based CO_2 capture technology. The CHP-MEA-HP configuration was found to be the most effective in terms of maximizing heat delivery to the DH system, clearly aligning with the plant owner's perspective.

The choice of CO_2 capture technology from the end-users' perspective: As described in Section 5.1, to observe the differences between the plant owners' and end-users' perspectives, first, the core functionality of the unabated plant must be retained. In this case, it is DH, an energy service that is primarily used by the end-user for space heating and domestic hot water. Figure 5-3a illustrates the exergy efficiencies of the different BECCS configurations within the plant boundaries. In contrast, Figure 5-3b illustrates the case in which all electric power delivered to the end-user is assumed to be consumed in GSHPs in a decentralized manner, as depicted in Figure 5-2.

Within the plant boundaries, the CHP-MEA plant, as expected, yielded the highest exergy efficiency (~35%), primarily due to its higher level of power preservation. As a result, the higher exergy efficiency confers this plant configuration with greater product flexibility, with the ability to vary the output load of a specific product by adapting product ratios between heat, power, and negative CO_2 emissions.

The bio-CHP plant fitted with the MEA process and large-scale heat pumps, therefore, exhibits greater availability of the higher-exergy energy carrier, electricity, which could be strategically used in heat pumps to increase the total DH output (up to 41%) or delivered to the electricity grid. This conclusion highlights the limitation of using energy as a figure of merit for technology comparison within plant boundaries, which previously led to the conclusion that the HPC process could be the optimal decarbonization technology from the plant owner's perspective.

Figure 5-4b illustrates the estimated system exergy efficiency range, with an assumed Carnot efficiency (η_{Carnot}) in the range of 40%–60% for the GSHPs. The maximum values in the box plots indicate the exergy efficiencies estimated for a DH supply temperature of 86°C. The minimum and median values represent the exergy efficiencies corresponding to typical end-use supply temperatures, in the range of 30°–60°C for space heating and domestic hot water, respectively. The system exergy efficiency is highest when the retained electric power output is consumed locally in decentralized GSHPs (CHP-MEA), followed by the situation in which it is consumed on-site in centralized large-scale heat pumps (CHP-MEA-HP), and finally, the CHP-HPC case, which exhibits the lowest system exergy efficiency owing to its lower power-to-heat ratio.

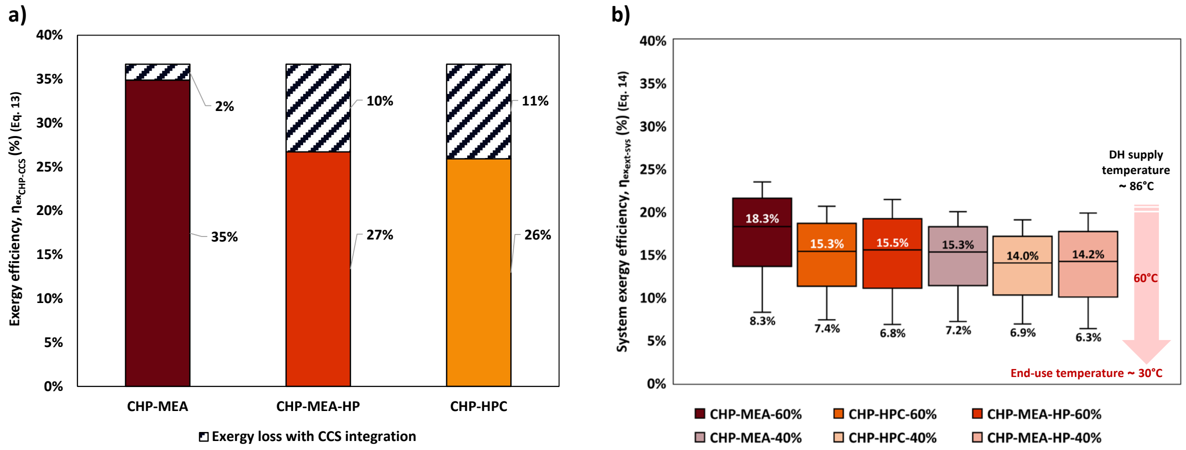

Figure 5-4: Exergy efficiencies of the CHP-CCS plant cases within their plant boundaries a) and extended system boundaries b), with ground-source heat pumps (GSHPs) operating with Carnot efficiencies η_{Carnot} in the range of 40%–60%. Source: Paper I.

These results reveal that the retained electric power output in the CHP-MEA configuration could be utilized in power-to-heat technologies, such as GSHPs in the local DH system, to ensure increased levels of DH delivery, thereby avoiding DH distribution losses. Therefore, the CHP-MEA configuration coupled with the uptake of GSHPs in its local DH systems emerges as the most effective option for maximizing system-level exergy efficiency in the broader system while achieving the same level of CO_2 emissions reduction as the other BECSS configurations.

From the end-users' perspective, this is also the preferred configuration, as it provides the flexibility to connect to the DH network or install substitute technologies to deliver the same energy service. Furthermore, end-users could optimize their indoor climate demand patterns by complementing their existing heating systems with heat pumps. This example of BECCS in DH systems highlights how plant owners' and end-users' perspectives on the optimal decarbonization technology or plant configuration may diverge. This divergence can be identified using the framework described in Section 5.1.1, which can be adapted to other industrial energy systems for which the plant-level and system-level objectives may differ.

5.2 Iterative combined exergy-pinch analysis

This section presents the framework developed in **Paper II** and its application to the air regeneration train of a propane dehydrogenation plant. Section 5.2.1 describes the iterative combined exergy-pinch (CEP) analysis, while Section 5.2.2 presents the key results from the case study.

5.2.1 Identifying promising decarbonization process configurations using iterative combined exergy-pinch analysis

The CEP analysis developed in **Paper II** builds on the method proposed by Feng et al. [134], which adopts the concepts of *avoidable* and *inevitable* exergy losses to set performance improvement targets aimed at improving energy efficiency in existing industrial systems. In **Paper II**, this method was adapted for identifying promising process modifications and targeting minimal exergy losses in net-zero CO_2 emissions process configurations. Feng et al. [134] introduced an exergy-energy (Ω-H) diagram to overcome the limitations of pinch analysis, which represents only heat transfer processes. This diagram was used to represent graphically the exergy losses across different processes within an industrial plant, including those that involve pressure or composition changes. The difference between the total and inevitable exergy losses was quantified to estimate the avoidable exergy losses for an individual piece of equipment. Based on this, their process modification strategy involved targeting the process equipment with the largest avoidable exergy losses first, while neglecting inevitable exergy losses.

Feng et al. [134] defined inevitable exergy loss as the minimum exergy loss or minimum driving force required for a process to operate at a desirable rate, thereby establishing the *theoretical maximum potential* for improvements that can be achieved through process modifications. In contrast, the avoidable exergy losses represent the *practical maximum potential* for improvement that can be achieved through process modifications under current technical and economic conditions. This distinction implies that exergy losses that have previously been considered inevitable may become avoidable with technological advancements and changes in economic conditions. While this distinction remains valid, the current context of improving resource efficiency and minimizing CO_2 emissions requires a reevaluation of what constitutes inevitable losses. In particular, process modifications can now be considered to replace combustion processes, which are typically one of the largest sources of inevitable exergy losses in industrial energy systems. For instance, process electrification for industrial process heating at higher temperature levels could provide the additional advantage of avoiding direct CO_2 emissions on-site while minimizing the exergy losses associated with combustion.

Accordingly, **Paper II** focused on the inevitable exergy losses due to the combustion of carbon-based fuels, which are inherently irreversible and the primary source of CO_2 emissions. To this end, an additional screening process was incorporated into the CEP analysis to address the inevitable exergy losses in combustion processes, using methods to replace or modify the existing combustion process. This screening step considers the temperature level at which the process requires energy and the possibility of minimizing combustion exergy losses through two options: (i) switching to electrified process heaters for process heating requirements >1,000°C (depending on heating element properties[38]); or (ii) direct or indirect integration of an industrial gas turbine (GT), for process heating requirements below 800°C.

---

[38] Maximum element temperature and maximum watt loading (W/m^2)

Direct electrification via heating elements enables uniform and controllable heat flux at the required temperature levels by converting electricity directly into heat. In contrast, the integration of gas-fired turbines is relatively straightforward, as the advanced materials used in the turbines enable enhanced utilization of fuel exergy between the adiabatic flame temperature and the turbine outlet temperature. This fraction of fuel exergy is typically lost in conventional process heaters and furnaces due to material constraints. A more detailed description of these options and their corresponding Ω-H diagram can be found in Section 2 of **Paper II**. Based on this, the merit order of process modifications starts with the screening step for the combustion-related exergy losses, followed by targeting process equipment in the reference process plant and the retrofitted decarbonization technology, spanning from the largest to the smallest avoidable exergy loss. Process modifications that are deemed compatible are implemented iteratively, and after each step, the economic performance is assessed to ensure that the exergy savings justify the required investment[39]. This approach enables the identification of a cost-optimal process configuration with minimal exergy losses relative to the unabated plant, with near-zero or net-zero CO_2 emissions.

Figure 5-5 provides an overview of this framework. The steps involved in the framework are described below in the context of an unabated PDH plant. However, they are generalizable and applicable to other process plants for techno-economic comparisons of alternative process configurations with relevant decarbonization technologies, allowing for the determination of an exergy- and cost-optimal decarbonized process plant configuration.

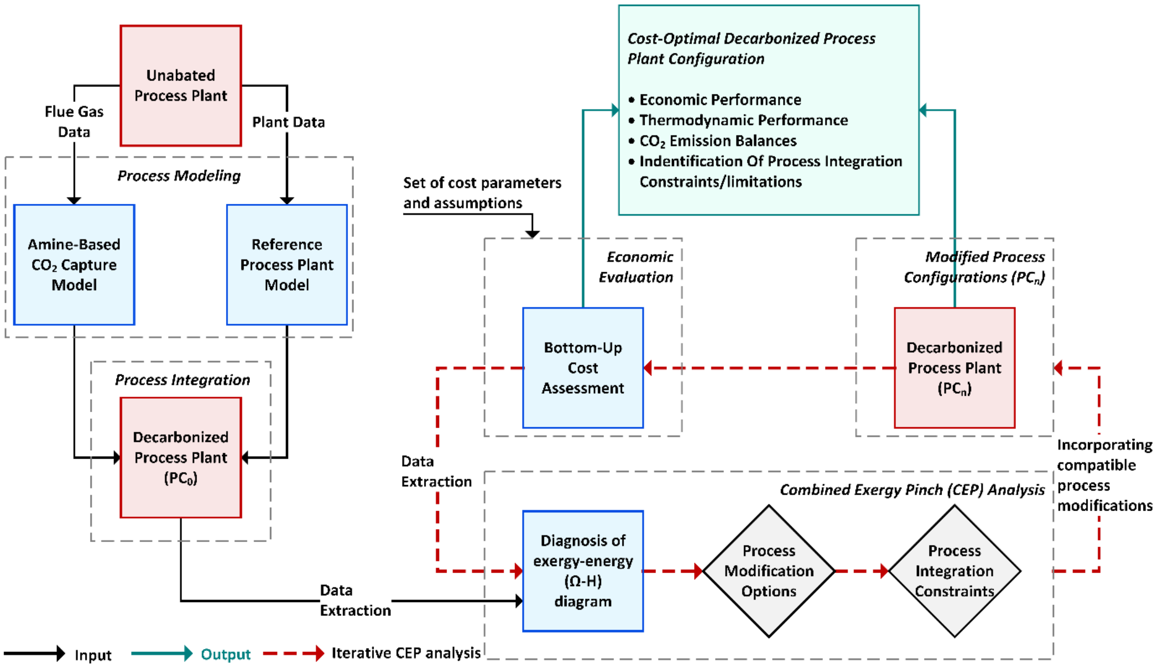

Figure 5-5: Overview of the applied methodological framework and method used, including process modeling, process integration, combined-exergy pinch, and techno-economic analysis, indicated with gray-dashed boxes. The blue boxes indicate the numeric models developed. The gray-shaded boxes indicate the evaluations of process modification options. Process configurations and main outputs are indicated in red and green boxes, respectively. The integrated process configurations are abbreviated as 'PC,' suffixed with a number, that indicates the number of stepwise implemented modifications. Source: Paper II

---

[39] The relationship between costs and process modifications are discussed in the Supplementary Matieral of **Paper II**.

5.2.2 Targeting minimal exergy losses towards net-zero CO_2 emissions - Propane dehydrogenation plant

Figure 5-6 illustrates the decarbonized-process configurations identified using the proposed framework for a PDH plant. Table 5-1 summarizes the process modifications implemented in each iteration of the CEP analysis and the corresponding influence on the composition of the flue gas at the end of the air-regeneration train. A more detailed description of the process configurations and the modifications identified using the CEP analysis can be found in **Paper II**. The potential and implications of the proposed PDH process (PC_2) are discussed in Section 5.4 of **Paper II**.

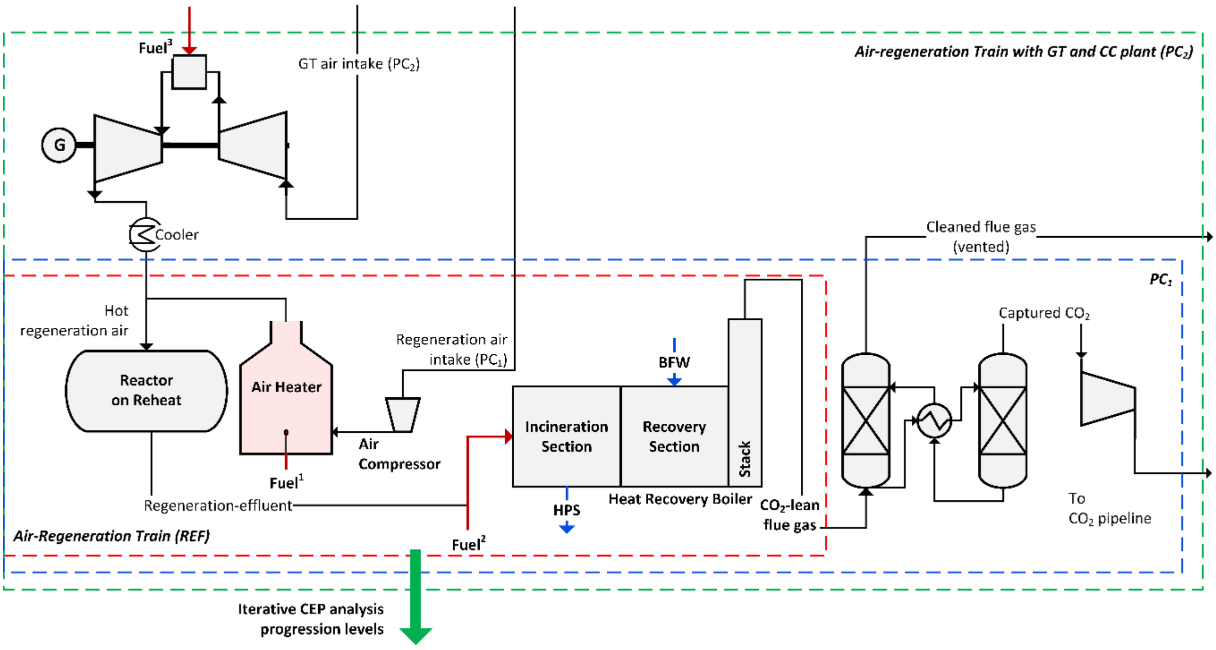

Figure 5-6: Process flowsheet diagram of the different process configurations of the air regeneration train and the progression of the CEP analysis. The CEP analysis starts with the reference air-regeneration train model (REF[40], indicated in the red dashed box), followed by the PC_1 configuration (blue-dashed box), which includes the CC plant, and finally, the proposed PDH configuration (PC_2, indicated in green dashed box), which includes the industrial gas turbine, the exhaust gases of which are used as the hot-regeneration air. In this case, the existing air compressor and air heater function as standby units. [1] The air heater utilizes H_2-rich fuel gas and natural gas at the main burners of the air heater under the reference conditions, REF and PC_1, respectively. [2] Volatile organic compounds in the reactor effluent are incinerated with natural gas in the heat recovery boiler in all the configurations.[3] The gas turbine utilizes natural gas as the primary fuel in the PC_2 configuration. Abbreviations: HPS, high-pressure steam; BFW, boiler feed water. Source: Paper II.

Figure 5-7 illustrates the technical and economic performances of the proposed process configuration (PC_2) identified using the framework developed in **Paper II**. Figure 5-7a shows that integrating new process equipment into an unabated PDH plant for decarbonization reduces the overall exergy efficiency (cf. reference PDH plant and PC_0), as expected. Retrofitting a CO_2 capture plant to the unmodified PDH plant (PC_0) results in a relative CO_2 avoidance[41] of 50%, primarily due to the higher specific regeneration duty at low CO_2 concentrations (2.5 vol.%) and the resulting indirect CO_2 emissions from natural gas-fired boilers to maintain the on-site steam balances.

---

[40] In the reference air-regeneration train, the air heater utilizes hydrogen-rich fuel gases recovered from the propane dehydrogenation plant (without a CO_2 capture unit).

[41] The relative CO_2 avoidance (Equation 16 in **Paper II**) is a key technical performance indicator used to compare the different process configurations (air regeneration train of the PDH plant) based on the absolute amount of CO_2 avoided (Equation 15 in **Paper II**) relative to the absolute amount of CO_2 generated in them.

Table 5-1: Description of implemented process modifications and corresponding process configurations.

Process configuration	Implemented process modification	Corresponding flue gas compositions prior to CO_2 capture	
		Main gas component	vol.%
PC_0	Straightforward retrofit of CC plant to the reference PDH process[40] without process modifications.	CO_2	2.5
		O_2	13.4
		H_2O	11.2
		N_2 (balanced)	72.9
PC_1	Fuel switched from H_2-rich fuel gas to methane, followed by retrofitting the amine-based CC plant.	CO_2	4.0
		O_2	12.2
		H_2O	9.0
		N_2 (balanced)	74.8
Proposed process configuration (PC_2)	Integration of industrial GT prior to the air heater. The GT exhaust gas is used as hot regeneration air in the air-regeneration train of the PDH process.	CO_2	5.5
		O_2	8.9
		H_2O	10.8
		N_2 (balanced)	74.8

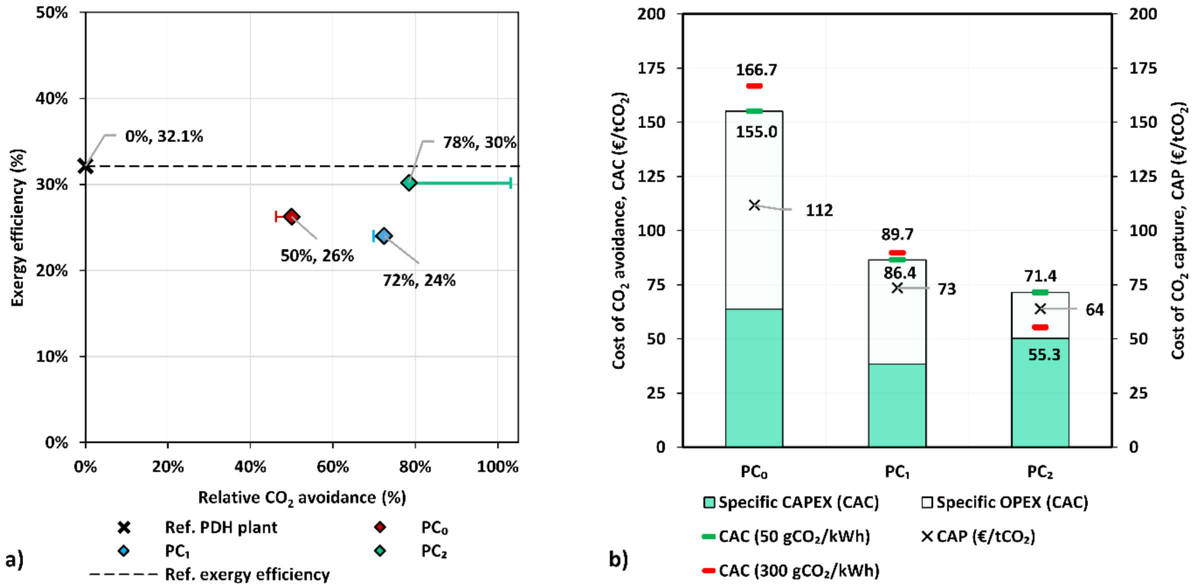

Figure 5-7: a) Comparison of the exergetic and CO_2 avoidance performances of the proposed PC_2 plant configuration with those of the intermediary process configuration (PC_0 and PC_1). These configurations assume a dedicated natural gas boiler to balance the steam demand in the CO_2 capture plant. The impact of grid emissions intensity on the overall CO_2 avoided is indicated with horizontal error bars (300 gCO_2/kWh), where the markers assume a reference grid carbon intensity of 50 gCO_2/kWh. b) Economic performances of the different decarbonized process configurations of the PDH plant. The stacked bars indicate the cost of CO_2 avoidance (CAC) in terms of specific CAPEX and specific OPEX. The black markers indicate the cost of CO_2 captured (CAP), while the green and red markers denote the avoidance costs, corresponding to a specific grid emissions intensity in the range of 50–300 gCO_2/kWh, respectively. Abbreviations: CC, carbon capture; CH, charge heater; HRB, heat recovery boiler stack; GT, gas turbine. Source: Paper II.

This retrofit results in an exergy efficiency of 26%, which is six percentage points lower than that of the unabated PDH plant (32%). The subsequent process modification, involving a switch from H_2-rich fuel gas to natural gas, increased the CO_2 concentrations in the flue gas (4%) and improved the relative CO_2 avoidance[42] by 22 percentage points compared to PC_0, although the exergy efficiency was two percentage points lower. This indicated that the exergy savings in the CO_2 capture plant were offset by combustion exergy losses elsewhere in the plant. These losses resulted from increased fuel consumption due to the lower energy content of natural gas compared to the H_2-rich fuel gas.

Overall, the proposed configuration (PC_2) achieved the highest relative CO_2 avoidance (72%) and the highest exergy efficiency (30%) compared to the other decarbonization configurations. Notably, its exergy efficiency was just two percentage points lower than that of the unabated air-regeneration train. The integration of the industrial gas turbine and the subsequent use of its exhaust gases as regeneration air resulted in three favorable outcomes. First, the CO_2 concentration increased substantially prior to the carbon capture plant, which in turn minimized the exergy loss in the CO_2 capture plant. Second, the oxygen concentrations prior to the CO_2 capture decreased compared to those in the reference plant (Table 5-1), which in turn reduces the risk of solvent losses due to oxidative degradation at high O_2 concentrations. Third, the generated electricity would have a significantly lower carbon intensity as the CO_2 capture plant at the end of the air-regeneration train captured emissions from both the industrial gas turbine and the air-regeneration train. Therefore, the higher CO_2 avoidance in the PC_2 configuration resulted directly from the low-carbon electricity produced on-site, which could be exported to the grid and reduce emissions elsewhere.

Considering the grid emissions intensity of the local energy system in which the PDH plant operates, Figure 5-7a indicates that the proposed PC_2 configuration has significant potential to increase further the relative CO_2 avoidance owing to the low-carbon electricity produced on-site. For instance, at an EU average grid emissions intensity of 300 gCO_2/kWh, the relative CO_2 avoidance increases by 25 percentage points. This is indicated by the horizontal positive error bars (green) in Figure 5-7a, where a relative CO_2 avoidance of 103% was estimated, indicating that the overall CO_2 avoidance exceeds the CO_2 generated on-site. Conversely, higher grid emissions intensity lowers the CO_2 avoidance achieved in the intermediary configurations (PC_0 & PC_1), due to their power consumption, as indicated by the negative error bars in Figure 5-7a. Other inferences from Figure 5-7a can be found in the Supplementary Material of **Paper II**.

Figure 5-7b illustrates the economic performance of the proposed configuration (PC_2) in comparison to those of the intermediary process configurations, which involve substantially diluted flue gas streams (Table 5-1). As expected, a significant and near-linear reduction in capture costs (CAP) was observed in each subsequent process configuration due to the increasing CO_2 concentrations and the absolute amount of CO_2 captured on-site (economy of scale). Interestingly, the difference between these process configurations is more pronounced when indirect CO_2 emissions and their corresponding CO_2 avoidance levels are considered.

---

[42] Absolute residual emissions decreased by 28% with fuel switching in PC_1 compared to PC_0.

In the PC_1 configuration[43], fuel switching reduced the CAC by approximately 44%–46% compared with CO_2 capture from the highly dilute flue gas stream from the unmodified PDH plant (PC_0). In the PC_2 configuration, the integration of GT conferred a significant economic advantage over its counterpart configurations, owing to the benefits of higher CO_2 concentrations, resulting in lower steam reboiler duty and the generation of low-carbon electricity from the turbine. The impact of grid carbon intensity on the CO_2 avoidance costs in PC_2 is both significant and contrasting compared to PC_0 and PC_1.

Amine-based capture plants typically exhibit higher CO_2 avoidance costs than CO_2 capture costs. However, integrating a gas turbine into PDH plants that are operating in regions with high grid carbon intensity can lead to lower avoidance costs (55 €/$tCO_{2,avo}$) than their corresponding capture costs (63 €/$tCO_{2,cap}$). This is due to the CO_2 emissions that are offset in the local energy system with the low-carbon electricity generated from the PC_2 configuration. The proposed configuration achieves an overall reduction of CO_2 avoidance cost of 58%–70% (55–71 €/$tCO_{2,avo}$), as compared with the PC_0 configuration (155–167 €/$tCO_{2,avo}$).

A sensitivity analysis was conducted in **Paper II** to evaluate the impact of energy costs on the estimated CO_2 avoidance costs. The results showed that the CO_2 avoidance cost of the PC_2 configuration was significantly influenced by electricity prices, albeit inversely, due to its low-carbon electricity production. Considering the full range of electricity and natural gas prices (see Table 3 in **Paper II**), a cost escalation factor in the range of 138%–621 % (Figure A2 in **Paper II**) would be required to obtain a CO_2 avoidance cost equivalent to that of the PC_0 configuration, where the lower bound represents a scenario with low electricity prices of 30 €/MWh. Notably, this lower bound is higher than the proposed retrofitting cost escalation factor (20%–105 % [36,38,137]) for newly integrated systems to account for unforeseen cost escalations due to system integration complexities. Overall, the proposed PC_2 configuration is comparable to the PC_0 configuration only under low electricity price scenarios and cost escalations that far exceed the expected cost escalations for such systems, emphasizing its superior economic performance.

It is important to note that these CAC estimates (Figure 5-7b) do not include additional costs associated with on-site processing of the captured CO_2 to meet either the pipeline or sea-export specifications. These costs were estimated to add 8–14 €/$tCO_{2,avo}$[44], with relatively lower costs for pipeline export than for export by sea. Assuming costs associated with long-distance transportation, intermediate and final storage could add up to 100 €/$tCO_{2,cap}$, the CAC estimates are expected to exceed[45] 281 €/$tCO_{2,avo}$, 202 €/$tCO_{2,avo}$, and 183 €/$tCO_{2,avo}$ for PC_0, PC_1, and PC_2, respectively. Nevertheless, the increasing absolute amount of CO_2 captured on-site with process modifications has only a weak impact on the overall trend of decreasing CO_2 avoidance costs towards the proposed PC_2 configuration, which has the lowest estimated avoidance cost.

---

[43] Here, the fuel gas price is assumed to be equivalent to the assumed average NG prices (6 €/GJ). Therefore, the price difference between the fuel gas and the alternate hydrocarbon fuel (with H/C <4) would ultimately determine the cost reduction attainable with the fuel switch in the PC_1 configuration.

[44] See Supplementary Material in **Paper II** for a detailed breakdown of the CAPEX and operational costs.

[45] Assuming an upper bound of 14 €/$tCO_{2,avo}$ for on-site processing (sea-export specification) and 100 €/$tCO_{2,cap}$ for long-distance transportation, intermediate storage, and final storage. The term *exceed* is used here to reflect the expected impacts of emissions and leakages along the CCTS supply chain, which would result in a CO_2 avoidance cost exceeding 100 €/$tCO_{2,cap}$.

5.3 Site-specific techno-economic analysis

This section presents the framework developed in **Paper III** and its application to the steam cracker plant case study. Section 5.3.1 outlines the methodology for quantifying and evaluating the quantitative and qualitative site-specific factors, while Section 5.3.2 presents the key results from the case study.

5.3.1 Methodological framework for incorporating site-specific factors

The framework developed in **Paper III** extends the standardized techno-economic assessment (s-TEA) methods by incorporating site-specific factors to improve early-stage comparisons of decarbonization options. In particular, it supports the early identification of the most-suitable[46] decarbonization technology for a specific industrial site by enhancing CO_2 avoidance cost estimates across the technology alternatives. The site-specific factors encompass spatial and time-related constraints that are contingent on the types and locations of unabated carbon-intensive industries.

The developed methodological framework was generalized and, together with the tools for estimating the spatial footprint and CO_2 interconnection cost, and can therefore serve as the basis for evaluating a wide array of decarbonization options in other large-scale process plants, such as pulp mills, cement plants, and oil refineries. Figure 5-8 illustrates the framework and the key steps involved in incorporating site-specific factors into standardized techno-economic assessments. These steps are:

(i) Identify and extract the pertinent site-specific factors that are expected to influence the relative CO_2 abatement costs **of** the different decarbonization technologies for a specific industrial site, and categorize them as quantitative or qualitative factors;

(ii) Quantify the site-specific factors using their respective estimation methods and tools (see Section 5.3.1.1);

(iii) Estimate the technology-specific *cost of retrofitability* (COR), calculated as the sum of all the quantified site-specific factors for each considered decarbonization technology (in €/$tCO_{2,avoided}$);

(iv) Calculate the *site-specific cost* of CO_2 capture (€/$tCO_{2,ss\text{-}cap}$) and avoidance (€/$tCO_{2,ss\text{-}avo}$)[47].

(v) Evaluate the qualitative factors (technology and site-level attributes) through expert elicitation using the retrofitability assessment matrix (see Section 5.3.1.2); and

(vi) Compile and visualize the results from the qualitative retrofitability assessment, sensitivity analysis, and site-specific costs in a diagnostics diagram, so as to obtain an enhanced visual indication of the optimal decarbonization pathway for the selected industrial site (see Section 5.3.1.3).

---

[46] In the context of **Paper III**, *most-suitable* refers to the technology selected based on both qualitative and quantitative site-specific factors, while *cost-optimal* denotes the technology option incurring the lowest CO_2 avoidance cost (compared to a non-exhaustive list of alternative decarbonization technologies) at a host process plant.

[47] Site-specific CO_2 capture and avoidance costs are the sum of technical cost of CO_2 capture and avoidance obtained from the s-TEA method (see Figure 5-2), and the estimated cost of retrofitability in terms of €/$tCO_{2,cap}$ or €/$tCO_{2,avo}$, respectively.

5.3.1.1 Methods and tools for quantifying key site-specific factors

Industrial sites are highly heterogeneous, not only across sectors but also among plants within the same industry. To account for this heterogeneity, generalized quantification methods and tools were developed to estimate the key quantitative site-specific factors, such as the opportunity costs associated with occupying available space on existing sites, energy supply costs, site-layout-dependent CO_2 interconnection costs, and costs incurred due to forced downtime and premature decommissioning of newly installed equipment as consequence of being locked into the residual lifetime of the host plant.

Essential site-specific information for quantifying these factors includes the existing site-energy system, site layout indicating available space and preferred placement of new technologies, maintenance schedules, and residual lifetimes of existing assets. The quantification methods and tools were designed to work with limited site-specific information from a particular site. For instance, aerial imagery using GIS tools was used to categorize the site layout and to identify the available space and on-site assets (e.g., stacks, tank farm, pipe racks, etc.).

When detailed site-specific information is unavailable, reasonable industry-specific assumptions can be applied. For example, factors such as the site energy system, turnaround times, and annual maintenance shutdown periods can be generalized based on the industry type. Sensitivity analysis is recommended for time-related factors such as forced downtime and premature decommissioning due to the technology lock-in effect, to evaluate disparities between the technologies with respect to expected cost escalations. This evaluation considers delays that occur during installation in the short term and deployment in the long term relative to the residual lifetime of the host plant. Outlined below is a brief description of the considered site-specific factors and the methods used for their quantification.

Opportunity costs: Figure 5-9 provides an overview of the method that was developed to quantify the opportunity cost of decarbonization technologies at a specific site. The opportunity cost (C_{OC}) refers to the cost of occupying available land with decarbonization technologies, where the alternative would be to continue operating the unabated process plant while incurring direct operational costs i.e., the added cost of emitting CO_2 or alternative use of the available land for installing, at a later time, an emerging low-carbon production technology, that both avoids CO_2 emissions and generates revenue.

To this end, a space-value graph was created based on the process design hierarchy[48] [54]. This graph used the plant's total annual revenue to assign a value to the space on-site, while the process design hierarchy enabled a generalized categorization of site layouts of different process industries with typically large spatial footprints. A modified onion-diagram was introduced[49], with its layers representing different plant sections. As the modified onion-diagram ranked the plant sections in increasing order of their value addition or contributions to the total annual revenue, accumulative site-specific value (SV) functions were assumed that represented the opportunity cost of occupying available space in different plant sections.

---

[48] Also referred to as the onion model for process design which illustrates the sequential nature of process design, where the synthesis and optimization of design parameters in the reactors section are prioritized, followed by the subsequent layers of the onion diagram, to obtain a complete design [164].

[49] Adapted to illustrate the increasing order of accumulative value additions or contributions to the total annual revenue of the process plant.

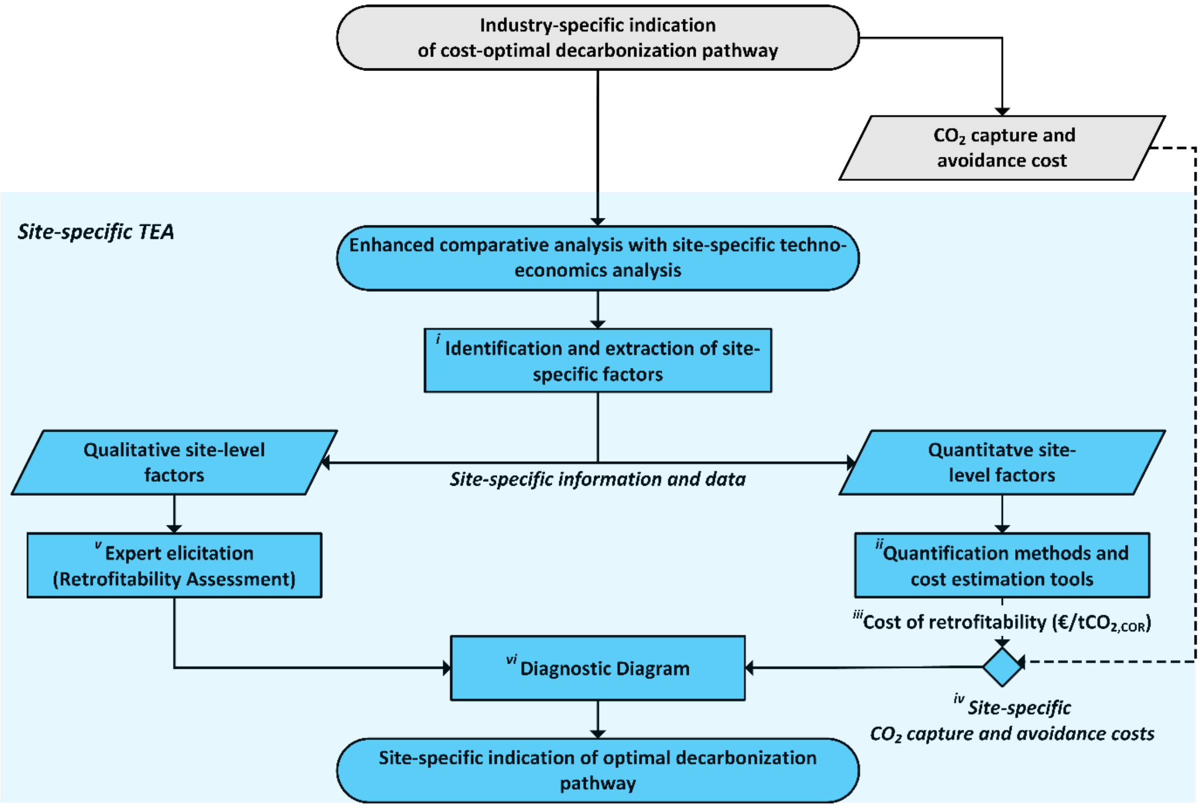

Figure 5-8: Overview of the framework methodology applied in Paper III to enhance the comparative analysis of the different decarbonization pathways, incorporating site-specific factors. The oval symbol indicates the start/end of the framework methodology, the parallelograms indicate input/calculated data, and the rectangles indicate methods. Gray-shaded shapes indicate the application of the standardized TEA method, while the blue-shaded shapes indicate the site-specific techno-economic analysis. Adapted from Paper III.

To address the subjectivity related to valuing site space, this method introduced a conservative (max/min) approach by assuming linear (VF_l) and non-linear (VF_{nl}) site-specific value functions[50] indicated with red and blue lines in Figure 5-10, respectively. These functions represent a plausible range of value-addition from each plant section to the total annual revenue. The space-value graph was complemented with a merit order for space utilization to determine where decarbonization equipment could be placed on-site at an early assessment stage. The merit order was ranked based on the available space within an existing process plant and its type, i.e., brownfield or greenfield areas. Unoccupied brownfield areas were prioritized first, followed by brownfield areas with redundant units (after removal/rearrangement) and finally greenfield areas. Based on the determined placement of decarbonization equipment within the plant and their estimated spatial footprints[51], the opportunity cost was calculated as the revenue forgone over the host plant's lifetime as shown in Equation 8. This cost also accounts for the emissions cost avoided following the installation of the decarbonization technology during the same period.

---

[50] The linear SV function sets the maximum, while the non-linear SV function sets the minimum. The linear SV function implies that all plant sections are valued equally by the plant owner, whereas the non-linear function represents the exponentially increasing land value as one progresses from the outer layers of the modified onion-diagram towards the inner plant sections. The gradient of the exponential function depends on the type of process plant, as the physical footprint of its core production units (reaction section) and their relative contributions to total annual revenue are expected to vary between plants.

The net present value method was used to discount the cumulative forgone annual revenue and avoided emissions costs for the remaining lifetime of the host process plant, as these cash flows are not realized until the end of a specific year of decarbonized operation.

Site-layout-dependent interconnections: Figure 5-9 illustrates the site-layout-dependent CO_2 interconnections, including the flue gas ductwork, solvent lines, and CO_2 pipelines, for post-combustion CO_2 capture within the plant boundaries. This example highlights how CO_2 network configurations can vary depending on site-layout constraints. To enable quantification of these interconnection costs, a simplified local CO_2 network cost estimation tool was developed in **Paper III.** This tool was based on the network design hierarchy introduced by Berghout et al. [138], which was used to determine the design and technical specifications of each component in the local CO_2 transportation network.

The main inputs to the network design calculations were the operating pressure and temperature of the pipeline, along with the flow rates and physicochemical properties of the transported gas or liquid. These costs were subject to limitations imposed by the site layout, for which an optimal network route within the plant boundary of the case study plant was determined using aerial images and additional site-specific information, such as the space available within the plant for accommodating and installing CO_2 capture equipment. The resulting site-layout-dependent interconnection costs are incurred as CAPEX during construction and expressed as the total specific CO_2 network costs (C_{netw},€/$tCO_{2,avo}$), normalized to the technology-specific annual CO_2 avoidance achieved.

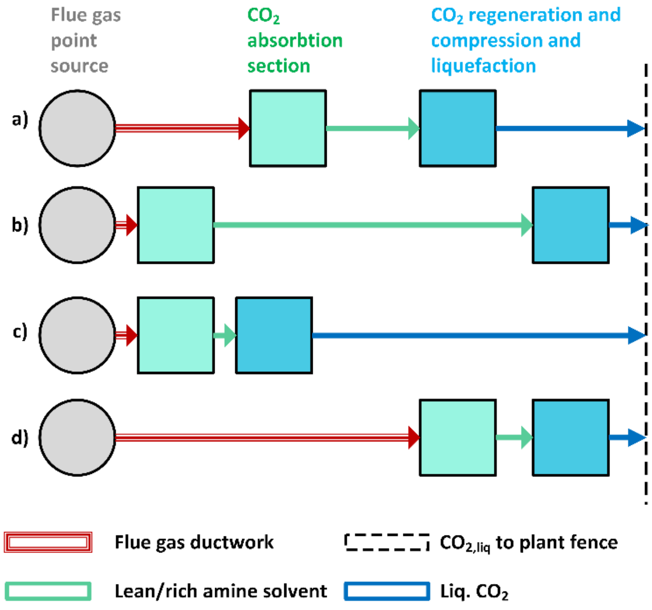

Figure 5-9: Illustrative example of the site-layout-dependent CO_2 interconnections for transporting CO_2 from single-point source emissions to the plant fence at space-constrained sites, adapted from Roussanaly et al. [139]**, where additional interconnection configurations for multiple-point source emissions can be found.**

---

[51] In **Paper III**, a spatial footprint estimation tool was developed to estimate the space required for installing an amine-based CO_2 capture plant, including compression and liquefaction units, at a specific site based on the flue gas properties, i.e., flue gas flow rate and CO_2 concentration. The tool uses publicly available data (e.g., FEED reports) for the area requirements of Post-CCS plants to derive correlations between the spatial footprint and flue gas properties. Further details are provided in the appended paper.

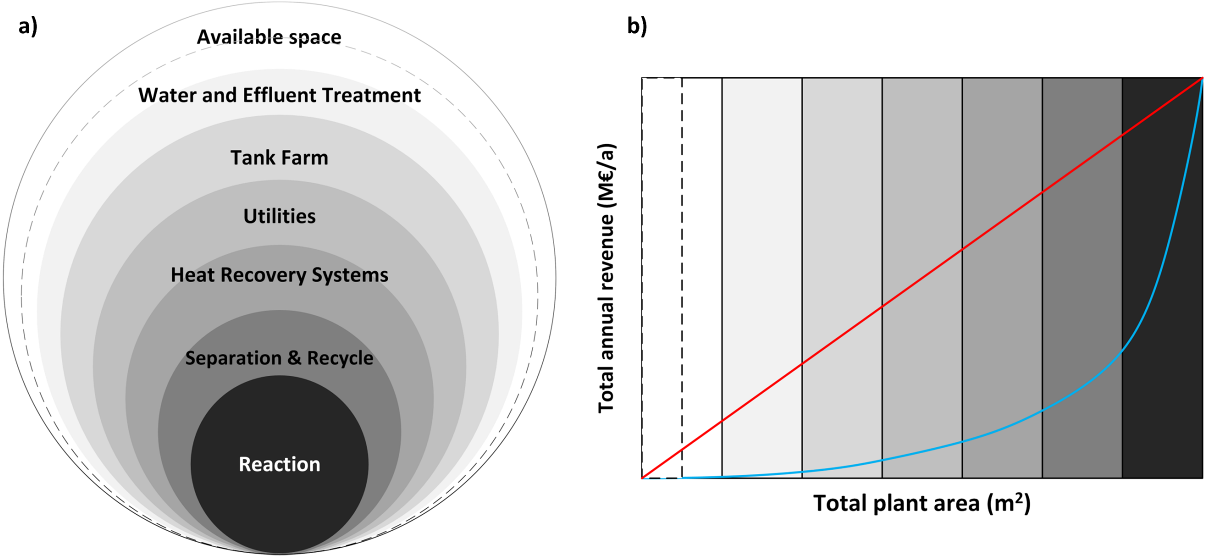

Categorization of site-layout based on process design hierarchy

Representation of different plant sections on the space-value graph

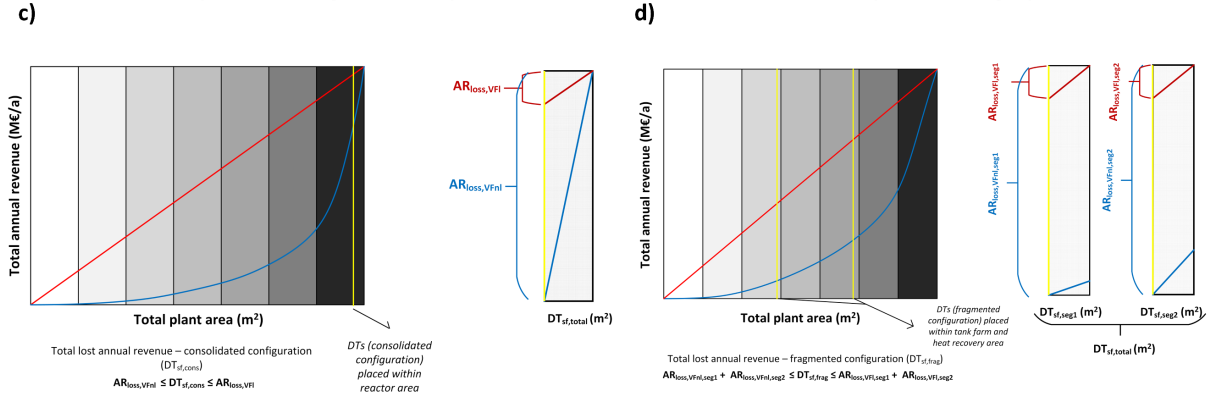

Figure 5-10: (a) Categorization of the site layout of a process plant based on the process design hierarchy [140] and (b) its representation on the space-value graph, which represents the different plant sections from the onion diagram. Note that all gray-shaded layers in the diagram shown in subplot (a) are assumed to have equal areas and are arranged in subplot (b) in increasing order (from left to right) based on their cumulative value addition or contribution to the total annual revenue of the process plant. The dashed vertical line indicates the categorization of available or allocated space for future expansion as brownfield and greenfield areas. Red and blue lines indicate the linear and non-linear space value functions. Overview of calculation procedure for estimating opportunity cost of occupying space available on-site with DTs that is dependent on its layout configurations – c) consolidated configuration (all DTs in one plant section), and d) fragmented configuration (distributed placement of DTs in multiple plant sections). Figure 14 in Paper III shows the outcome of the applied method to the steam cracker plant. Abbreviations: SF – spatial footprint, AR – annual revenue, VF –value function, seg–segment.

$$\mathrm{C_{OC}} = \sum_{j=0}^{\mathrm{RLT}} \left({}^{\left(\mathrm{DT}_{\mathrm{sf}_{\mathrm{cons/frag}}}\right)}\!\Big/_{(1+\mathrm{i})^{\mathrm{j}}} \right) - \sum_{j=0}^{\mathrm{RLT}} \left({}^{\left(\dot{\mathrm{m}}_{\mathrm{CO}_{2\,\mathrm{cap/avo}}} * \mathrm{CO}_{2_{\mathrm{avg}_{\mathrm{tax}}}}\right)}\!\Big/_{(1+\mathrm{i})^{\mathrm{j}}} \right) \left[\frac{€}{\mathrm{tCO}_{2,\mathrm{cap/avo}}} \right] \qquad (8)$$

Forced downtime: The cost of forced downtime (C_{FD}) was quantified as lost revenue (M€), corresponding to the time for which a process plant is shut down, assuming that integration of decarbonization technologies renders the host process plant non-operational beyond the timeframe of the scheduled maintenance shutdown. Depending on the year of operation and the type of industry, this timeframe could last up to 2–4 weeks in a regular year and 1–3 months in a turnaround year. Given that it is rather challenging to foresee commissioning delays, a sensitivity analysis was performed to assess the potential revenue losses from the forced downtime. These costs were accounted for as CAPEX during the construction of the decarbonization technology, and were normalized to the technology-specific annual CO_2 avoidance so as to obtain the specific cost of the forced downtime. In **Paper III**, Figure 16 illustrates the sensitivity of forced downtime costs to the plant stoppage or downtime duration.

Cost of premature decommissioning (lock-in effect): Figure 5-11 illustrates an example of how delayed adoption or deployment of CCS relative to the lifetime of the host process plant can lead to cost escalations. The lock-in effect of the decarbonization pathway, with its host process plant, was demonstrated with the capital recovery factor applied to its total capital requirement, where the operational lifetime of the decarbonization technology (DT_{OLT}) was assumed to be equal to the residual lifetime of the decarbonized process plant (where $DT_{OLT}<DT_{ELT}$), in order to obtain the cost of premature decommissioning (C_{PD}).

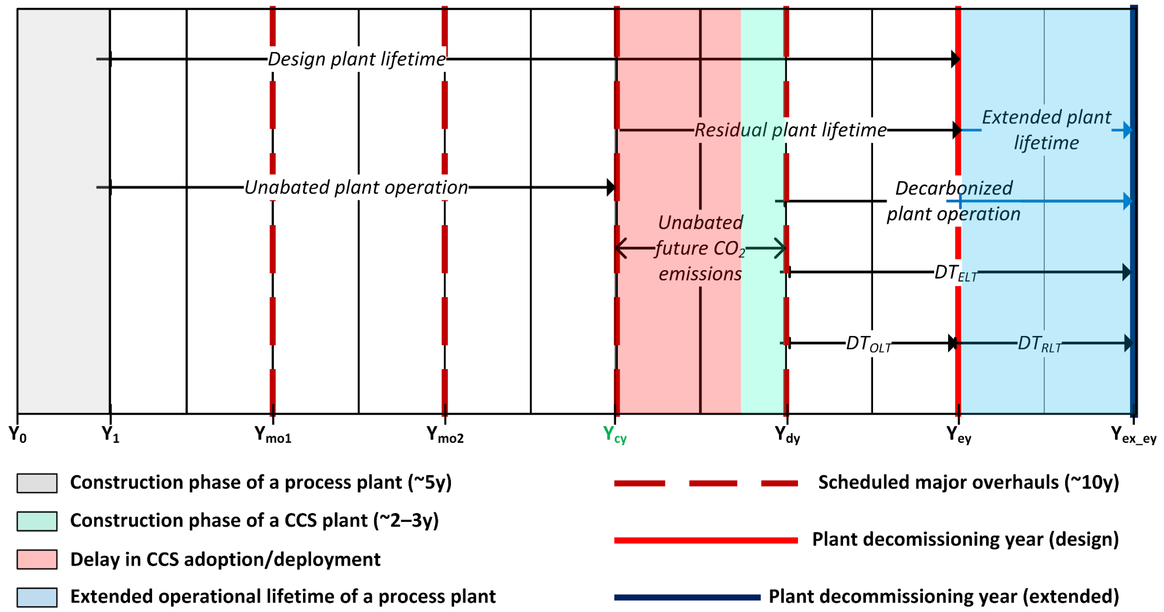

Figure 5-11: Illustrative example of delayed adoption/deployment of CCS relative to the lifetime of the host process plant. Each vertical gridline corresponds to a five-year operation period. Figure abbreviations: Y_0 –Year of process plant construction, Y_1 – First year of plant operation, Y_{mo} –Scheduled major overhaul year, Y_{cy} – Current year of operation, Y_{dy} – Planned year of commissioning of decarbonization equipment, Yey – Scheduled process plant decommissioning year, Y_{ex_ey}–Extended plant decommissioning year with reinvestments, DT_{ELT} – Economic lifetime of the installed decarbonization technology, DT_{OLT} –Expected operational lifetime of the decarbonization technology, DT_{RLT} – Residual economic lifetime of the decarbonization technology.

In contrast, a decarbonization technology with the possibility to operate as a stand-alone process plant, such as the Pre-CCS pathway, is not considered to be locked into its host process plant. Therefore, the operational lifetime of the newly installed equipment could be assumed to be equal to its design lifetime. However, the timing of the deployment becomes critical for the alignment of the design lifetime of the equipment and the residual lifetime of the host plant. Figure 5-12 shows the results of applying this method to the steam cracker plant case study, visualizing how CO_2 capture costs and avoidance costs escalate with delays in the installation and deployment of decarbonization technologies that tend to be locked into their host plant.

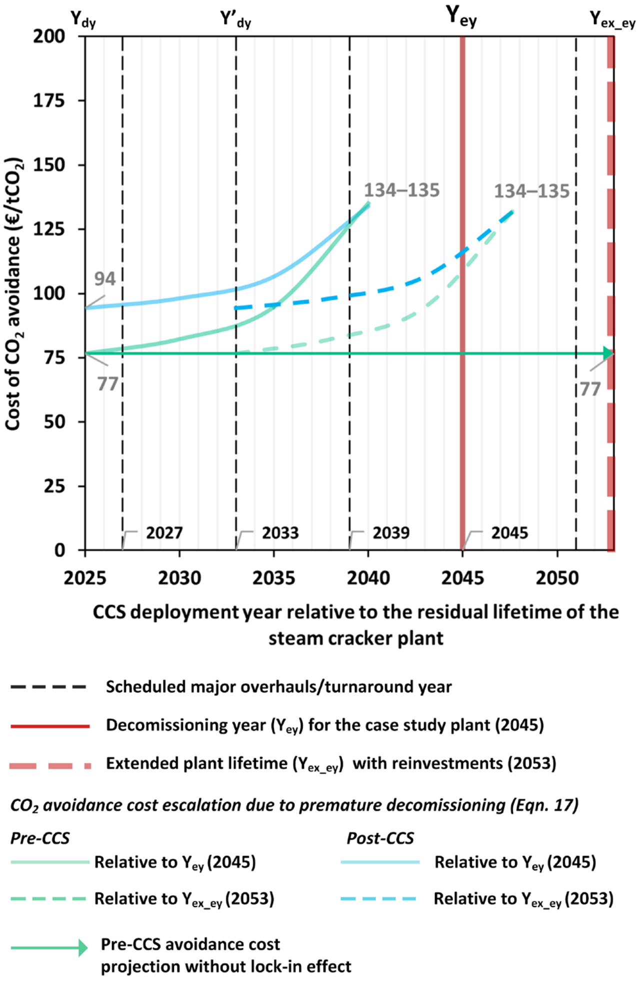

Figure 5-12: CO_2 avoidance cost escalation (C_{PD_total}) due to premature decommissioning relative to the residual lifetime of the steam cracker plant. Red solid line – scheduled decommissioning year of 2045 (Y_{ey}~2045); Red dashed line – extended decommissioning year (Y_{ex_ey}~2053); Black dashed lines – turnaround years that occur every six years. Figure abbreviations: Y_{dy} – CCS deployment year, Y'_{dy} – Synchronized deployment with turnaround year, which enables full utilization of CCS design lifetime until Y_{ex_ey}.

Cost of energy supply options and their emissions intensity: The site energy system varies across industrial plants due to differences in the feedstock slate and fuel mix at the site, whereas the electricity source and associated emissions intensities depend on the location of the plant. Therefore, energy supply costs and emissions intensity represent additional site-specific factors that could influence the equivalent CO_2 avoidance[52], and, in turn, affect the technology-specific cost of CO_2 avoidance. To capture this uncertainty, a two-way sensitivity analysis was conducted to assess the impact of indirect CO_2 emissions on the equivalent CO_2 avoidance, as well as the variation in CO_2 avoidance costs in different energy supply cost scenarios for the decarbonization technologies considered. Additional details and the calculation procedures can be found in **Paper III**.

Cost of retrofitability: The cost of retrofitability (C_{COR}) was defined as the sum of all the quantified site-specific cost factors, which excluded the technical cost of CO_2 avoidance from the s-TEA method, as shown in Equation 5. The site-specific cost of avoidance ($CAC_{site\text{-}specific}$) was then calculated as the sum of the cost of retrofitability and baseline avoidance cost estimates obtained from the s-TEA method (CAC, Equation 4), as shown in Equation 10.

$$\text{Cost of retrofitability } (C_{COR}) = C_{OC} + C_{netw} + C_{FD} + C_{PD} \left[\frac{€}{tCO_{2,avo}}\right] \tag{9}$$

$$\text{Site} - \text{specific cost of } CO_2 \text{ avoided } \left(CAC_{site-specific}\right) = CAC + C_{COR} \left[\frac{€}{tCO_{2,avo}}\right] \tag{10}$$

5.3.1.2 Retrofitability assessment matrix

To evaluate factors that may support or hinder the integration of decarbonization technologies at a specific industrial site, **Paper III** introduced a qualitative *retrofitability assessment matrix*. This approach involved expert elicitation on factors such as dependence on external energy supply, reliance on external infrastructure (electricity grid, CO_2 pipelines), sensitivity to fuel and electricity prices, complexity of system integration, adaptability to future feedstock switches, availability of resources, alternative utilization of CO_2 capture equipment, and the feasibility of achieving 100% carbon recovery for CO_2 utilization pathways.

The retrofitability assessment matrix incorporates generalized definitions for each qualitative factor, which are applicable to any unabated process plant of interest (see Supplementary Materials in **Paper III**). The expert elicitation on site-specific factors involved a qualitative assessment based on their perceptions of the expected impact of a certain decarbonization technology on the host process plant. Each site-specific qualitative factor was assigned a 0–1 impact score. An impact score of 1 indicated that the evaluated factor has a higher overall impact on the host plant, implying more severe perceived risks and unforeseen costs, while a score of 0 indicated a lack of impact on the host plant.

---

[52] Equivalent CO_2 avoidance is defined as the amount of CO_2 avoided relative to the host plant (see Equation 3 in **Paper III**).

5.3.1.3 Combining quantitative and qualitative site-specific factors

A diagnostic diagram, presented as a spider plot with a scale of 0–1, combines the outcomes for the quantified site-specific factors, sensitivity analysis, and the retrofitability assessment matrix. A broader spread in the spider plot for a decarbonization technology indicates a sub-optimal choice, as compared with other options depicted in the same plot. The spider plot serves the purpose of comparing factors that are not directly comparable with one another and are not, per se, the primary determinants for selecting a cost-optimal decarbonization technology. No weighting factors were applied for the case study in **Paper III**. However, weighting factors could be assigned to the individual qualitative site-specific factors deemed important for other industrial sites. The calculation method used for plotting the site-specific factors in the diagnostic diagram is detailed in **Paper III**.

5.3.2 Impact of site-level constraints on the technology choice and CO_2 abatement costs – Steam cracker plant

Figure 5-13 illustrates how the baseline CO_2 avoidance cost estimates derived from the standardized TEA method (gray bars) can escalate when site-specific cost factors (red solid floating bars) are added. These resulting in the site-specific costs of avoidance for the Post-CCS (blue) and Pre-CCS (green) pathways considered for the steam cracker plant case study in **Paper III**. These cost escalations are estimated according to the set of baseline site-specific assumptions (Table 6 in **Paper III**), to illustrate the differences in a conservative manner. To capture the full scope of the expected cost escalation beyond these assumptions, **Paper III** presents a sensitivity analysis of each site-specific factor.

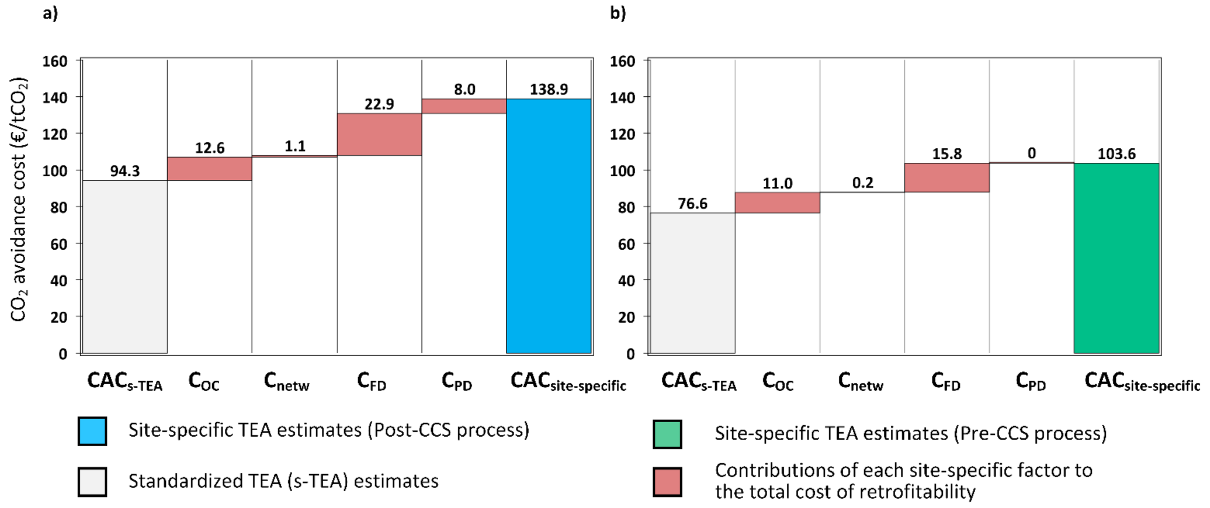

Figure 5-13: Site-specific cost of CO_2 avoidance for (a) Post-CCS and (b) Pre-CCS pathways. Note that the average value of opportunity costs (estimated for different space-value functions) was taken here, with the baseline assumptions listed in Table 6 in Paper III. Including additional costs for CO_2 transportation and final storage (104 €/tCO_2 [40]), the total CO_2 avoidance costs amount to 243 €/tCO_2 for the Post-CCS pathway and 208 €/tCO_2 for the Pre-CCS pathway. Figure abbreviations: s-TEA – standardized TEA, C_{OC} – Opportunity cost, C_{netw} – CO_2 network costs, C_{FD} – Forced downtime costs, C_{PD} – Premature decommissioning costs due to technology lock-in effect. Source: Paper III.

The forced downtime has by far the strongest impact on the site-specific CO_2 avoidance cost, followed by the opportunity costs of space available on-site and the technology-specific lock-in effect in relation to the residual lifetime of the case study plant. Accounting for avoided CO_2 emissions, the cost difference between the two decarbonization alternatives widens significantly, as shown in Figure 5-13a–b. The site-specific avoidance costs increase by roughly 47% and 35% for Post-CCS and Pre-CCS (139 €/t$CO_{2,avo}$ and 104 €/t$CO_{2,avo}$) from their respective baseline CO_2 avoidance cost estimates of 94 €/t$CO_{2,avo}$ and 76 €/t$CO_{2,avo}$.

This difference is primarily due to the technology-specific characteristics of the Pre-CCS pathway, which utilizes a relatively smaller space on-site and remains unaffected by the lock-in effect, as the newly installed process equipment can be run as a standalone hydrogen production plant that utilizes natural gas from the grid. Although the Pre-CCS pathway entails higher installation complexity[53] and has a higher probability of forced downtime, the incurred cost escalation remains lower than the estimated C_{FD} for the Post-CCS pathway, owing to the significantly higher level of CO_2 avoidance achieved with the Pre-CCS option. With the inclusion of site-specific factors, the relative differences in the CO_2 avoidance cost estimates between the two decarbonization options increase from approximately 20% with conventional TEA methods to 29% with the site-specific TEA method.

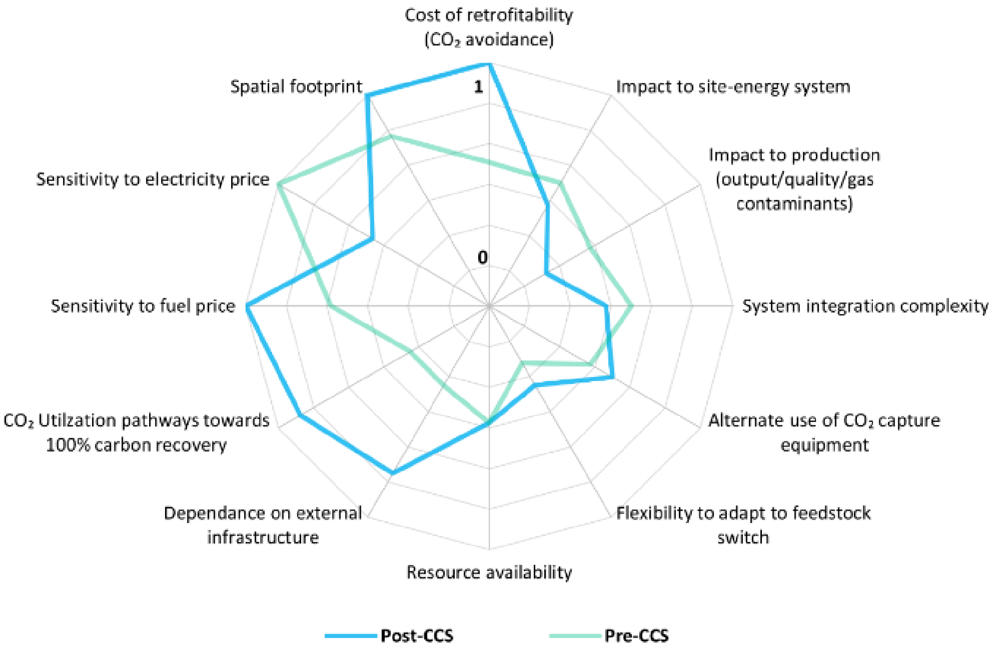

Figure 5-14: Diagnostic diagram combining quantitative site-specific factors (cost of retrofitability, spatial footprint, and sensitivities to fuel and electricity prices) with the results of the qualitative retrofitability assessment obtained through expert elicitation for the steam cracker plant. The averaged values of the expert elicitation on qualitative factors are plotted. Source: Paper III.

---

[53] For revamping the existing fuel gas system and replacing or modifying burners to enable hydrogen firing in existing cracker furnaces.

Figure 5-12 shows the diagnostic diagram that combines the quantitative site-specific results with a qualitative assessment of the site-specific factors, so as to obtain an enhanced indication of the optimal decarbonization technology for the case study plant. Based on expert elicitation, qualitative factors such as flexibility to adapt to future feedstock switches, resource availability, alternative use of CO_2 capture equipment, the possibility of achieving 100% carbon recovery towards CO_2 utilization pathways, cost of retrofitability in terms of CO_2 avoidance, spatial footprint, and reduced sensitivity to fuel prices generally favor the Pre-CCS process. In contrast, factors such as system integration complexity, sensitivity to electricity prices, dependence upon external energy supply, and reliance on external infrastructure favor the Post-CCS process. Utilizing the diagnostic diagram, the Pre-CCS option, with an average score of 0.47 (showing a narrower spread on the diagnostic diagram), was determined to be the preferred decarbonization alternative over the Post-CCS pathway (average score, 0.59), implying relatively higher risks related to technical and economic uncertainties.

5.4 Integrated hydrogen production systems

This section presents the framework developed in **Paper IV** and its application to the steam cracker plant introduced in Section 3.3.3, with an expanded scope, as detailed in Section 3.2.4. Section 5.4.1 describes the framework, while Section 5.4.2 presents the key results that illustrate the impact of site- and price-specific conditions on the integrated hydrogen production system and compares its performance with that of standalone systems.

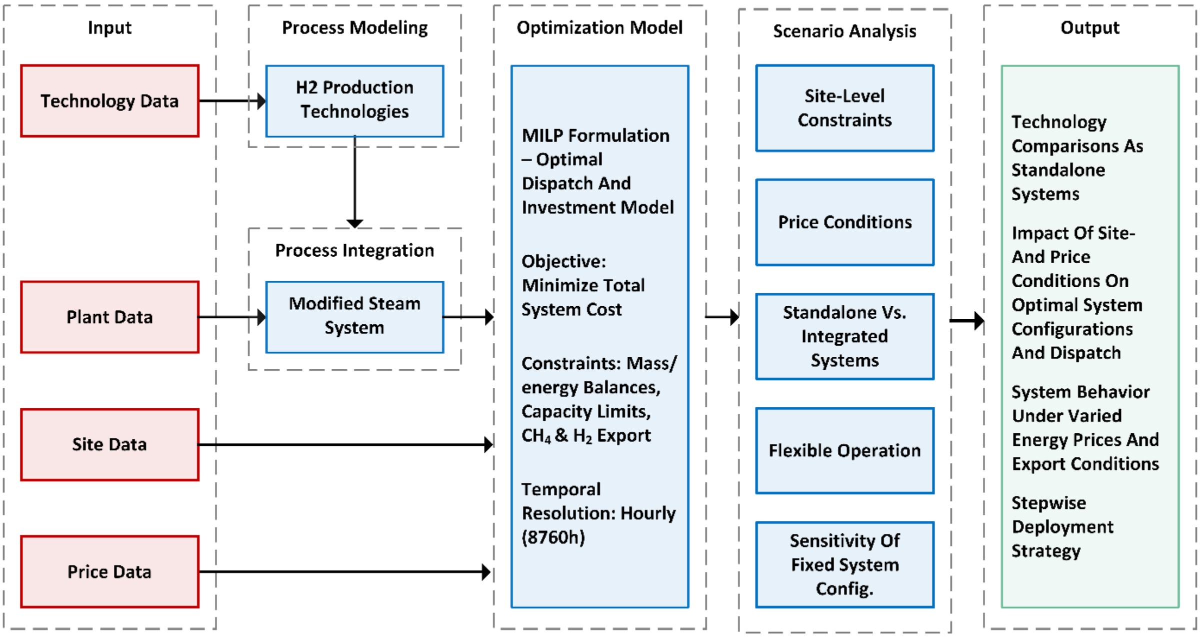

Figure 5-15: Overview of the framework methodology applied in Paper IV. Red indicates inputs, green indicates outputs, and the blue boxes represent the numerical models developed and the scenarios investigated in this work.

5.4.1 Methodological framework for cost-optimal design and operation of an integrated hydrogen production system under site constraints and energy market uncertainty

In **Paper IV**, the framework combines steady-state process modeling, process integration, and cost optimization methods to determine cost-optimal hydrogen supply strategies through the integrated hydrogen production system within a petrochemical cluster, as illustrated in Figure 5-13. At the core of the framework is a mixed-integer linear programming (MILP) model that was formulated as an investment and dispatch model designed to optimize the technology mix and hourly hydrogen dispatch strategy. The model minimizes the total system costs (TSC), while being subject to a set of technical, operational, and site-specific constraints. The key constraints are grid transmission capacity, ammonia tank capacity, fuel gas availability, minimum load limits, and ramp rate restrictions. A complete model description, including the nomenclature, input data, and related assumptions, can be found in the Supplementary Material of **Paper IV**. Although this framework was demonstrated using a steam cracker plant in **Paper IV**, it can be applied to other industries or industrial clusters that have significant hydrogen demands. The key steps of the framework are as follows:

i) Select a set of complementary hydrogen production technologies that are appropriate for the site. The selection should be guided by both the specific constraints of the selected site and technology-specific attributes, such as energy efficiency, ramping limits, operational range, and costs. Most importantly, complementary technologies are recommended, as they can help to balance the trade-offs between cost, combining operational flexibility and energy dependence. This may involve combining fast- and slow-ramping technologies, electrified options with those requiring additional fuels or feedstocks, and technologies that rely on domestic supply with those that are dependent upon imports.

ii) Evaluate opportunities for shared infrastructure and material integration. Hydrogen production technologies may exchange utilities such as fuel gas, steam, and byproducts (e.g., oxygen), through integration with the site energy system. In **Paper IV**, the hydrogen production technologies were modeled to establish their mass and energy balances and integrated with the steam network of the steam cracker plant, whereby surplus on-site steam and steam recovered from newly installed equipment were used to supply the steam generator of the SOEC. Such integration can reduce the overall system costs by offsetting utility demands through internal resource use.

iii) Estimate the current or future hydrogen demand for a specific industry or its surrounding cluster, depending on the scope of the assessment. Low-emissions hydrogen can replace existing gray hydrogen or be used as fuel in furnaces and process heaters. Current demand can be estimated based on existing on-site gray hydrogen use (e.g., in refineries) or the fired duties of furnaces and heaters[54]. Since most CO_2 emissions in clusters originate from fuel gas combustion, any byproduct fuel gas not used for hydrogen production or export would otherwise require CO_2 capture. Accordingly, the future hydrogen demand can be approximated as the amount required to convert all the captured CO_2 into a single end-product (e.g., methanol), representing a high-demand scenario for hydrogen use in the cluster.

---

[54] If gray hydrogen is currently produced from internal byproduct fuel gas rather than natural gas, replacing it with low-emissions hydrogen may require repurposing of the fuel gas as feedstock or its export. This may involve recovering hydrogen using pressure swing adsorption (PSA) to reduce the internal hydrogen demand, and purifying the remaining hydrocarbon tail gas to meet natural gas grid specifications.

iv) Identify the relevant site-specific constraints and assign reasonable lower and upper bounds for each constraint in order to develop site-level scenarios[55]. Constraints such as grid transmission capacity, ammonia storage capacity, and fuel gas availability were considered in **Paper IV**. However, these can be adapted to the selected technologies and extended to include additional factors, such as on-site space availability (accounting for technology-specific spatial footprints).

v) Define two extreme price scenarios, i.e., low-price and high-price conditions, by setting each economic parameter[56] to its respective lower and upper bounds. These scenarios establish plausible cost ranges (LCOH and OHSC) for the considered hydrogen production technologies as standalone systems or integrated systems under various site conditions.

vi) Conduct a combined scenario and sensitivity analysis by varying the site-specific constraints and price scenarios. A structured scenario matrix based on a full factorial design can be used to estimate the impacts of site conditions on system costs and OHSC. For example, in **Paper IV**, the grid capacity and fuel gas availability were mapped along the *x*- and *z*-axes, while ammonia storage was varied at two discrete levels along the *y*-axis (see Figure 5-14). Based on this plot, one can identify plausible cost ranges for the optimized configuration of the integrated system, or conversely, determine the site and price conditions required to achieve the lowest system costs and corresponding OHSC.

vii) Formulate or adapt the MILP optimization model in **Paper IV** to determine the cost-optimal technology mix and dispatch strategy, based on the defined site-specific constraints and price scenarios.

viii) Evaluate the impacts of electricity and methane pricing structures, along with the possibility for hydrogen export, on the operation of the integrated system. First, select a plausible future site condition (i.e., a specific combination of site-specific constraints) and determine the optimal system configuration under the baseline price conditions. Then, fix this configuration and run the optimization model for combinations of different pricing structures and export options, to evaluate the trade-offs between price certainty (e.g., through PPAs) and flexible operation (for details, see Section 4.2.3 in **Paper IV**).

ix) Compare the hydrogen production technologies used as standalone systems with the optimized configurations of the integrated system that were identified by considering site-specific constraints. In **Paper IV**, this comparison is illustrated using a two-dimensional plot, where the *y*-axis shows the estimated LCOH or OHSC ranges, the primary *x*-axis represents total annual system cost (M€/y), and a secondary *x*-axis relates these system costs to the corresponding CO_2 abatement costs (€/tCO_2). In this plot, the degree of overlap between the optimized integrated system configurations (represented as markers) and the standalone systems (shown as shaded regions) indicates their relative cost competitiveness[57].

---

[55] For example, the lower bound could represent current site conditions, while the upper bound could be based on reasonable assumptions or projections in relation to price (see Table 2 in **Paper IV**).

[56] For example, electricity, ammonia, fuel gas, EU ETS emissions allowance price (see Table 1 in **Paper IV**).

[57] Note that standalone systems are evaluated independently of site-specific conditions, whereas the integrated systems are evaluated considering the site-specific constraints. When a standalone system appears to outperform an integrated system, it is important to consider whether the corresponding site conditions are realistic in the near term or align with targeted emissions reduction trajectories. Conversely, when the integrated system performs better than the standalone systems, this may reflect favorable site conditions, such as increased availability of byproduct fuel gas, which are not accounted for in the fixed baseline assumptions of the standalone systems.

x) Derive an indicative stepwise deployment strategy in which each technology is deployed based on the technology-specific CO_2 abatement cost estimates relative to EU ETS emissions allowance price projections. A more detailed and robust deployment strategy could be derived if the site and price factors are known with greater certainty, e.g., ammonia prices (through long-term contracts), fuel gas availability, grid capacity, renewable electricity prices (e.g., via PPAs), and the potential for hydrogen export based on expected offtake prices.

5.4.2 Techno-economic performance of integrated hydrogen production system and stepwise deployment strategy

5.4.2.1 Impacts of site- and price conditions on hydrogen production costs

Figure 5-14 illustrates the impacts of site-specific constraints such as ammonia tank capacity, grid transmission capacity, and the availability of byproduct fuel gas on the optimal system configuration, comprising SOEC, AC, and ATR-CCS, under low-price (Figure 5-14a) and high-price (Figure 5-14b) conditions.

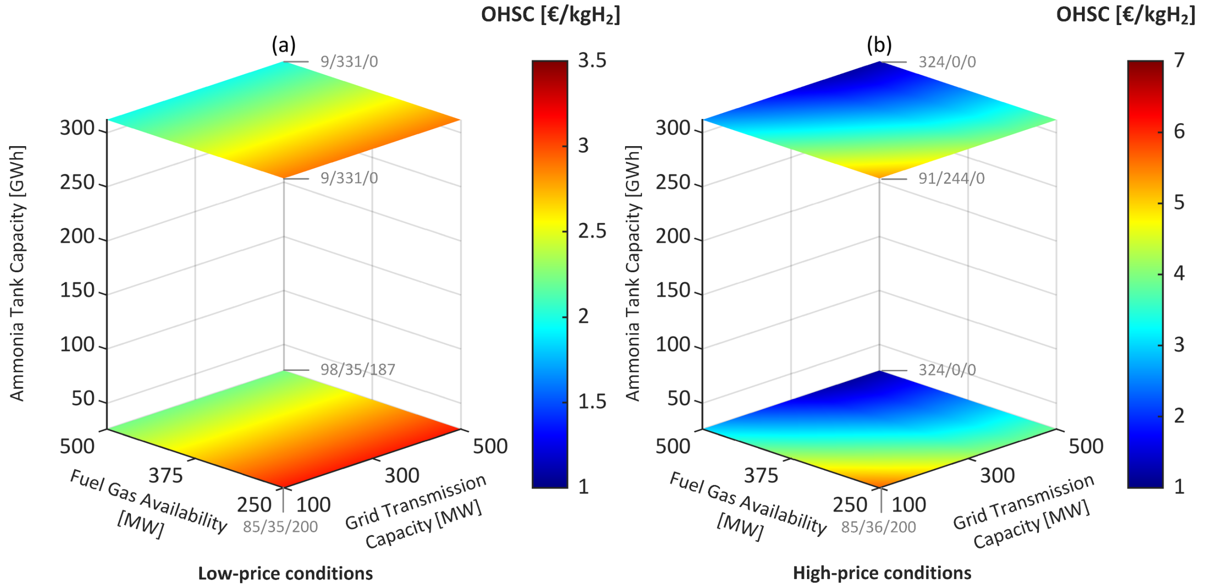

Figure 5-16: Impact of site-specific factors on the on-site hydrogen supply costs (€/kgH_2) under (a) low-price and (b) high-price conditions, accounting for offsets from repurposing or exporting methane recovered from the fuel gas. The optimal system configurations at the minimum and maximum estimated OHSC in the top and bottom planes of each subplot are annotated as SOEC/AC/ATR in MW, indicating the installed capacities of each technology (see Figure S.3 in the Supplementary Materials of Paper III). Note: the OHSC scales differ between the two subplots.

The scenario analysis reveals two clear trends. First, access to more fuel gas increases the potential for methane export, which results in a significantly lower OHSC. For instance, under low-price conditions (Figure 5-14a), the LCOH was in the range of 3.0–3.7 €/kgH_2, while the OHSC was in the range of 2.0–3.1 €/kgH_2. This offset was even more pronounced under high-price conditions (Figure 5-14b), whereby the LCOH range is 5.6–7.9 €/kgH_2 and the OHSC range is 1.2–5.7 €/kgH_2. Second, the optimal installed capacities remained relatively consistent under low-price conditions, whereas high-price conditions led to notable changes in the system configuration with increasing hydrogen production costs (see Figure S.3 in **Paper IV**). These shifts reflect how site limitations constrain technology selection, often favoring technologies with higher hydrogen production costs.

Under low-price conditions (Figure 5-14a), ATR-CCS dominated the optimal system configuration. However, its installed capacity was strongly influenced by the availability of on-site ammonia storage, leading to the installation of larger ammonia crackers. When both ammonia storage and grid transmission capacities were limited, the integrated hydrogen system shifted towards reformer-dominated configurations, regardless of the energy price. These configurations typically relied heavily on internal methane use, thereby limiting the system's ability to export methane. In contrast, when at least one of the two capacities was available, methane export was consistently favored.

When sufficient ammonia storage was available (~312 GWh), ammonia cracking emerged as the dominant hydrogen supply option, meeting 97% of the demand. The remaining 3% was supplied by the SOEC. In this case, the shift towards ammonia cracking was driven by the potential to reduce TSC through the export of byproduct methane in the integrated system configuration. Unlike the standalone ATR-CCS systems, in which methane is repurposed as feedstock without incurring any additional cost, the optimized model treats methane use as a cost to ensure fair comparison. This reflects the opportunity cost of using methane internally rather than increasing the capacities of other technologies and exporting the methane.

Under high-price conditions (Figure 5-14b), the highest OHSC (>5.3 €/kgH_2) was observed in those scenarios in which both grid transmission capacity (100 MW) and fuel gas availability (250 MW) were limited. SOEC dominated the optimal configuration when the grid transmission capacity exceeded 260 MW. Below this threshold, ammonia cracking replaced SOEC as the dominant source to meet the hydrogen demand and minimize the TSC through methane exports. Although ammonia cracking exhibited the highest LCOH (8.4 €/kgH_2) among the three technologies under high-price conditions (see Figure 3 in **Paper IV**), this shift was primarily driven by the high price for methane (90 €/MWh), which made exporting methane more favorable economically than using it as a feedstock for ATR-CCS. Furthermore, when the transmission capacity exceeded 420 MW, the optimal configuration consisted exclusively of SOEC, and nearly all the methane was exported to minimize the TSC, which also corresponded to the lowest LCOH across all the scenarios shown in Figure 5-14b. However, this configuration remains optimal only under the assumption that byproduct methane can be exported year-round at prices that are consistently around 90 €/MWh, as SOEC is not the least-cost option as a standalone system (see Figure 3 in **Paper IV**).

5.4.2.2 Comparison of standalone and integrated hydrogen production systems

Figure 5-15 compares the performances of standalone and integrated hydrogen production systems under varying site and price-specific conditions. It presents their relationships to the TSC, levelized cost of hydrogen (LCOH), on-site hydrogen supply costs (OHSC), and CO_2 abatement costs. The estimated LCOH and OHSC ranges for standalone systems (from Figure 3 in **Paper IV**) are plotted against their corresponding TSC values, depicted as solid and hatched shaded regions, respectively. In Figure 5, the markers (○) indicate the optimal system configurations (from Figure 5-14). Furthermore, Figure 5 illustrates the relationship between the TSC and the corresponding CO_2 abatement costs. The three vertical dashed lines indicate the EU ETS allowance price projections, modeled in Ref. [141]. Detailed inferences drawn from the results shown in Figure 5-15 can be found in **Paper IV**. Here, the key observations are summarized.

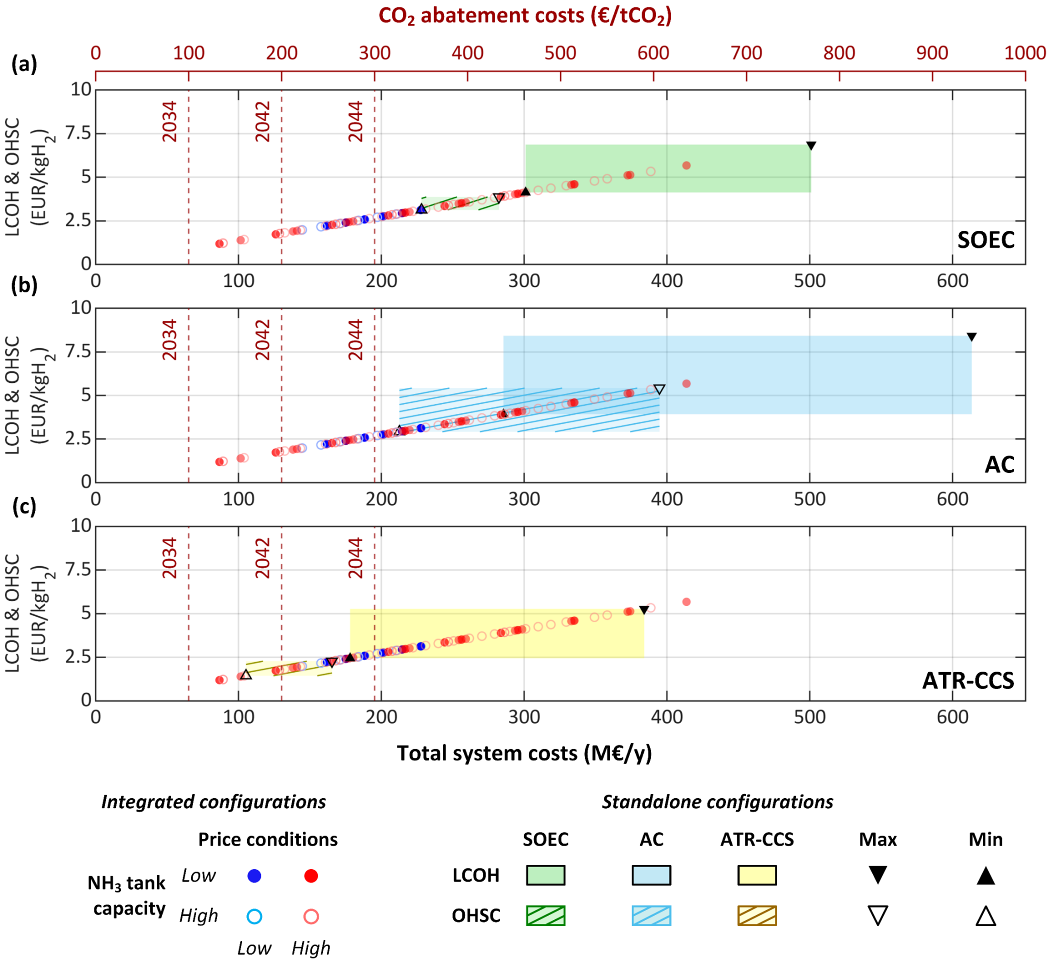

Figure 5-17: Comparisons of the standalone and optimal system configurations under different site and price conditions and their relationships to the total system costs, levelized cost of hydrogen, on-site hydrogen supply costs, and CO_2 abatement costs. Standalone systems are shown as shaded regions, with diagonally hatched areas indicating costs that account for the offsets from repurposing or exporting methane. Optimal system configurations are represented by markers, where filled markers indicate limited ammonia storage (26 GWh), and unfilled markers indicate a larger storage capacity (312 GWh).

Standalone configurations: Among the standalone systems evaluated, ATR-CCS consistently achieved the lowest system cost and CO_2 abatement cost (172–272 €/tCO_2), making it the most viable option in the near term. In contrast, the SOEC and AC systems exhibited prohibitively high abatement costs (348–467 €/tCO_2), even when accounting for methane offsets, which implies that, as standalone systems, these technologies are not economically attractive for steam cracker plants, as they would likely require EU ETS allowance prices higher than 300 €/tCO_2, which are not expected until after 2044 based on current projections [141].

Integrated configurations: Three key observations can be made regarding the data in Figure 5-15. First, integrated systems largely remain comparable with ATR-CCS, in terms of OHSC, and to a lesser extent with AC and SOEC, as evidenced by the markers overlapping with the shaded regions. This indicates that, should site limitations restrict the deployment of a standalone ATR-CCS, the integrated system would become the next viable option, provided that a combination of favorable site and price conditions is established. Second, a majority of the integrated system configurations lie below the lower bounds of the standalone system cost ranges. This is due to the broader sensitivity range assumed for fuel gas availability in the scenario analysis (250–500 MW), which exceeds the fixed methane export potential for standalone systems (~278 MW). This enables more fuel gas to be exported when sufficient transmission capacity (>260 MW) is available for deploying larger SOEC units, which reduces the OHSC. Third, the availability of ammonia storage capacity has a negligible impact on the overall costs indicated by the close proximity of filled and unfilled markers in Figure 5-15. This is primarily due to the limited installed capacities of ammonia crackers in most of the scenarios (see Figure S2 in **Paper IV**).

Overall, the lowest costs are expected when a combination of favorable site and price conditions is in place. Favorable site conditions include: (i) increased availability of fuel gas; (ii) sufficient grid infrastructure to support large-scale SOEC deployment; and (iii) adequate ammonia storage to support moderately sized AC when the grid capacity is limited. Favorable price conditions include: (i) low electricity prices for SOEC; (ii) low ammonia feedstock prices for AC; and (iii) high methane prices to offset hydrogen production costs. In practice, this entails securing price certainty through low-cost PPAs, securing long-term ammonia supply contracts, or attributing a higher value to exported methane as recycled carbon fuels (see Section 6.1.5 in **Paper IV**). Finally, given the uncertainty regarding both site- and price-specific conditions, these results highlight the value of clustering multiple production technologies and aligning them with site-specific conditions to minimize system costs and reduce the risks associated with standalone systems.

5.4.2.3 Stepwise deployment strategy

Figure 5-5 presents an indicative stepwise deployment strategy derived from the techno-economic comparisons of standalone and integrated hydrogen production systems shown in Figure 5-15. A key limitation of the proposed integrated system is that cost-effective implementation may require stepwise deployment of individual technologies, as favorable site-specific and market conditions are expected to emerge over time. Therefore, practical implementation must consider the order in which technologies are introduced, the timing of their deployment, and the ways in which deployment can be coordinated within the cluster.

In this context, the choice of technology ultimately depends on the costs for CO_2 abatement relative to the alternative cost for emitting CO_2. The scenario analysis shows that favorable conditions for deployment of each technology emerge at different EU ETS allowance price levels: for ATR-CCS, ~253–621 €/tCO_2; for AC, ~320–977 €/tCO_2; and for SOEC, ~345–793 €/tCO_2). Excluding methane feedstock costs, ATR-CCS was found to be viable at allowance price levels of 115–215 €/tCO_2. Based on these estimates, the potential deployment sequence is likely to be: ATR-CCS initially, followed by AC, and finally SOEC.

Four key factors must be considered when determining the appropriate timing of the deployment. First, recent forecasts suggest an EU ETS allowance price range of 77–160 €/tCO_2 by Year 2030, followed by a gradual increase in allowance price until Year 2039, with a more pronounced rise expected in the early to mid-2040s [141,142]. This indicates that, for the considered technologies, economic feasibility may not be achievable until the latter part of the 2030s. However, ambitious emissions reduction targets could prevail over EU ETS allowance price signals as the primary driver of deployment timing. Second, considering planning and construction lead times (3–5 years), deployment must begin early enough to ensure that each technology is operational when the EU ETS allowance price levels match their estimated abatement costs. Third, while this timeline allows for the scaling up of critical infrastructure, only three scheduled turnarounds at the cracker plant are expected before Year 2045, thereby limiting the integration opportunities without operational disruptions. Finally, policy-related uncertainties must also be considered, especially concerning the future classification of exported methane as a recycled carbon fuel.

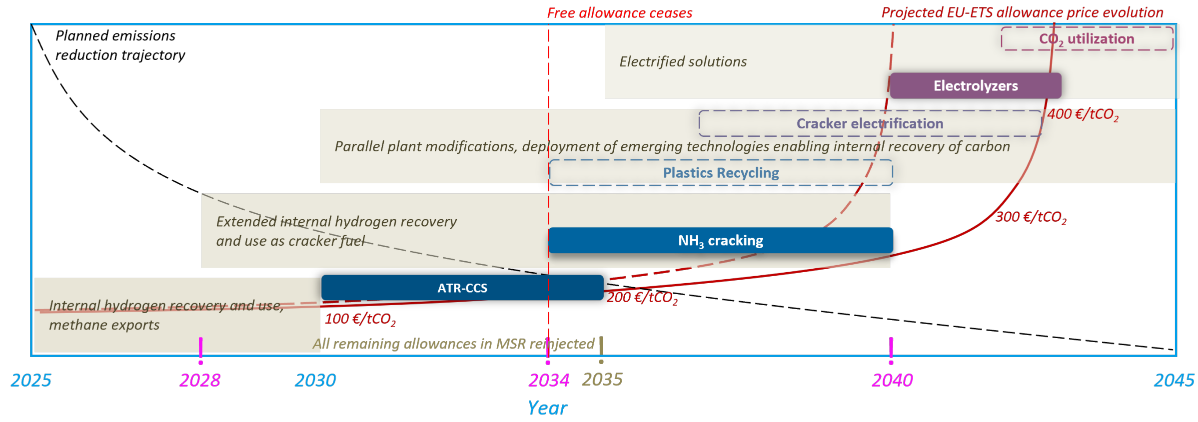

Figure 5-18: Indicative stepwise deployment strategy for a steam cracker plant within a petrochemical cluster, aligned with the projected EU ETS price evolution (red curves), emissions reduction targets (black dashed curve), and scheduled turnaround years (pink markers). Two EU ETS allowance price trajectories are shown: one assuming the remaining allowances in the Market Stability Reserve (MSR) are not reinjected (red dashed curve), and one including their reinjection after the phase-out of free allowances in 2034 (red solid curve), based on Ref. [141]. Technologies evaluated in this work are indicated with solid-shaded boxes, while technologies such as electrified crackers and plastics recycling, which could be deployed in parallel but are outside the scope of this work, are shown with dashed boxes. Note that the figure is illustrative and not drawn to scale.

In the short-to-medium term (2028–2034), ATR-CCS systems could be deployed due to their relatively low abatement costs (115–215 €/tCO_2), which fall within the projected EU ETS allowance price ranges during this period. The actual deployment of such systems will depend on the availability of a CO_2 transport and storage infrastructure. The installed capacities would have to be determined based on the trade-off between the cost savings from methane exports and the emissions reductions achieved through ATR-CCS during this period. In general, larger ATR-CCS systems are more favorable, as they benefit from economies of scale and have a stronger capability to accommodate the anticipated increase in on-site fuel gas availability through cracker electrification or plastic waste recycling.

In the medium term (2034–2040), alternative hydrogen production technologies must be deployed and operational before the final scheduled turnaround in Year 2040. The technology selection will largely depend on the prevailing market conditions, the availability of renewable electricity, and access to sufficient grid transmission capacity. In principle, if cheap renewable electricity with sufficient transmission capacity becomes available, direct electrification of cracker furnaces should be prioritized. However, if direct electrification of existing crackers is proven to be technically unfeasible, or if the electricity and grid capacities do not materialize, ammonia may become indispensable during this period for its use either as a fuel or as a feedstock for hydrogen production.

Beyond Year 2040, electrolyzers could be deployed as part of integrated hydrogen production systems. In this regard, early installation of electrolyzers would allow for extended operation alongside ATR-CCS and AC, enabling the synergies demonstrated in this work. Given the limitations linked to the modular scale-up of electrolyzer systems, investment in overcapacity may be required. Nevertheless, integrated systems with overcapacity tend to offer greater flexibility in terms of responding to price fluctuations while maintaining high capacity utilization. Alternatively, this deployment could be phased, initially targeting the remaining hydrogen demand at the cracker plant and thereafter expanding to meet the green hydrogen demand across the cluster. This would ensure a future hydrogen supply within the cluster, facilitating CO_2 utilization and recycling pathways towards the circular use of materials [143].

6 Discussion

This chapter summarizes the results from Papers **I–IV** *(Section 6.1), discusses the implications for the case study plants (Section 6.2), presents general reflections on the methodological frameworks (Section 6.3), and highlights the limitations (Section 6.4).*

6.1 Summary of results

Figure 1-1 illustrates the generalized[58] assessment framework that integrates the individual frameworks developed in this work to overcome the identified limitations of incumbent process integration and techno-economic methods. These methodological frameworks were demonstrated through case studies of decarbonization in a bio-CHP plant operating in a district heating system (**Paper I**), a propane dehydrogenation plant (**Paper II**), and steam cracker plant (Papers **III–IV**).

In **Paper I**, the framework highlighted the advantage of choosing CO_2 capture technology that preserves the electric power production at future BECCS plants, which inherently offers greater product flexibility[59] and higher exergetic efficiency. The integration of an amine-based CO_2 capture technology retained approximately 80% of the electric power output of the unabated bio-CHP plant. Complementing this BECCS configuration with large-scale heat pumps on-site could enable an increase in district heating output by 21% compared to the unabated bio-CHP plant. Furthermore, the results showed that centralized large-scale heat pumps could further enhance the product flexibility (heat, power, and negative CO_2 emissions) of the future BECCS plants in the district heating system in response to fluctuating energy market conditions or demand levels.

In **Paper II**, the framework identified a novel and cost-effective decarbonized propane dehydrogenation process configuration, which features an industrial gas turbine (GT) immediately upstream of the air heater in the air-regeneration train, and an amine-based CO_2 capture plant downstream of these units (see Figure 5-6). This integration enabled the use of the GT exhaust gases to replace the current hot air intake for the regeneration sequence in the reactors. This process modification resolved the two key decarbonization challenges inherent to the propane dehydrogenation technology: i) the highly diluted (CO_2) flue gas stream, and ii) the high oxygen concentrations that may cause relatively high solvent losses from the amine-based CO_2 capture process. The identified configuration enhanced fuel exergy utilization, thereby enabling the propane dehydrogenation process to become a net producer of low-carbon electricity. Substantial benefits were observed in the techno-economic analysis, primarily due to the economies of scale in the CO_2 capture plant and the generation of low-carbon electricity that can be sold to the grid.

---

[58] Although the methodology shown in Figure 1-1 suggests a top-down approach, initiating with systems-level considerations followed by plant-level and site-level considerations, the methods employed within the individual methodological frameworks developed in **Papers I–Paper IV** take a bottom-up approach.

[59] The ability of the plant to vary a specific product output, in this case, heat, power, and negative CO_2 emissions.

In **Paper III**, the site-specific techno-economic analysis applied to the steam cracker plant highlighted that the impact on current and potential future plant production has the highest impact on the total cost of retrofitability, followed by the opportunity cost of occupying valuable space available at existing sites. Considering site-specific factors of the reference steam cracker plant, the CO_2 avoidance cost was roughly 46% and 36% higher than the baseline estimates for the Post-CCS and Pre-CCS processes, respectively, obtained with a standardized techno-economic assessment method. Furthermore, the cost of retrofitability or the escalation of CO_2 avoidance costs due to site-specific factors was approximately 80% higher for the Post-CCS decarbonization process (43 €/tCO_2) than for the Pre-CCS process (24 €/tCO_2), highlighting the varied impact of these factors on different decarbonization technologies.

Overall, including the added cost for CO_2 transportation and storage (~104 €/tCO_2 [40]), the avoidance costs were 243 €/tCO_2 and 208 €/tCO_2 for the Post-CCS and Pre-CCS pathways, respectively. The qualitative retrofitability assessment revealed pertinent site-specific factors such as adequate access to external infrastructure such as the electricity grid and CO_2 supply infrastructure, the flexibility to adapt to future feedstock switches, the importance of decoupling the decarbonization technology and the host process plant's residual lifetime, and the possibility of reaching 100% carbon recovery through CO_2 utilization pathways as factors that could tip the favor from one decarbonization technology to another.

Paper IV builds on the outcomes of **Paper III**, which identified hydrogen firing as the cost-optimal decarbonization option for the steam cracker plant, considering its site-specific factors. This work proposed the concept of an integrated hydrogen production system that combines multiple distinct hydrogen production technologies to meet demand for low-emissions hydrogen as fuel for steam cracker furnaces. The results showed that integrating multiple hydrogen production technologies confers significant advantages over standalone systems, not only in terms of economic performance but also in enhancing operational flexibility and system redundancy. This integrated system enabled cost reductions through flexible operation under varying price and export conditions, with minimal impact on the overall capacity utilization. Scenario analyses revealed that site-specific constraints, including grid transmission capacity, methane availability, and ammonia storage, significantly influenced the optimal technology mix. The scenario analysis further highlighted the importance of securing price certainty through low-cost, long-term contracts for system configurations that are dominated by a single technology. Alternatively, in the absence of price certainty, the risk of cost escalation could be mitigated by installing comparable or excess capacities across technologies, so as to enable flexible operation. In addition, overcapacity can reduce on-site hydrogen supply costs through hydrogen exports to other potential offtakers in the cluster.

Together, these industrial case studies show that the technology choice for decarbonization depends strongly on the industrial context and the scope of assessment. For instance, the post-combustion pathway was clearly identified as sub-optimal in the context of a steam cracker plant. In contrast, for the propane dehydrogenation process, the post-combustion pathway was found to be the only practicable solution, given its complexity in integration with alternative decarbonization pathways, albeit at an extremely high abatement cost. By adopting a more detailed approach in **Paper II**, however, the framework revealed process modifications that transformed what had previously been the only practicable but prohibitively expensive decarbonization option into a viable solution with much lower abatement costs.

The cost of CO_2 avoidance is a recurring economic performance indicator in this thesis (Papers **II–IV**). The wide range of avoidance costs estimated in the case studies indicates that conditions for deployment arise at different points in time. However, for all the considered technologies, these costs far exceed current EU ETS allowance prices. A key condition for their deployment is EU ETS allowance prices >200 €/tCO_2, which are not foreseeable until the late 2030s. This implies that, without targeted subsidies or investment support, near-term implementation of these identified decarbonization measures within the studied industries is unlikely.

6.2 Implications

This section presents broader implications for the industries considered as case studies in this thesis, while more specific implications can be found in the appended papers.

Bio-CHP plants: Bio-CHP, and to some extent, waste-CHP plants operating in a district heating system could be transformed into large-scale sites for carbon dioxide removal through the integration of end-of-pipe CO_2 technology. As demonstrated in **Paper I**, the choice of CO_2 capture technology has implications beyond the plant boundaries. An analysis by Beiron et al. [144], however, suggested that the choice between the two capture technologies is ultimately determined by trade-offs at the city energy system rather than by technology performance alone. Specifically, the trade-off is between reduced annual heat production (~30% with MEA) and increased annual electricity imports (~44% with HPC), which are strongly linked to system-level factors such as biomass and electricity prices, as well as local conditions including grid connection capacity and the portfolio of production units in the district heating system. At the plant level, however, cost minimization through product flexibility (heat, electricity, negative emissions) ultimately depends on preserved electricity output and its efficient use, for example, in centralized industrial heat pumps rather than in flue gas compressors for HPC technology. Such cost optimization is particularly important for bio-CHP plants, which operate relatively few full-load hours annually, making investments in such applications less attractive. Further implications of deploying CCS in bio-CHP plants, and the value of recovering heat from CCS units using heat pumps, have been evaluated in other contributions by the author [105,145].

Propane dehydrogenation plant: The decarbonized propane dehydrogenation process configuration identified in **Paper II**, with the lowest specific CO_2 avoidance costs, also opens the possibility of enhancing CO_2 avoidance through partial or complete feedstock switching from fossil-based propane to bio-propane. Bio-propane, typically obtained as light ends in the production of biofuels such as sustainable aviation fuel and renewable diesel via either the HVO route[60] or Fischer–Tropsch route [146,147], could be sourced as feedstock for propylene production. It could also be sourced from future methanol-to-olefins plants that use sustainable methanol[61] as feedstock, where bio-propane is obtained as a byproduct. Since these production routes typically have higher-value products (transport fuels), it could become economically viable for these future plants to sell the byproduct bio-propane [148]. Subsequent use of the produced bio-based propylene in a downstream polypropylene plant would, to some extent, decouple the production of carbon-based materials from fossil resource extraction, contributing to circular economy systems [149].

---

[60] Hydrotreated vegetable oil (HVO), also known as renewable diesel, is produced by hydrogenating and hydrocracking vegetable oils and animal fats using hydrogen and catalysts at high temperatures and pressures [147]

[61] Produced with captured biogenic CO_2 and renewable electricity–based hydrogen [165].

Furthermore, the feedstock switch could enable net-negative CO_2 emissions at significantly lower costs. Overall, the feedstock switch would provide a cost-effective route to producing low-carbon electricity and bio-based propylene, with the added benefit of net-negative CO_2 emissions. However, the economic viability of such a feedstock switch would depend on the market price of both the bio-propane byproduct and the carbon removal credits in the voluntary carbon market. The combination of fuel switching and feedstock switching in the proposed decarbonized plant configuration would generate byproduct bio-hydrogen that could qualify as an advanced biofuel, under the EU RED III directives [150,151], provided it is recovered from the fuel gas system. Finally, while the case study plant is the only facility in the EU to adopt the CATOFIN Lummus PDH technology, the proposed configuration is especially relevant for decarbonizing the substantial PDH capacity being built outside the EU [114].

Steam cracker plants: The case study in **Paper III** showed that the post-combustion CO_2 capture pathway is inherently limited in its CO_2 abatement potential and effectively ties the economic lifetime of the capture plant to the residual lifetime of the steam cracker plant. In the context of steam cracker plants in the EU, many are at risk of closure due to overcapacity elsewhere, and most have limited residual lifetimes, with only a few scheduled turnarounds remaining before 2050. Therefore, synchronization of the design lifetime of the post-combustion CO_2 capture pathway (~20–25 years) with the residual plant lifetime would be required to avoid stranded assets. For the case study plant, this implies that the installation of the post-combustion CO_2 capture pathway should start as early as 2025 and, at the latest, 2033. The post-combustion CO_2 capture pathway is therefore not expected to play a major role in steam cracker plants. In contrast, the pre-combustion CO_2 capture pathway could remain relevant well beyond the residual lifetime of the existing cracker, as it enables continued production of blue hydrogen from natural gas supplied through the grid.

The case study in **Paper IV** demonstrated steam cracker plants as a practical starting point for scaling up low-emissions hydrogen production within petrochemical clusters. In this context, several advantages were identified: i) using low-emissions hydrogen as a cracker fuel enables significant cost reductions through the export of recovered methane from the displaced fuel gas; ii) the combined possibility of hydrogen firing and methane exports helps to circumvent the absence of both hydrogen and CO_2 transport and storage infrastructure in the short-to-medium-term; iii) it avoids the need for costly hydrogen compression and storage systems by using hydrogen as it is produced; and iv) this approach offers the possibility to redirect hydrogen to preferred end-uses with higher CO_2 abatement potential, as more-efficient substitute technologies, such as electrified crackers, become available over time. Other implications, including the impact of displaced methane from the steam cracker plants on fossil fuel gas imports to the EU and the associated CO_2 abatement, can be found in **Paper IV**.

6.3 Methodological reflections

This section reflects on the methodological frameworks developed in this thesis, focusing on their usefulness, implications, and limitations. Several considerations guided their development. The urgency of implementing CCS, together with the changing energy and policy landscape, necessitated a reassessment of incumbent ex-ante assessment methods and their efficacy in identifying cost-effective decarbonization solutions across different industrial sectors. Earlier work in the field had primarily focused on technology comparisons, often through Nth-of-a-kind (NOAK) evaluations addressing 'what-if' and 'what-will' questions [36], without fully considering the constraints and trade-offs that shape practical deployment.

To this end, the methodological frameworks developed in this thesis, built on incumbent process integration and ex-ante techno-economic assessment methods, were aimed at addressing specific limitations across different industrial contexts. Although technology comparison was a recurring theme in the case studies, the purpose was not limited to establishing the technical or economic superiority of one option over another. Instead, these comparisons were initially designed to address questions pertinent to specific industry sectors (**Papers I–II**) and later evolved to address shortcomings in existing methods for complex industries (e.g., petrochemicals) where outcomes of comparative technology assessments are strongly influenced by context and site-specific factors (**Papers III–IV**).

In **Paper I**, the framework applied exergy as a figure of merit together with system boundary expansion to highlight differences in technical performance between two inherently different CO_2 capture technologies in the context of a CHP plant operating within a district heating system. The method was specifically framed to address prevailing arguments in favor of HPC over MEA capture technology, owing to its lower energy penalty and higher recoverable heat that could be sold as district heating. The application of the framework revealed that conclusions based solely on energy as a metric within plant-level system boundaries can be misleading, since they fail to account for the value of preserved electricity output in terms of its utility for both the plant operator and the end-users in the district heating system. While valuable in highlighting this distinction, the framework required further generalization (as described in Section 5.1.1) to enable its application beyond the context of CHP plants.

In **Paper II**, the framework combined exergy–pinch analysis with techno-economic assessment in an iterative manner to identify promising process modifications for decarbonizing a propane dehydrogenation plant. The motivation for this approach came from our technology prescreening, which showed that this process had limited compatible decarbonization options beyond end-of-pipe CO_2 capture, and even this option was economically unattractive due to its highly diluted flue gases. This indicated a need for a method to systematically identify compatible process modifications that could deliver cost reductions. To address this, the exergy-pinch analysis by Feng et al. [134] was adopted and combined with techno-economic analysis, which was iteratively performed to allow process modifications to be adopted or rejected at successive design stages based on their economic viability. Consequently, this framework indicated a technically feasible and exergy-efficient configuration that conventional piecewise-comparative analyses would have overlooked. While this demonstrated the usefulness of the developed framework, it is both time- and data-intensive. Therefore, its transferability to other industries may require tools that streamline its application.

In **Paper III**, shortcomings in standardized TEA methods were addressed by incorporating site-specific factors expected to influence abatement costs, and thereby the choice of technology for decarbonizing a given industrial site. This detailed approach was considered necessary given the many comparative TEA studies reporting CO_2 abatement costs within a narrow range, leaving the choice of technology to site-specific contexts. The objective was not to reconcile early-stage cost estimates with the actual cost of CCS implementation at specific sites, but to provide a generalized method for systematically evaluating both quantitative and qualitative site-level factors. While the case study demonstrated the strength of the framework in providing a concrete and holistic indication of the optimal choice of decarbonization technology, its application also highlighted challenges with the availability of site-level data, which are generally not disclosed due to confidentiality. To overcome this limitation, the framework relied on certain assumptions and made use of open-source tools and publicly available front-end engineering design reports.

Building on this, in **Paper IV**, a generalized optimization framework was developed that incorporated site-specific constraints that reflected technology-specific barriers to deployment. This framework was less complex relative to the other frameworks developed in this thesis. The focus was on evaluating the potential for cost reductions through technology diversification, flexible operation, and leveraging integration benefits and short-term policy incentives that are unique to steam cracker plants. Although the developed optimization tool can be adapted to other industrial clusters, a key limitation is its reliance on perfect foresight, which does not capture uncertainties in energy market conditions and may overestimate the cost-effectiveness of the proposed system.

In summary, the developed frameworks and their application to different industrial case studies in this thesis highlighted the value of combining both broader and more detailed approaches when conducting technology comparisons for industrial decarbonization. Another aspect to consider is the balance between generalizing methods for their wider applicability and tailoring methods to ensure their relevance to specific industries. Together, these reflections show that while industry-specific indications are valuable, the implementation of decarbonization strategies ultimately depends on site-specific conditions, opportunities, and constraints.

6.4 Limitations

This section presents broader limitations of the frameworks developed in this thesis, while more specific limitations related to the tools and case study plants are discussed in the appended papers. The frameworks developed in this work were demonstrated through industrial case studies under the assumption of unchanged feedstock consumption, energy use, and product demand (**Papers I–IV**). However, it is essential to consider the impact of factors such as process changes at steam cracker plants, the increasing availability of renewable electricity, and stronger incentives for the adoption of heat pumps in district heating systems, among others, on the outcomes of this work. For example, the decommissioning of older cracker furnaces within a steam cracker plant would reduce the demand for hydrogen as cracker fuel. In such situations, the post-combustion CO_2 capture pathway could become increasingly competitive relative to the pre-combustion pathway, as the latter is both capital-intensive and relies heavily on economies of scale.

While the developed frameworks were generalized for application to other carbon-intensive industries, the methods and tools developed in **Papers II–IV** are highly adapted to the respective industrial case study, which makes their transferability to other industries cumbersome. In this context, the frameworks developed in **Papers III** and **IV** pose additional challenges as they were designed to provide site-specific indications, which inherently limit comparability between studies within the same industrial sector. Nevertheless, some broader industry-specific trends could still emerge through their application.

The site-specific techno-economic assessment method (**Paper III**) primarily focused on comparing mature decarbonization pathways available for near-term implementation at the steam cracker plant, given their lower uncertainties regarding technical performance and cost structures compared to emerging process technologies. However, the indication of the optimal decarbonization pathway for any industrial site remains contingent on the number of decarbonization options compared in the assessment. Therefore, the indication of the pre-combustion CO_2 capture pathway as the optimal decarbonization pathway should be interpreted in relation to the other alternative considered in the study, i.e., the post-combustion CO_2 capture pathway.

Decarbonization measures, such as direct process electrification or installation of substitute production technologies, are likely to affect the material and energy balances at a specific site. Take, for example, the electrification of a steam cracker furnace or changes to the feedstock slate of the cracker plant. Cracker electrification would increase the availability of fuel gas, which would have to be exported or repurposed as feedstock for low-emissions hydrogen production. Furthermore, it could directly impact the available excess heat within the plant, as demonstrated in a case study by Wiertzema et al. [32] on an oxo-synthesis plant with electrified syngas production. Therefore, the consequences of process changes in terms of changes to heat and material flows at existing sites must be accounted for in the generalized assessment framework.

7 Conclusions

This thesis presents a generalized assessment framework for enhanced early-stage identification of optimal decarbonization pathways in carbon-intensive industries, accounting for their site-, plant-, and system-level contexts. This framework integrates a set of methodological approaches, each addressing specific limitations of incumbent process integration and comparative ex-ante techno-economic assessments. The main contribution of the thesis lies in the development and demonstration of this framework to varied industrial contexts, enabling the identification of exergy- and cost-optimal decarbonization pathways that facilitate decision-making toward near-term implementation.

At the systems level, the inconsistencies between the plant owner and the end-user perspectives on the choice of decarbonization technologies were addressed. By extending system boundaries and applying exergy as a figure of merit, the framework enables a more consistent comparison of CO_2 capture technologies with inherently different exergy demands (**Paper I**).

At the plant level, the limitation of pinch-based methods, which consider only heat transfer processes, was addressed by combining exergy-pinch analysis with ex-ante techno-economic assessment. This framework enables the identification of process modifications that maximize exergy utilization when retrofitting decarbonization technologies to existing unabated process plants, yielding configurations with minimal exergy losses and lower CO_2 avoidance costs (**Paper II**).

At the site level, a site-specific techno-economic analysis method was developed to enhance early-stage ex-ante assessment methods (**Paper III**). This framework reveals site-specific factors and technology-specific attributes that influence technology selection and provides tools to both quantify and qualitatively assess them through a retrofitability matrix, thereby enhancing comparative assessments of decarbonization technologies at specific industrial sites.

Finally, to overcome existing deployment barriers for low-emissions hydrogen, an integrated system combining distinct low-emissions hydrogen production technologies was proposed and evaluated with a generalized optimization framework (**Paper IV**). This framework enables the identification of cost-optimal hydrogen supply configurations and system operation while accounting for site-level constraints, technology-specific limitations, and energy market uncertainties. This provides the basis for deriving stepwise deployment strategies for the timely and cost-effective introduction of hydrogen production technologies at petrochemical clusters. Some general conclusions can be drawn from the applications of the developed frameworks to industrial case studies:

- The amine-based CO_2 capture process clearly demonstrates a significant advantage over the hot-potassium carbonate capture process for enabling BECCS, as it inherently offers greater product flexibility (i.e., the ability of the plant to vary the relative output of heat, electricity, and negative CO_2 emissions) with higher preservation of electric power output relative to the unabated bio-CHP plant.
- Post-combustion CO_2 capture process is the only practicable decarbonization pathway available for a state-of-the-art propylene production technology due to process constraints. However, straightforward retrofit of such plants is prohibitively expensive due to the highly diluted flue gases (<3 vol.% CO_2).

- The decarbonized propane dehydrogenation configuration identified through the developed framework incorporates an industrial gas turbine immediately upstream of the air heater in the air-regeneration train. This integration pre-concentrates CO_2 in the flue gases prior to entering the amine-based capture plant, thereby reducing energy demand for solvent regeneration, resulting in substantially lower avoidance costs and higher relative CO_2 avoidance.
- The impact on current or potential production has the largest influence on the total cost of retrofitability. Significant cost escalation could be avoided by synchronizing CCS deployment with scheduled maintenance shutdowns during turnaround years to minimize the possibility of unforeseen forced downtime.
- The qualitative retrofitability assessment revealed pertinent site-specific factors such as sufficient access to external infrastructure such as the electricity grid and CO_2 supply infrastructure, the flexibility to adapt to future feedstock switches, the importance of decoupling the decarbonization technology and the process plant's lifetime, and the possibility of reaching 100% carbon recovery towards CO_2 utilization pathways as factors that could tip the favor from one decarbonization technology to another.
- The post-combustion CO_2 capture pathway is not expected to play a significant role in the decarbonization of steam cracker plants, given its significantly lower CO_2 emissions avoidance performance. It is limited to a maximum equivalent CO_2 avoidance of 85% while the pre-combustion CO_2 capture pathway process attains a maximum equivalent CO_2 avoidance of 96%.
- Co-location and integration of distinct hydrogen production technologies could mitigate deployment barriers and investment uncertainty facing low-emission hydrogen by providing operational flexibility and system redundancy. Through technology diversification, hydrogen supply at the cluster remained unaffected by limited access to renewable electricity and grid transmission capacity

In summary, the generalized assessment framework can be utilized to acquire a comprehensive early-stage indication of the optimal decarbonization technological pathway. At the systems level, it is imperative to consider end-users' perspectives to avoid the selection of sub-optimal decarbonization technology and, in general, to achieve exergy-efficient energy systems. At the plant level, it is essential to consider modifying exergy-destructive operations, such as fuel combustion for high-temperature heat, with either direct process electrification or direct process-to-process integration of an industrial gas turbine. Finally, site-level considerations provide the possibility of obtaining enhanced cost estimates for different decarbonization technologies at specific industrial sites. These cost estimates not only provide insights into the hidden costs of decarbonization, often not considered in academic or advanced cost-engineering studies, but also facilitate informed technology selection. Moreover, integrating these enhanced site-specific cost estimates with the technology-specific cost of retrofitability into energy-systems level studies can improve the level of detail translated to higher-level analyses, such as national-level marginal abatement cost curves, or the evaluation of cascading cost of decarbonization pathways on the final consumers, providing critical information for policymakers in this domain.

8 Recommendations for future work

The generalized assessment framework (Figure 1-1) developed in this thesis provides a basis for future comparative assessments for early-stage identification of optimal decarbonization pathways suitable for implementation at the studied industrial site. Given that this framework is built upon a combination of methodological frameworks with select industrial case studies that best highlight the limitations in existing process integration and techno-economic methods, future research efforts should prioritize adopting these frameworks across a wider range of industries.

The reasons for this are threefold. First, this would broadly validate the relevance of the proposed frameworks for other industries. Second, this would enable identification of site-specific differences both within and between industries, as well as potentially differing perspectives between the plant owner and end-users regarding optimal decarbonization pathways. Third, application of the frameworks in other industrial contexts could potentially reveal further limitations of the developed frameworks, apart from those mentioned in Section 6.4, which should then be addressed to enhance the robustness of the generalized assessment framework. In addition to these broader recommendations, some specific directions for future work are outlined below.

- The case study in **Paper I** demonstrated how underlying market conditions in a DH system could potentially favor sub-optimal decarbonization solutions at the plant level. Although such disparities may be inconsequential in industrial contexts with limited interaction with local energy systems, future efforts could focus on identifying similar disparities between plant- and systems-level perspectives on competing decarbonization pathways, contingent on either incumbent or proposed policies within this domain.
- The framework methodologies developed in **Papers III** and **IV** could be extended to include emerging technologies, such as e-crackers and advanced thermochemical recycling technologies [117,143], as well as carbon dioxide removal technologies[62] at the cluster level. Such extensions should be guided by the hybrid-costing method[63]. It is also important to ensure that key technology-specific attributes, such as physical footprint, are available or can be reasonably estimated.
- Careful curation of site-specific data is warranted to better understand the similarities and differences among industrial sites, which are typically heterogeneous even within the same industry category. This would enable the formulation of well-informed assumptions, thereby simplifying the site-specific techno-economic analysis. In particular, applying object detection in aerial imagery to identify assets and categorize layouts, could provide early estimates of available space for retrofitting technologies at existing industrial sites.

---

[62] Such an integration would enable mitigation of residual industrial CO_2 emissions by utilizing the large amounts of industrial waste heat, access to the electricity grid and potential future access to shared infrastructure for CO_2 capture, utilization, transport and storage. Specifically, the adsorption-based direct air capture technologies that require low-grade waste heat at around 80–100°C (1600 kWh/tCO_2) and electricity (400 kWh/tCO_2) [166].

[63] A hybrid-costing approach integrates engineering–economic and experience-curve methods for advanced technologies, accounting for future cost trajectories based on technology maturity and anticipated learning rates [36].

- The stepwise deployment strategy outlined in **Paper IV** could be evaluated quantitatively using a multi-stage stochastic programming approach, incorporating uncertainties regarding technology readiness, infrastructure availability, and price developments. This would enable a realistic assessment of the deployment potential of low-emissions hydrogen production and other emerging technologies at existing petrochemical clusters. This framework could also be to address broader questions on infrastructure planning for CO_2 transport, hydrogen networks, and electricity grids. In addition, the framework could be extended with deep uncertainty methods[64], applied either at the plant or system level, to craft robust and adaptive strategies that account for a broad spectrum of uncertainties potentially impeding the transition toward sustainable industrial decarbonization.

---

[64] Stenström et al. [167] applied Decision-Making under Deep Uncertainty (DMDU) methods to demonstrate how robustness against uncertainty could support investment decisions in BECCS deployment.

References

[1] Copernicus: 2024 is the first year to exceed 1.5°C above pre-industrial level 2025. https://climate.copernicus.eu/copernicus-2024-first-year-exceed-15degc-above-pre-industrial-level (accessed August 30, 2025).

[2] IEA, CO_2 Emissions in 2022. Int Energy Agency 2023. https://www.iea.org/reports/co2-emissions-in-2022 (accessed January 7, 2024).

[3] Ritchie H. How much CO_2 can the world emit while keeping warming below 1.5°C and 2°C? 2023. https://ourworldindata.org/how-much-co2-can-the-world-emit-while-keeping-warming-below-15c-and-2c (accessed January 7, 2024).

[4] European Commission. Directorate-General for Climate Action. EU Climate Action Plan. 2050 long-term strategy. 2024. https://climate.ec.europa.eu/eu-action/climate-strategies-targets/2050-long-term-strategy (accessed February 7, 2024).

[5] European Commission. Directorate-General for Communication. Recommendations for 2040 targets to reach climate neutrality by 2050. 2024. https://commission.europa.eu/news/recommendations-2040-targets-reach-climate-neutrality-2050-2024-02-06_en (accessed February 7, 2024).

[6] European Council. European Green Deal. 2023. https://www.consilium.europa.eu/en/policies/green-deal (accessed January 7, 2024).

[7] European Commission. Directorate-General for Communication. Free Allocation. 2022. https://climate.ec.europa.eu/eu-action/eu-emissions-trading-system-eu-ets/free-allocation (accessed January 7, 2024).

[8] Nurdiawati A, Urban F. Towards Deep Decarbonisation of Energy-Intensive Industries: AReview of Current Status, Technologies and Policies. Energies 2021;14. https://doi.org/10.3390/en14092408.

[9] Official Journal of the European Union. Commission Delegated Decision (EU) 2019/708 of 15 February 2019 supplementing Directive 2003/87/EC of the European Parliament and of the Council concerning the determination of sectors and subsectors deemed at risk. 2019.

[10] Official Journal of the European Union. Commission Decision of 29 June 2021 instructing the Central Administrator of the European Union Transaction Log to enter the national allocation tables of Belgium, Bulgaria, Czechia, Denmark, Germany, Estonia, Irela. 2021/C 302/01 2021.

[11] Fit for 55. 2023. https://www.consilium.europa.eu/en/policies/green-deal/fit-for-55-the-eu-plan-for-a-green-transition/ (accessed February 15, 2024).

[12] Schreyer F, Ueckerdt F, Pietzcker R, Rodrigues R, Rottoli M, Madeddu S, et al. Distinct roles of direct and indirect electrification in pathways to a renewables-dominated European energy system. One Earth 2024;7:226–41. https://doi.org/10.1016/j.oneear.2024.01.015.

[13] 2050 long-term strategy 2023. https://climate.ec.europa.eu/eu-action/climate-strategies-targets/2050-long-term-strategy_en#documentation (accessed August 9, 2023).

[14] European Commission. Clean Industrial Deal 2025. https://ec.europa.eu/commission/presscorner/detail/en/ip_25_550?utm_source=chatgpt.com (accessed September 7, 2025).

[15] Odenweller A, Ueckerdt F. The green hydrogen ambition and implementation gap 2024;2023. https://doi.org/10.1038/s41560-024-01684-7.

[16] Global CCS Institute. The Global Status of CCS:Global Status of CCS 2024 Collaborating for a net-zero future. 2024:1–89.

[17] IEA. Net Zero by 2050 2021. https://www.iea.org/reports/net-zero-by-2050 (accessed December 15, 2024).

[18] International Energy Agency (IEA). Net zero roadmap: A global pathway to keep 1.5 °C goal in reach – 2023 update. IEA Publ 2023:1–226.

[19] Carbon capture in 2021: Off and running or another false start? – Analysis - IEA 2021. https://www.iea.org/commentaries/carbon-capture-in-2021-off-and-running-or-another-false-start (accessed September 7, 2025).

[20] Equinor. First CO2 volumes stored at Northern Lights 2025. https://www.equinor.com/news/20250825-first-co2-volumes-stored-at-northern-lights (accessed August 25, 2025).

[21] Stockholm Exergi - World's Largest Facilities for Removing Carbon Dioxide - Beccs Stockholm 2025. https://beccs.se/news/stockholm-exergi-to-build-one-of-the-worlds-largest-facilities-for-removing-carbon-dioxide-from-the-atmosphere/ (accessed September 5, 2025).

[22] Greensand 2025. https://greensandfuture.com/ (accessed September 7, 2025).

[23] CO_2 reduction through storage under the North Sea - Porthos 2025. https://www.porthosco2.nl/en/ (accessed September 7, 2025).

[24] Antwerp@C | Port of Antwerp-Bruges 2025. https://www.portofantwerpbruges.com/en/our-port/climate-and-energy-transition/antwerpc (accessed September 7, 2025).

[25] The European Hydrogen Backbone (EHB) initiative | EHB European Hydrogen Backbone 2025. https://ehb.eu/ (accessed September 5, 2025).

[26] Subraveti SG, Rodríguez Angel E, Ramírez A, Roussanaly S. Is Carbon Capture and Storage (CCS) Really So Expensive? An Analysis of Cascading Costs and CO_2 Emissions Reduction of Industrial CCS Implementation on the Construction of a Bridge. Environ Sci Technol 2023;57:2595–601. https://doi.org/10.1021/acs.est.2c05724.

[27] Hörbe Emanuelsson A, Johnsson F. The Cost to Consumers of Carbon Capture and Storage—A Product Value Chain Analysis. Energies 2023;16. https://doi.org/10.3390/en16207113.

[28] Rootzén J, Johnsson F. Managing the costs of CO_2 abatement in the cement industry. Clim Policy 2017;17:781–800. https://doi.org/10.1080/14693062.2016.1191007.

[29] Rootzén J, Johnsson F. Paying the full price of steel – Perspectives on the cost of reducing carbon dioxide emissions from the steel industry. Energy Policy 2016;98:459–69. https://doi.org/10.1016/j.enpol.2016.09.021.

[30] Tanzer SE, Ramírez A. When are negative emissions negative emissions? Energy Environ Sci 2019;12:1210–8. https://doi.org/10.1039/c8ee03338b.

[31] Tan M, Igor PI, Ramírez AR. Understanding the Level of Integration in Existing Chemical Clusters : Case Study in the Port of Rotterdam 2024.

[32] Wiertzema H, Svensson E, Harvey S. Bottom–Up Assessment Framework for Electrification Options in Energy-Intensive Process Industries. Front Energy Res 2020;8. https://doi.org/10.3389/fenrg.2020.00192.

[33] Umeda T, Harada T, Shiroko T. A thermodynamic approach to the synthesis fo heat integration systems in chemical processes. Comput Chem Eng 1979;3:273–82.

[34] Kemp I. Pinch Analysis and Process Integration: A User Guide on Process Integration for the Efficient Use of Energy. 2nd Editio. Elsevier Science & Technology; 2007.

[35] de Raad B, van Lieshout M, Stougie L, Ramirez A. Improving plant-level heat pump performance through process modifications. Appl Energy 2024;358:122667. https://doi.org/10.1016/j.apenergy.2024.122667.

[36] Roussanaly S, Berghout N, Fout T, Garcia M, Gardarsdottir S, Nazir SM, et al. Towards improved cost evaluation of Carbon Capture and Storage - a white paper. vol. 106. SINTEF Energi AS; 2021. https://doi.org/10.5281/zenodo.4940264.

[37] van der Spek M, Sanchez Fernandez E, Eldrup NH, Skagestad R, Ramirez A, Faaij A. Unravelling uncertainty and variability in early stage techno-economic assessments of carbon capture technologies. Int J Greenh Gas Control 2017;56:221–36. https://doi.org/10.1016/j.ijggc.2016.11.021.

[38] Greig C, Garnett A, Oesch J, Smart S. Guidelines for Scoping and Estimating Early Mover CCS Projects. 2014.

[39] COWI. CinfraCap – Gemensam infrastruktur för transport av koldioxid – Förstudierapport. Report nr A209494-4-06-REP-0001. COWI AB, Göteborg, Sweden. 2021.

[40] Detterfelt L, Hellström A. Renova AB - Sävenäs 2024 2024.

[41] Becattini V, Riboldi L, Burger J, Nöhl J, Oeuvray P, Reyes-Lúa A, et al. Rolling-out pioneering carbon dioxide capture and transport chains from inland European industrial facilities: A techno-economic, environmental, and regulatory evaluation. Renew Sustain Energy Rev 2024;205. https://doi.org/10.1016/j.rser.2024.114803.

[42] Karlsson S, Normann F, Odenberger M, Johnsson F. Modeling the development of a carbon capture and transportation infrastructure for Swedish industry. Int J Greenh Gas Control 2023;124:103840. https://doi.org/10.1016/j.ijggc.2023.103840.

[43] Becattini V, Gabrielli P, Antonini C, Campos J, Acquilino A, Sansavini G, et al. Carbon dioxide capture, transport and storage supply chains: Optimal economic and environmental performance of infrastructure rollout. Int J Greenh Gas Control 2022;117:103635. https://doi.org/10.1016/J.IJGGC.2022.103635.

[44] Kalyanarengan Ravi N, Van Sint Annaland M, Fransoo JC, Grievink J, Zondervan E. Development and implementation of supply chain optimization framework for CO2 capture and storage in the Netherlands. Comput Chem Eng 2017;102:40–51. https://doi.org/10.1016/J.COMPCHEMENG.2016.08.011.

[45] Christensen P, Burton DJ. Cost Estimate Classification System – As Applied in Engineering , Procurement , and Construction for the Process Industries. Construction 2005:10.

[46] Hills T, Leeson D, Florin N, Fennell P. Carbon Capture in the Cement Industry: Technologies, Progress, and Retrofitting. Environ Sci Technol 2016;50:368–77. https://doi.org/10.1021/acs.est.5b03508.

[47] Rubin ES. Understanding the pitfalls of CCS cost estimates. Int J Greenh Gas Control 2012;10:181–90. https://doi.org/10.1016/j.ijggc.2012.06.004.

[48] van der Spek M, Ramirez A, Faaij A. Challenges and uncertainties of ex ante techno-economic analysis of low TRL CO_2 capture technology: Lessons from a case study of an NGCC with exhaust gas recycle and electric swing adsorption. Appl Energy 2017;208:920–34. https://doi.org/10.1016/j.apenergy.2017.09.058.

[49] Martorell JL, Rochelle GT, Baldea M, Elliott W, Bauer C. Lessons Learned: Comparing Two Detailed Capital Cost Estimates for Carbon Capture by Amine Scrubbing. Ind Eng Chem Res 2023;62:4433–43. https://doi.org/10.1021/acs.iecr.2c04311.

[50] Stepchuk I, Pérez-Fortes M, Ramírez A. Assessing impacts of deploying bio-based isobutene for MTBE production in an existing petrochemical cluster. J Clean Prod 2025;503. https://doi.org/10.1016/j.jclepro.2025.145114.

[51] ISPT, QuoMare, Deltalinqs. A scenario study of transition in the Rotterdam Harbor Industrial Cluster - Carbon feedstock transition of the petrochemical industry under spatial limitations 2025.

[52] Power2X, Deltalings. A sustainable carbon future - Feedstock Transition for Harbor Industrial Cluster Rotterdam 2022.

[53] Kuramochi T, Ramírez A, Turkenburg W, Faaij A. Comparative assessment of CO_2 capture technologies for carbon-intensive industrial processes. Prog Energy Combust Sci 2012;38:87–112. https://doi.org/10.1016/j.pecs.2011.05.001.

[54] Tsupari E, Kärki J, Arasto A, Pisilä E. Post-combustion capture of CO_2 at an integrated steel mill - Part II: Economic feasibility. Int J Greenh Gas Control 2013;16:278–86. https://doi.org/10.1016/j.ijggc.2012.08.017.

[55] Cormos C. Evaluation of reactive absorption and adsorption systems for post-combustion CO_2 capture applied to iron and steel industry. Appl Therm Eng 2016;105:56–64. https://doi.org/10.1016/j.applthermaleng.2016.05.149.

[56] Ho MT, Bustamante A, Wiley DE. Comparison of CO_2 capture economics for iron and steel mills. Int J Greenh Gas Control 2013;19:145–59. https://doi.org/10.1016/j.ijggc.2013.08.003.

[57] Biermann M, Langner C, Roussanaly S, Normann F, Harvey S. The role of energy supply in abatement cost curves for CO_2 capture from process industry – A case study of a Swedish refinery. Appl Energy 2022;319. https://doi.org/10.1016/j.apenergy.2022.119273.

[58] Berghout N, Broek M Van Den, Faaij A. International Journal of Greenhouse Gas Control Techno-economic performance and challenges of applying CO_2capture in the industry : A case study of five industrial plants 2013;17:259–79. https://doi.org/10.1016/j.ijggc.2013.04.022.

[59] Andersson V, Franck PÅ, Berntsson T. Techno-economic analysis of excess heat driven post-combustion CCS at an oil refinery. Int J Greenh Gas Control 2016;45:130–8. https://doi.org/10.1016/j.ijggc.2015.12.019.

[60] Gardarsdottir SO, De Lena E, Romano M, Roussanaly S, Voldsund M, Pérez-Calvo JF, et al. Comparison of technologies for CO_2 capture from cement production—Part 2: Cost analysis. Energies 2019;12:542. https://doi.org/10.3390/en12030542.

[61] Cormos CC. Decarbonization options for cement production process: A techno-economic and environmental evaluation. Fuel 2022;320. https://doi.org/10.1016/j.fuel.2022.123907.

[62] Johansson D, Sjöblom J, Berntsson T. Heat supply alternatives for CO_2 capture in the process industry. Int J Greenh Gas Control 2012;8:217–32. https://doi.org/10.1016/j.ijggc.2012.02.007.

[63] IEA (2023), Tracking Clean Energy Progress 2023, IEA, 2023. https://www.iea.org/reports/tracking-clean-energy-progress-2023.

[64] Incer-Valverde J, Korayem A, Tsatsaronis G, Morosuk T. “Colors” of hydrogen: Definitions and carbon intensity. Energy Convers Manag 2023;291:117294. https://doi.org/10.1016/j.enconman.2023.117294.

[65] Schlund D, Schulte S, Sprenger T. The who’s who of a hydrogen market ramp-up: A stakeholder analysis for Germany. Renew Sustain Energy Rev 2022;154:111810. https://doi.org/10.1016/j.rser.2021.111810.

[66] Ramboll. Achieving affordable green hydrogen production plants 2023.

[67] Shafiee RT, Schrag DP. Carbon abatement costs of green hydrogen across end-use sectors. Joule 2024:1–9. https://doi.org/10.1016/j.joule.2024.09.003.

[68] European Commission. COMMISSION DELEGATED REGULATION (EU) 2023/1184 of 10 February 2023 supplementing Directive (EU) 2018/2001 of the European Parliament and of the Council establishing a Union methodology setting out detailed rules for the production of renewable liquid and 2023.

[69] Mac Dowell N, Sunny N, Brandon N, Herzog H, Ku AY, Maas W, et al. The hydrogen economy: A pragmatic path forward. Joule 2021;5:2524–9. https://doi.org/10.1016/j.joule.2021.09.014.

[70] Roshan Kumar T, Beiron J, Marthala VRR, Pettersson L, Harvey S, Thunman H. Enhancing early-stage techno-economic comparative assessment with site-specific factors for decarbonization pathways in carbon-intensive process industry. Carbon Capture Sci Technol 2025;14:100338. https://doi.org/10.1016/j.ccst.2024.100338.

[71] Kountouris I, Bramstoft R, Madsen T, Gea-bermúdez J, Münster M, Keles D. A unified European hydrogen infrastructure planning to support the rapid scale-up of hydrogen production 2024:1–13. https://doi.org/10.1038/s41467-024-49867-w.

[72] Ganter A, Gabrielli P, Sansavini G. Near-term infrastructure rollout and investment strategies for net-zero hydrogen supply chains. Renew Sustain Energy Rev 2024;194:114314. https://doi.org/10.1016/j.rser.2024.114314.

[73] Terlouw T, Bauer C, McKenna R, Mazzotti M. Large-scale hydrogen production via water electrolysis: a techno-economic and environmental assessment. Energy Environ Sci 2022;15:3583–602. https://doi.org/10.1039/d2ee01023b.

[74] Biermann M, Normann F, Johnsson F, Hoballah R, Onarheim K. Capture of CO_2 from Steam Reformer Flue Gases Using Monoethanolamine: Pilot Plant Validation and Process Design for Partial Capture. Ind Eng Chem Res 2022;61:14305–23. https://doi.org/10.1021/acs.iecr.2c02205.

[75] Antonini C, Treyer K, Streb A, van der Spek M, Bauer C, Mazzotti M. Hydrogen production from natural gas and biomethane with carbon capture and storage - A techno-environmental analysis. Sustain Energy Fuels 2020;4:2967–86. https://doi.org/10.1039/d0se00222d.

[76] Nguyen T, Abdin Z, Holm T, Mérida W. Grid-connected hydrogen production via large-scale water electrolysis. Energy Convers Manag 2019;200:112108. https://doi.org/10.1016/j.enconman.2019.112108.

[77] Cooper N, Horend C, Röben F, Bardow A, Shah N. A framework for the design & operation of a large-scale wind-powered hydrogen electrolyzer hub. Int J Hydrogen Energy 2022;47:8671–86. https://doi.org/10.1016/j.ijhydene.2021.12.225.

[78] Pissot S, Thunman H, Samuelsson P, Seemann M. Production of negative-emissions steel using a reducing gas derived from dfb gasification. Energies 2021;14. https://doi.org/10.3390/en14164835.

[79] Carolina D, Castilla GM, Pallar D, Johnsson F, Thunman H. Thermochemical Energy Storage with Integrated District Heat Production – A Case Study of Sweden 2023.

[80] Parra SQ, Romano MC. Decarbonization of cement production by electrification. J Clean Prod 2023;425:138913. https://doi.org/10.1016/j.jclepro.2023.138913.

[81] Walter V, Göransson L, Taljegard M, Öberg S, Odenberger M. Low-cost hydrogen in the future European electricity system – Enabled by flexibility in time and space. Appl Energy 2023;330. https://doi.org/10.1016/j.apenergy.2022.120315.

[82] Devkota S, Cha JY, Shin BJ, Mun JH, Yoon HC, Mazari SA, et al. Techno-economic and environmental assessment of hydrogen production through ammonia decomposition. Appl Energy 2024;358:122605. https://doi.org/10.1016/j.apenergy.2023.122605.

[83] Ahmad AH, Darmanto PS, Hariana H, Darmawan A, Aziz M, Juangsa FB. Integration ammonia cracking process and co-firing of natural gas in combined cycle power plant: A thermodynamic analysis. Energy 2024;304:132098. https://doi.org/10.1016/j.energy.2024.132098.

[84] Niermann M, Beckendorff A, Kaltschmitt M, Bonhoff K. ScienceDirect Liquid Organic Hydrogen Carrier (LOHC) e Assessment based on chemical and economic properties. Int J Hydrogen Energy 2019;44:6631–54. https://doi.org/10.1016/j.ijhydene.2019.01.199.

[85] Ishimoto Y, Voldsund M, Nekså P, Roussanaly S, Berstad D, Gardarsdottir SO. Large-scale production and transport of hydrogen from Norway to Europe and Japan: Value chain analysis and comparison of liquid hydrogen and ammonia as energy carriers. Int J Hydrogen Energy 2020;45:32865–83. https://doi.org/10.1016/j.ijhydene.2020.09.017.

[86] Tiggeloven JL, Faaij APC, Kramer GJ, Gazzani M. Optimization of Electric Ethylene Production: Exploring the Role of Cracker Flexibility, Batteries, and Renewable Energy Integration. Ind Eng Chem Res 2023;62:16360–82. https://doi.org/10.1021/acs.iecr.3c02226.

[87] Tiggeloven JL, Faaij APC, Kramer GJ, Gazzani M. Optimizing Emissions Reduction in Ammonia - Ethylene Chemical Clusters: Synergistic Integration of Electrification, Carbon Capture, and Hydrogen 2025. https://doi.org/10.1021/acs.iecr.4c03817.

[88] Ibrahim Y, Al-Mohannadi DM. Optimization of low-carbon hydrogen supply chain networks in industrial clusters. Int J Hydrogen Energy 2023;48:13325–42. https://doi.org/10.1016/j.ijhydene.2022.12.090.

[89] Mirza N, Kearns D. State of the Art: CCS Technologies 2024. Glob CCS Inst Melbourne, Aust 2022.

[90] Technology Readiness and Costs of CCS - Global CCS Institute 2021. https://www.globalccsinstitute.com/resources/publications-reports-research/technology-readiness-and-costs-of-ccs/ (accessed September 7, 2025).

[91] Kumar TR, Beiron J, Biermann M, Harvey S, Thunman H. Plant and system-level performance of combined heat and power plants equipped with different carbon capture technologies. Appl Energy 2023;338:120927. https://doi.org/10.1016/j.apenergy.2023.120927.

[92] Autothermal Reforming Hydrogen | Johnson Matthey | Johnson Matthey 2025. https://matthey.com/hydrogen-autothermal-reforming-atr-ghr (accessed September 7, 2025).

[93] Autothermal reforming (ATR): reforming the future with low-carbon hydrogen | Air Liquide 2025. https://www.airliquide.com/stories/hydrogen/autothermal-reforming-atr-reforming-future-low-carbon-hydrogen (accessed September 7, 2025).

[94] Ueckerdt F, Verpoort PC, Anantharaman R, Bauer C, Beck F, Longden T, et al. On the cost competitiveness of blue and green hydrogen. Joule 2024;8:104–28. https://doi.org/10.1016/j.joule.2023.12.004.

[95] Bauer C, Treyer K, Antonini C, Bergerson J, Gazzani M, Gencer E, et al. On the climate impacts of blue hydrogen production. Sustain Energy Fuels 2022;6:66–75. https://doi.org/10.1039/d1se01508g.

[96] Matthey J. LCH™ Process for the production of blue hydrogen 2022.

[97] Axelsson L, Edvall M, Harvey S, Roshan Kumar T, Jannasch A-K, Westin J, et al. Future hydrogen supply in Stenungsund Pre-study of a SOEC pilot plant and analysis of large-scale integration of SOEC and ammonia cracking plants. 2024.

[98] TOPSOE. All about SOEC for PtX. 2024.

[99] Hoegh EVI - FSRU 2025. https://hoeghevi.com/solutions/clean-energy-solutions/ (accessed April 28, 2025).

[100] TOPSOE. H2Retake™ - an ammonia cracking solution ready to go 2024. https://www.topsoe.com/our-resources/knowledge/our-products/process-licensing/h2retake-process (accessed October 4, 2024).

[101] Thyssenkrupp. Ammonia cracking – Closing the energy value chain 2024. https://www.thyssenkrupp-uhde.com/en/ammonia-cracking (accessed April 24, 2024).

[102] KBR. Empowering Transition℠ H2ACT℠ Ammonia Cracking Technology : A pathway to sustainable energy. 2023.

[103] Stylianou E. KBR Ammonia Cracking , H2ACT℠ - A roadmap from clean energy source to sustainable hydrogen supply. 2023.

[104] Dufour M, Möllersten K, Zetterberg L. How to maintain environmental integrity when using state support and the VCM to co-finance BECCS projects - a Swedish case study. Front Environ Sci 2024;12:1–12. https://doi.org/10.3389/fenvs.2024.1387138.

[105] Stenström O, Kumar TR, Rydén M. A million scenarios to identify conditions for robust bioenergy carbon capture in Sweden. Int J Greenh Gas Control 2025;145. https://doi.org/10.1016/j.ijggc.2025.104411.

[106] Åberg M, Fälting L, Lingfors D, Nilsson AM, Forssell A. Do ground source heat pumps challenge the dominant position of district heating in the Swedish heating market? 2020;254. https://doi.org/10.1016/j.jclepro.2020.120070.

[107] Levihn F. CHP and heat pumps to balance renewable power production: Lessons from the district heating network in Stockholm. Energy 2017;137:670–8. https://doi.org/10.1016/j.energy.2017.01.118.

[108] Levihn F. CHP and heat pumps to balance renewable power production: Lessons from the district heating network in Stockholm. Energy 2017;137:670–8. https://doi.org/10.1016/J.ENERGY.2017.01.118.

[109] IEA Bioenergy. Large biomass CHP plant in Stockholm Sweden 2018. https://www.ieabioenergy.com/wp-content/uploads/2018/02/8-LargeCHP-Värtaverket_SE_Final.pdf (accessed June 22, 2022).

[110] Amghizar I, Vandewalle LA, Van Geem KM, Marin GB. New Trends in Olefin Production. Engineering 2017;3:171–8. https://doi.org/10.1016/J.ENG.2017.02.006.

[111] Honeywell UOP. Filling the Propylene Gap – Shaping the Future with On-Purpose Technologies. Honeywell UOP 2019:1–9.

[112] Features P, Benefits P, Feedstocks T. CATOFIN ® Dehydrogenation 2020.

[113] GlobalData. (October 12, 2023). Production capacity of propylene worldwide in 2018 and 2022, with a forecast to 2030 (in million metric tons) [Graph]. In Statista. 2023. https://www.statista.com/statistics/1065879/global-propylene-production-capacity (accessed June 25, 2024).

[114] Tullo A. Contracts awarded for propylene in China. Chem Eng News 2022;100:10–10. https://doi.org/10.1021/CEN-10019-BUSCON8.

[115] Clariant launches new CATOFIN® 312 propane dehydrogenation catalyst 2024. https://www.clariant.com/en/Corporate/News/2024/04/Clariant-launches-new-CATOFIN-312-propane-dehydrogenation-catalyst (accessed June 25, 2024).

[116] The heart of the chemical park goes electric - www.svp.de 2021. https://www.svp.de/en/the-heart-of-the-chemical-park-goes-electric/ (accessed September 5, 2025).

[117] Accelerating electrification with the "Cracker of the Future" Consortium - Borealis 2021. https://www.borealisgroup.com/news/accelerating-electrification-with-the-cracker-of-the-future-consortium (accessed October 25, 2022).

[118] Manalal JT, Pérez-Fortes M, Ramírez A. Re-wiring petrochemical clusters: impact of using alternative carbon sources for ethylene production. Green Chem 2025. https://doi.org/10.1039/d4gc06042c.

[119] Lawrence G. Cost estimating for turnarounds 2012. https://www.digitalrefining.com/article/1000335/cost-estimating-for-turnarounds (accessed November 18, 2023).

[120] Europe Cracker Closures | ICIS 2025. https://www.icis.com/explore/resources/cracker-closures-europe/ (accessed September 5, 2025).

[121] A Perfect Storm? Europe's steam cracker closures highlight continent's struggles with competitiveness | S&P Global 2025. https://www.spglobal.com/commodity-insights/en/news-research/latest-news/chemicals/070725-a-perfect-storm-europes-steam-cracker-closures-highlight-continents-struggles-with-competitiveness (accessed September 5, 2025).

[122] Northern Lights, Quality Specification for Liquified CO_2. 2023. https://norlights.com/ (accessed October 10, 2023).

[123] Northern Lights. Liquid CO_2 Quality Specifications (Updated) 2024. https://norlights.com/wp-content/uploads/2024/02/Northern-Lights-GS-co2-Spec2024.pdf (accessed February 20, 2024).

[124] Borealis AB. Krackeranläggningen Miljörapport. Stenungsund: 2021.

[125] Northern Lights. Northern Lights, Quality Specification for Liquified CO2. 2023. https://norlights.com/ (accessed October 10, 2023).

[126] European Hydrogen Observatory. The European hydrogen market landscape. Clean Hydrog Partnersh 2023:1–95.

[127] European Commission. Hydrogen 2025. https://energy.ec.europa.eu/topics/eus-energy-system/hydrogen_en (accessed September 5, 2025).

[128] Clean Air Task Force. Hydrogen Hub 2025. https://www.catf.us/hydrogen/hydrogen-hubs/.

[129] Eliasson Å, Fahrman E, Biermann M, Normann F, Harvey S. Efficient heat integration of industrial CO2 capture and district heating supply. Int J Greenh Gas Control 2022;118:103689. https://doi.org/10.1016/j.ijggc.2022.103689.

[130] Deng H, Roussanaly S, Skaugen G. Techno-economic analyses of CO_2 liquefaction: Impact of product pressure and impurities. Int J Refrig 2019;103:301–15. https://doi.org/10.1016/j.ijrefrig.2019.04.011.

[131] Antwerp@C Development Studies Pre Feed Report 2021.

[132] Axelsson L, Edvall M, Harvey S, Roshan Kumar T, Jannasch A-K, Westin J, et al. Future hydrogen supply in Stenungsund : Pre-study of a SOEC pilot plant and analysis of large-scale integration of SOEC and ammonia cracking plants 2024.

[133] Hackl R, Harvey S. Applying exergy and total site analysis for targeting refrigeration shaft power in industrial clusters. Energy 2013;55:5–14. https://doi.org/10.1016/j.energy.2013.03.029.

[134] Feng X, Zhu XX. Combining pinch and exergy analysis for process modifications. Appl Therm Eng 1997;17:249–61. https://doi.org/10.1016/s1359-4311(96)00035-x.

[135] Feng X, Zhu XX, Zheng JP. A practical exergy method for system analysis [of steam power plants]. IECEC 96. Proc. 31st Intersoc. Energy Convers. Eng. Conf., vol. 3, 1996, p. 2068–71 vol.3. https://doi.org/10.1109/IECEC.1996.553438.

[136] Gardarsdóttir SÓ, Normann F, Andersson K, Johnsson F. Postcombustion CO_2 capture using monoethanolamine and ammonia solvents: The influence of CO_2 concentration on technical performance. Ind Eng Chem Res 2015;54:681–90. https://doi.org/10.1021/ie503852m.

[137] Hughes S. NETL's Cost of Capturing CO_2 from Industrial Sources and Industrial Carbon Capture Retrofit Database 2023.

[138] Berghout N, Kuramochi T, Broek M van den, Faaij A. Techno-economic performance and spatial footprint of infrastructure configurations for large scale CO_2 capture in industrial zones. A case study for the Rotterdam Botlek area (Part A). Int J Greenh Gas Control 2015;39:256–84. https://doi.org/10.1016/j.ijggc.2015.05.019.

[139] Roussanaly S, Berghout N, Fout T, Garcia M, Gardarsdottir S, Nazir SM, et al. Towards improved cost evaluation of Carbon Capture and Storage from industry. vol. 106. 2021.

[140] Smith R. Chemical Process Design and Integration. Second Edi. John Wiley & Sons, Ltd; 2016.

[141] Enerdata. Carbon price forecast under the EU ETS 2023:1–11.

[142] Homaio. What are the EUA price forecasts for 2030? 2024. https://www.homaio.com/post/what-are-the-eua-price-forecasts-for-2030.

[143] Thunman H, Berdugo Vilches T, Seemann M, Maric J, Vela IC, Pissot S, et al. Circular use of plastics-transformation of existing petrochemical clusters into thermochemical recycling plants with 100% plastics recovery. Sustain Mater Technol 2019;22:e00124. https://doi.org/10.1016/j.susmat.2019.e00124.

[144] Beiron J, Normann F, Johnsson F. Carbon capture from combined heat and power plants – Impact on the supply and cost of electricity and district heating in cities. Int J Greenh Gas Control 2023;129. https://doi.org/10.1016/j.ijggc.2023.103973.

[145] Hoseinpoori S, Roshan Kumar T, Beiron J, Johnsson F, Svensson E, Pallarès D. Integration of sorbent-based direct air capture into combined heat and power plants with post-combustion carbon capture. Energy 2025;328. https://doi.org/10.1016/j.energy.2025.136509.

[146] Hannula I, Kurkela E. Liquid transportation fuels bed gasification of lignocellulosic biomass. vol. 91. 2013.

[147] ETIP Bioenergy. HVO / HEFA 2023. https://old.etipbioenergy.eu/value-chains/products-end-use/products/hvo-hefa (accessed September 3, 2025).

[148] Slome S, Velson JC, Fox T. The problem with on-purpose bio-propane 2023. https://www.nexanteca.com/blog/202205/problem-purpose-bio-propane (accessed November 9, 2023).

[149] Cañete Vela I, Berdugo Vilches T, Berndes G, Johnsson F, Thunman H. Co-recycling of natural and synthetic carbon materials for a sustainable circular economy. J Clean Prod 2022;365. https://doi.org/10.1016/j.jclepro.2022.132674.

[150] Di Nardo A, De Rinaldis S, Di Benedetto A. Bio and green hydrogen: A comparative review of regulatory trends, industrial feasibility, and technological perspectives. Int J Hydrogen Energy 2025;154:150254. https://doi.org/10.1016/J.IJHYDENE.2025.150254.

[151] Official Journal of the European Union. DIRECTIVE (EU) 2023/2413 OF THE EUROPEAN PARLIAMENT AND OF THE COUNCIL of 18 October 2023 amending Directive (EU) 2018/2001, Regulation (EU) 2018/1999 and Directive 98/70/EC as regards the promotion of energy from renewable sources, and repealing Council 2023.

[152] European Commission. Carbon Border Adjustment Mechanism 2023. https://taxation-customs.ec.europa.eu/carbon-border-adjustment-mechanism (accessed December 26, 2023).

[153] International Energy Agency (IEA). Hydrogen 2025. https://www.iea.org/energy-system/low-emission-fuels/hydrogen (accessed August 30, 2025).

[154] US Department of Energy. Technology Readiness Assessment Guide DOE G413.3-4A, 9-15-2011, Office of Management, U.S. Department of Energy, Washington, D.C. 2011.

[155] Roussanaly S, Gundersen T, Ramirez A. Putting the costs and benefits of carbon capture and storage into perspective: a multi-sector to multi-product analysis. Prog Energy 2025;7. https://doi.org/10.1088/2516-1083/ad9075.

[156] Shell and Dow start up e-cracking furnace experimental unit | Shell Global 2025. https://www.shell.com/business-customers/chemicals/media-releases/2022-media-releases/shell-and-dow-start-up-e-cracking-furnace-experimental-unit.html (accessed September 8, 2025).

[157] Technology: Electrification Solutions | Coolbrook 2025. https://coolbrook.com/electrification-solutions/ (accessed September 8, 2025).

[158] Borcycle™ C - Borcycle™ - Circular Economy - Borealis 2025. https://www.borealisgroup.com/circular-economy/borcycle/borcycle-c (accessed September 8, 2025).

[159] Further Assessment of Emerging CO_2 Capture Technologies for the Power Sector and their Potential to Reduce Costs - IEAGHG 2019. https://ieaghg.org/publications/further-assessment-of-emerging-co2-capture-technologies/ (accessed September 8, 2025).

[160] Karlsson S, Svensson E, Riboldi L, Roussanaly S, Anantharaman R. Estimating the potential and costs for carbon dioxide removal in the European pulp and paper industry 2025:5–7.

[161] Roshan Kumar T, Beiron J, Marthala VRR, Pettersson L, Harvey S, Thunman H. Combining exergy-pinch and techno-economic analyses for identifying feasible decarbonization opportunities in carbon-intensive process industry: Case study of a propylene production technology. Energy Convers Manag X 2025;25:100853. https://doi.org/10.1016/j.ecmx.2024.100853.

[162] European Commission. COMMISSION DELEGATED REGULATION (EU) 2023/1185 of 10 February 2023 supplementing Directive (EU) 2018/2001 of the European Parliament and of the Council establishing a Union methodology setting out detailed rules for the production of renewable liquid and 2023.

[163] WBCSD and WRI, “The Greenhouse Gas Protocol - A Corporate Accounting and Reporting Standard,” 2012. 2012.

[164] Smith R. Chemical Process Design and Integration. Second. John Wiley & Sons, Ltd; 2016.

[165] Perstorp. Project Air. 2024. https://projectair.se/en/.

[166] Young J, Garcı-Dıez E, Garcia S, van der Spek M. The impact of binary water–CO_2 isotherm models on the optimal performance of sorbent-based direct air capture processes 2021;14:5377–94. https://doi.org/10.1039/d1ee01272j.

[167] Stenström O, Khatiwada D, Levihn F, Usher W, Rydén M. A robust investment decision to deploy bioenergy carbon capture and storage—exploring the case of Stockholm Exergi. Front Energy Res 2023;11:1–20. https://doi.org/10.3389/fenrg.2023.1250537.

Nomenclature

Symbols[65]

AVO_{EX}	Avoidable exergy loss
INE_{EX}	Inevitable exergy loss
EX_{total}	Total exergy loss
Ω	Energy level (ratio of exergy and energy)
H	Energy input
C_{OC}	Opportunity costs
C_{netw}	Cost of all CO_2 interconnections
C_{FD}	Cost of forced downtime
C_{PD}	Cost of premature decommissioning
C^{tot}	Total system cost
$p_{n,t}$	hydrogen produced by technology n at time step t [MWh/h]
$c_t^{CH_4}$	natural gas price at time step t [€/MWh]

Subscripts

avo	avoided
reb	reboiler temperature
source	heat source
ss-cap	site-specific cost of CO_2 capture
ss-avo	site-specific cost of CO_2 avoidance
l	linear
nl	non-linear

---

[65] See Table S.3 in the Supplementary Materials of **Paper IV** for the full description and nomenclature of the optimization model.

Appendix A.

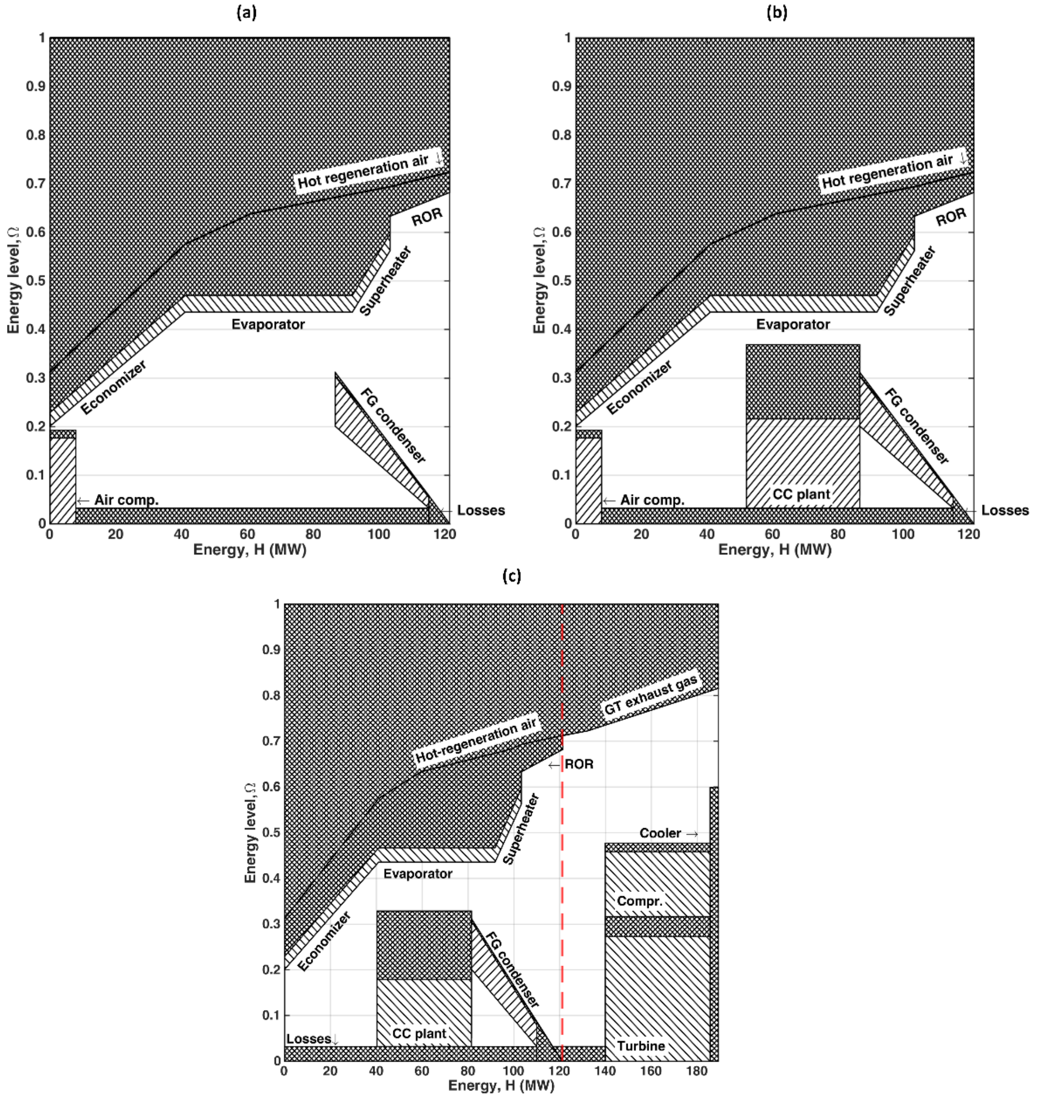

Figure A1: Ω-H diagram of the a) the reference air-regeneration train without the CC plant, b) PC_1 configuration and c) PC_2 configuration. Diagonal and cross-hatched regions indicate the avoidable and inevitable exergy losses, respectively. Note the increase in the X-axis scale in PC_2 configuration, with the integration of the industrial gas turbine. The red-dashed vertical line indicates the total exergy input to the previous process configurations, as depicted by the X-axis scales in sub-plots (a) and (b), prior to this modification. Source: Paper II.